

Journal of Life Sciences

Volume 5, Number 3, March 2011 (Serial Number 35)



David Publishing Company
www.davidpublishing.com

Publication Information

Journal of Life Sciences is published monthly in hard copy (ISSN1934-7391) and online (ISSN 1934-7405) by David Publishing Company located at 1840 Industrial Drive, Suite 160, Libertyville, Illinois 60048, USA.

Aims and Scope

Journal of Life Sciences, a monthly professional academic journal, covers all sorts of researches on molecular biology, microbiology, botany, zoology, genetics, bioengineering, ecology, cytobiology, biochemistry, and biophysics, as well as other issues related to life sciences.

Editorial Board Members

Dr. Stefan Hershberger (USA), Dr. Suiyun Chen (China), Dr. Farzana Perveen (Pakistan), Dr. Francisco Torrens (Spain), Dr. Filipa João (Portugal), Dr. Masahiro Yoshida (Japan), Dr. Reyhan Erdogan (Turkey), Dr. Grzegorz Żurek (Poland), Dr. Ali Izadpanah (Canada), Dr. Barbara Wiewióra (Poland), Dr. Valery Lyubimov (Russia), Dr. Amanda de Moraes Narcizo (Brasil), Dr. Marinus Frederik Willem te Pas (The Netherlands), Dr. Anthony Luke Byrne (Australia), Dr. Xingjun Li (China), Dr. Stefania Staibano (Italy), Dr. Wenle Xia (USA), Hamed Khalilvandi-Behroozyar (Iran).

Manuscripts and correspondence are invited for publication. You can submit your papers via Web Submission, or E-mail to life-sciences@davidpublishing.com or life-sciences@hotmail.com. Submission guidelines and Web Submission system are available at <http://www.davidpublishing.com>.

Editorial Office

1840 Industrial Drive, Suite 160, Libertyville, Illinois 60048

Tel: 1-847-281-9826, Fax: 1-847-281-9855

E-mail: life-sciences@davidpublishing.com, life-sciences@hotmail.com

Copyright©2011 by David Publishing Company and individual contributors. All rights reserved. David Publishing Company holds the exclusive copyright of all the contents of this journal. In accordance with the international convention, no part of this journal may be reproduced or transmitted by any media or publishing organs (including various websites) without the written permission of the copyright holder. Otherwise, any conduct would be considered as the violation of the copyright. The contents of this journal are available for any citation. However, all the citations should be clearly indicated with the title of this journal, serial number and the name of the author.

Abstracted / Indexed in

Database of EBSCO, Massachusetts, USA

Cambridge Scientific Abstracts (CSA), USA

Chinese Database of CEPS, American Federal Computer Library Center (OCLC), USA

Ulrich's Periodicals Directory, USA

Chinese Scientific Journals Database, VIP Corporation, Chongqing, China

Summon Serials Solutions

Subscription Information

Price (per year): Print \$420, Online \$300, Print and Online \$560

David Publishing Company

1840 Industrial Drive, Suite 160, Libertyville, Illinois 60048

Tel: 1-847-281-9826, Fax: 1-847-281-9855

E-mail: order@davidpublishing.com



David Publishing Company
www.davidpublishing.com

JLS

Journal of Life Sciences

Volume 5, Number 3, March 2011 (Serial Number 35)

Contents

Research Papers

- 167 **Binding of Mono, Bi and Tridomain Proteins to Zwitterionic and Anionic Vesicles: Asymmetric Location of Anionic Phospholipids in Mixed Zwitterionic/Anionic Vesicles and Cooperative Binding**
Francisco Torrens and Gloria Castellano
- 182 **Photosynthetic Excitation Pressure Causes Violaxanthin De-epoxidation in Aging Cabbage (*Brassica Oleracea* L.) Leaves**
Amarendra Narayan Misra, Dariusz Latowski and Kazimierz Strzalka
- 192 **Gene Expression Profiles in Porcine Tissues of Liver and Kidney**
Glazko Tatiana, Khlopova Nataliya, Fahrenkrug Scott, Garbe John and Glazko Valeriy
- 201 **Antiproliferative Activity of *Kappaphycus Alvarezii* Extract on Three Cancer Cell Lines (NCIH 460, HCT 116 and U 251)**
Madhavarani Alwarsamy and Ramanibai Ravichandran
- 206 **Evaluation of Emmer Wheat Genetic Resources Aimed at Dietary Food Production**
Zdeněk Stehno, Ivana Paulíčková, Jana Bradová, Petr Konvalina, Ivana Capouchová, Eva Mašková, Dana Gabrovská, Marie Holasová, Vlasta Fiedlerová, Renáta Winterová, Jarmila Ouhrabková and Ladislav Dotlačil
- 212 **Separated Hydrolysis and Fermentation of Water Hyacinth Leaves for Ethanol Production**
Buddhiporn Sornvoraweat and Jirasak Kongkiattikajorn
- 220 **Allelopathic Potentials of Some Crop Residues on the Germination and Seedling Growth of *Chromolaena Odoratum* L.**
Modupe Janet Ayeni and Joshua Kayode

Reviews

- 224 **Conditional Mutations in *Drosophila***
Boris F. Chadov, Nina B. Fedorova, Eugenia V. Chadova and Helena A. Khotskina
- 241 **Status, Impact and Management of Certain Alien Plant Pests Proven to Be Invasive to Thailand's Ecology**
Malee Thungrabeab and Suthap Tongma

Binding of Mono, Bi and Tridomain Proteins to Zwitterionic and Anionic Vesicles: Asymmetric Location of Anionic Phospholipids in Mixed Zwitterionic/Anionic Vesicles and Cooperative Binding

Francisco Torrens¹ and Gloria Castellano²

1. *Institute for Molecular Science, University of Valencia, Valencia E-46071, Spain*

2. *Energenesis Chair of Interdisciplinary Technology, Saint Vincent Martyr Catholic University of Valencia, Valencia E-46003, Spain*

Received: June 09, 2010 / Accepted: September 29, 2010 / Published: March 30, 2011.

Abstract: Lysozyme, myoglobin and BSA were used as models of globular proteins covering a wide range of pI. The purpose is to extend the studies to anionic lipid bilayers. Electrostatics is studied in cationic protein adsorption to zwitterionic PC and anionic mixed PC/PG SUVs. Protein adsorption is investigated in SUVs along with changes of fluorescence emission spectra. Partition coefficients and cooperativity parameters are calculated. At pI binding obtains maximum while at lower or higher pHs binding decreases. In Gouy-Chapman formalism activity coefficient goes with square charge, which deviations indicate asymmetric location of anionic phospholipid in the inner leaflet, in mixed SUVs for lysozyme- and myoglobin-PC/PG systems, in agreement with experiments and molecular dynamics simulations. Vesicles bind myoglobin anti-cooperatively while lysozyme-BSA cooperatively. A model is proposed for both, which composes two protein sub-layers with different structures and properties. Hill coefficient reflects subunit cooperativity of bi and tridomain proteins.

Key words: Protein-lipid interaction, sigmoid adsorption isotherm, transbilayer asymmetry, anionic phospholipid asymmetric location, cooperative binding, hill plot.

Abbreviations: ATP, adenosine triphosphate; BSA, bovine serum albumin; CA, cluster analysis; CL, cardiolipin; DNC, monodansylcadaverine; FRET, Foerster resonance energy transfer; MOPS, 3-(*N*-morpholino)-propanesulphonic acid; PC, phosphatidylcholine; PCA, principal component analysis; PG, phosphatidylglycerol; PI, phosphatidylinositol; pI, isoelectric point; PS, phosphatidylserine; SA, stearic acid; SP, surfactant protein; SUV, small unilamellar vesicle.

1. Introduction

Cationic cell penetrating peptides offer a promising, non-invasive platform for delivering molecules that are otherwise impermeable to cell membranes. They adsorb at the lipid membrane-water interface, disrupt headgroup interactions and produce local defects within the membrane that allow therapeutic molecules to enter the cell. Despite being net-neutral, PC melting

temperature and cooperativity were reduced with increasing the alkyl linkage separating cationic residues and peptide concentration. Bilayer disruption was more pronounced when anionic lipid was added, as peptides were able to bind to anionic headgroups, significantly affecting melting behaviour and inducing domain formation. Mixed zwitterionic/anionic phospholipid bilayers mimic some characteristics of the plasma membranes' lipid composition, since negatively charged components are present at 10-20%. Partition to zwitterionic bilayers decreases as apolar >

Corresponding author: Francisco Torrens, Ph.D., lecturer, research field: biomacromolecules. E-mail: francisco.torrens@uv.es.

polar > anionic > cationic solutes; to negatively charged bilayers is increased to cationic species, decreased to anionic and unaltered for apolar and polar molecules. In eukaryotic cell plasma membrane, anionic PS is predominantly exposed on the cytosolic leaflet [1]. Two mechanisms occur: a direct interaction of PS with the proteins of the cytoskeleton and an ATP-dependent inward-translocation (flip-flop) pumping of PS *via* translocase enzymes (e.g., flippases).

Allosterism is a property displayed by many oligomeric proteins. The binding of a molecule at one site induces a change in the binding properties of another site of the protein. Negatively cooperative receptor sites do not have a fixed affinity; rather, the affinity of the receptors decreases *vs.* the occupancy of the receptor population and is usually measured by ligand-accelerated tracer dissociation in an infinite dilution procedure. Negative cooperativity increases the range of the effective concentrations of the ligands. Myoglobin is the simplest monomeric haemoprotein and its physicochemical properties, e.g., reversible $O_{2(aq)}$ binding, are well known (cooperativity coefficient $h = 1$) [2]. However in intact muscle myoglobin shows positive cooperativity ($h = 1.46$, normal respiration), although it varies from non-respiration to hyper-respiration ($h = 1.00-2.23$). As with allosteric enzymes, which enable cells to gain control of metabolic activity *via* the abrupt, cooperative behaviour of enzyme subunits, cells also profit from the cooperative behaviour of membranes. Phase separation creates a compositional phase boundary with a unique status: the phase boundaries are the physical sites at which the membrane properties change abruptly. Cells can use the sharp differences in membrane properties to co-localize some components and separate others. Because phase separations depend on lipid composition, binding of ions and molecules to membrane and aggregation state of membrane components, small changes in parameters can control phase behaviour; e.g., phase separations may be driven

by the loss of certain lipid components together with the addition of new ones, as occurs because of the activity of lipid kinases, phosphatases and hydrolases during signalling reactions, or by changes in Ca^{2+} concentration, or by the aggregation of immune receptors. As a complication, a cooperative transition during a membrane phase change can either be fast or extremely slow.

In earlier publications the bindings of vinyl polymers to anionic SUVs [3], polyanionic electrolytes to cationic micelles [4], melittin to zwitterionic SUVs [5], and lysozyme, myoglobin and BSA to zwitterionic SUVs [6, 7] were studied by spectrofluorimetry and liquid chromatography. Valence-topological charge-transfer indices for multifunctional amino acids were applied to lysozyme [8, 9]. In the present report lysozyme, myoglobin and BSA were used as models of water-soluble, globular proteins with known three-dimensional structures, covering a wide range of pI 5-11. The objective of this report is to extend the studies to anionic lipid bilayers, given the involvement of anionic headgroups in cell activity. Bidomain lysozyme and monodomain myoglobin are smaller than tridomain BSA [10]; their surface hydrophobicity is relatively low in native state [11, 12]. They show no major conformational changes at pH 4-10 [13].

2. Materials and Methods

2.1 Materials

The PG, PS, PI, CL, hen egg-white lysozyme, horse heart myoglobin and BSA were from Sigma (St. Louis, MO). Egg-yolk PC was purchased from Merck (Darmstadt, Ger.) and purified according to Singleton, et al. [14]. Salt, buffers and reagents were of the highest purity available.

2.2 Vesicle Preparation

The SUVs composed of PC and PC/PG mixtures of various compositions, SP, PI and CL were prepared dissolving an appropriate amount of lipid in chloroform/methanol. The solvent was evaporated

under a stream of N_{2(g)} and the lipid was dried under vacuum overnight. The 0.010 mol·L⁻¹ MOPS-NaOH buffer pH 7.0, acetate buffer pH 4.0 or glycine buffer pH 9.0, at a given NaCl concentration in the range 0-1 mol·L⁻¹, was added to the dry film and the suspension was extensively vortexed. The lipid dispersion was next sonicated for 20 min, at a temperature above the phase transition temperature of the phospholipid, using an ultrasonic generator, with a microtip probe (Vibra cell, Sonics and Materials, Inc., Danbury, CT), at a power setting 4 and 50% duty cycle. The samples were then centrifuged for 15 min, at 35,000 g, to remove probe particles and the remaining multilamellar aggregates. The lipid content, in the resulting SUV preparations, was determined by a phosphorus assay [15]. The integrity of SUV preparations was controlled by negative-stain electron microscopy [16].

2.3 Fluorescence Spectroscopy

Steady-state fluorescence measurements were recorded using a Perkin Elmer (Beaconsfield, UK) LS-50 fluorescence spectrophotometer, with 1.0×1.0 cm quartz cuvette. The excitation-emission bandwidths were 5 nm. The excitation wavelength was set to 280 nm for all proteins. Spectra were corrected by comparison to quinine sulphate standard. In the binding experiments, the fluorescence emission spectra of the proteins, in MOPS-NaOH, acetate or glycine buffer, were monitored from 300 to 440 nm. Titrations were performed by addition of small aliquots of the SUV solution to the protein, at a desired concentration in 1 mL, and the shown data are representative of several independent experiments. The possible weak fluorescence contribution, because of the buffer and/or lipid solutions without proteins, was always used as baseline in all experiments and subtracted. In lipid-protein mixtures the changes of the emission fluorescence intensity, at $\lambda = 345$ nm (lysozyme, BSA) or $\lambda = 337$ nm (myoglobin), I^λ , were analyzed vs. R_i (lipid/protein molar ratio) and, from the fluorescence

intensity increase, the fraction of bound protein $\alpha = (I^\lambda - I^\lambda_{\text{free}})/(I^\lambda_{\text{bound}} - I^\lambda_{\text{free}})$ was estimated as described [17-20]. The I^λ_{bound} value was extrapolated from a double-reciprocal plot. Total protein concentration was 1 $\mu\text{mol}\cdot\text{L}^{-1}$.

2.4 Binding and Partition Equilibrium Models

The partition coefficient for the protein, between the lipid and aqueous phases, is defined as the ratio of the protein activity in the lipid phase a_p^L to that in the aqueous phase a_p^A :

$$K_r = \frac{a_p^L}{a_p^A} = \frac{c_p^L \gamma_p^L}{c_p^A \gamma_p^A} \quad (1)$$

where c_p^L and c_p^A are the protein concentrations in the corresponding phases, and γ_p^L and γ_p^A the activity coefficients. When lipid volume is negligible with regard to solvent one:

$$\frac{c_p^L}{c_p^A} = \frac{(\alpha/R_i^*)}{(1-\alpha)[P]_T \bar{v}_L} \quad (2)$$

where \bar{v}_L is the lipid partial molar volume (0.785 L·mol⁻¹ [21]) and $(1-\alpha)[P]_T$ the aqueous free protein concentration. Since the protein has access only from the vesicle outside, $\alpha/R_i^* = (\alpha/R_i)/\beta$ is corrected by the fraction of lipid in the outer leaflet $\beta = 0.65$. Substituting Eq. (2) in Eq. (1):

$$\frac{(\alpha/R_i^*)}{(1-\alpha)[P]_T} = \frac{K_r \bar{v}_L}{\gamma} = \frac{\Gamma}{\gamma} \quad (3)$$

where the activity coefficient $\gamma = \gamma_p^L/\gamma_p^A$. Parameter Γ is proportional to the partition coefficient:

$$\Gamma = K_r \bar{v}_L = C \bar{v}_L \exp\left(\frac{\Delta\bar{G}_p^{o,A} - \Delta\bar{G}_p^{o,L}}{RT}\right) \quad (4)$$

where constant C depends on the molar masses and densities of water and lipid, and $\Delta\bar{G}_p^{o,A}$ and $\Delta\bar{G}_p^{o,L}$ are protein molar free energies in the corresponding phases. The $\Delta\bar{G}_p^{o,A}$ is explained in Ref. [22]:

$$\begin{aligned} \frac{\Delta\bar{G}_p^{o,A}}{RT} = & -\frac{N_A (z_p^+)^2 e^2}{2RT(R_p + 2R_w) 4\pi\epsilon_o} \left(1 - \frac{1}{\epsilon_w}\right) + \frac{\Delta G_{\text{env}}}{RT} - \frac{4N_A z_p^+ e \mu_w}{RT(R_p + R_w)^2 4\pi\epsilon_o} \\ & + \frac{4N_A z_p^+ e \theta_w}{2RT(R_p + R_w)^3 4\pi\epsilon_o} - \frac{4N_A (z_p^+)^2 e^2 \alpha_w}{2RT(R_p + R_w)^4 4\pi\epsilon_o} \end{aligned} \quad (5)$$

where R_p is effective radius of protein ion, z_p^+ actual protein charge in solution, N_A Avogadro number, $e = 1.6021892 \times 10^{-19}$ C proton charge, $R = 8.3143$ J·mol⁻¹·K⁻¹

gas constant, $T = 293$ K temperature, $\varepsilon_0 = 8.854 \times 10^{-12}$ $C^2 \cdot N^{-1} \cdot m^{-2}$ absolute permittivity of vacuum, $R_w = 2.8 \text{ \AA}$ effective radius of solvation of water, $\varepsilon_w = 78.5$ relative permittivity, $\mu_w = 1.86$ D dipole moment, $\theta_w = 3.9 \times 10^{-26}$ statC·cm² quadrupole moment and $\alpha_w = 1.65 \times 10^{-40}$ C²·m²·J⁻¹ polarizability. For monovalent ions $z_p^+ = q$ (physical charge) makes Gouy-Chapman model to coincide with experiment; however multivalent ion fitting gives $z_p^+ < q$; thus protein z_p^+ is expected to be smaller than q . Cavitation energy is:

$$\Delta G_{\text{cav}} = \tau A_{\text{cav}} + W_o = \tau A_{\text{cav}} - RT \ln(1 - V_{\text{cav}} \rho_w^n) \quad (6)$$

where τ is the water-air surface tension ($435 \text{ J} \cdot \text{\AA}^{-2}$ at 298 K), $A_{\text{cav}} = 4\pi R_p^2$ and $V_{\text{cav}} = 4\pi R_p^3/3$ the cavity surface area and volume assumed spherical [23], W_o the cavitation work for a zero-surface solute and ρ_w^n the water number density. An expression similar to Eq. (5) is obtained for $\Delta \bar{G}_p^{o,L}$:

$$\frac{\Delta \bar{G}_p^{o,L}}{RT} = -\frac{N_A (z_p^+)^2 e^2}{2RT R_p 4\pi \varepsilon_o} \left(1 - \frac{1}{\varepsilon_L}\right) + \frac{N_A z_p^+ z_L e^2}{RT 4\pi \varepsilon_L \varepsilon_o R_p (1 + \kappa R_p)} \quad (7)$$

where ε_L is the relative permittivity of a lipid membrane,

$$\kappa = \left(\frac{2e^2 N_A I}{\varepsilon_w \varepsilon_o kT}\right)^{1/2} \quad (8)$$

is the inverse Debye screening length, z_L the phospholipid head charge and k Boltzman constant. The protein effective interfacial charge for the membrane-bound state ν is [24]:

$$\ln \gamma = 2\nu \sinh^{-1} \left[\nu b (\alpha/R_i^*) \right] \quad (9)$$

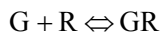
where parameter b :

$$b = \frac{20e}{\beta A_L (8\varepsilon_w \varepsilon_o RTI)^{1/2}} = 3.10(400/I)^{1/2} \quad (10)$$

is determined by the ionic strength I of the bulk electrolyte and $A_L = 70 \text{ \AA}^2$ the phospholipid head area [25]. For low surface coverages as $\Gamma \propto \gamma$ at constant ν it is expected:

$$\ln \Gamma \propto \ln \gamma \propto z_L \sinh^{-1}(z_L) \approx z_L^2 \quad (11)$$

Suppose one has a ligand G and receptor R the reaction can be written:



with *dissociation constant* of reaction K_D at equilibrium. The degree of adsorption is:

$$P_B = \frac{B}{B_{\text{max}}} = \frac{F}{K_D + F} \quad (12)$$

where $B_{\text{max}} = r_T$ is maximum B , B the equilibrium molar concentration of *bound ligand*, F the molar concentration of *free ligand* and K_D the *dissociation constant* of binding reaction. *Scatchard B/F-B plot* is a straight line if model holds [26, 27]. A Scatchard plot use is as a diagnostic of the type of departure from model. An upwardly concave curve is obtained for negatively cooperative binding, in which binding at one site makes it less likely that binding will occur at some other sites. In contrast a Scatchard plot with downward concavity could mean positively cooperative binding. The mathematical model of ligand-receptor interaction is:

$$P_B = \frac{B}{B_{\text{max}}} = \frac{F^n}{K_D^n + F^n} \quad (13)$$

where $n < 1$ indicates negative cooperativity and $n > 1$ positive cooperativity. For proteins with n binding sites for ligands, negative cooperativity occurs when binding at one site interferes with binding at an adjacent site. Eq. (12) can be transformed into a straight line writing:

$$\frac{P_B}{1 - P_B} = \left(\frac{F}{K_D}\right)^n$$

and taking logarithms of both sides:

$$\log\left(\frac{P_B}{1 - P_B}\right) = h \log F - h \log K_D \quad (14)$$

where n was replaced by h for the general case of nonperfect cooperativity. *Hill logP_B/(1-P_B) - logF plot* will be a straight line with slope h [28]. Experimental slope is *Hill coefficient* h , which increases with the extent of cooperativity up to a maximum possible value of the total number of sites n . An $h < 1$ could indicate negative cooperativity. For systems where cooperativity is complete $h = n$. Proteins that exhibit only a partial degree of positive cooperativity.

3. Results and Discussion

3.1 Binding Interface of Lysozyme into Lipid Bilayer

Lysozyme charges 12.0, 8.0 and 6.0 e.u. at pHs 4.0, 7.0 and 9.0 decay rapidly as isoelectric point at pH 10.7

is approached. Its binding curves were analyzed using partition equilibrium model with z_p^+ as adjustable parameter, assuming $\epsilon_L = 20$ and that protein was solvated in both phases; a globular shape for lysozyme ($R_p = 20.3 \text{ \AA}$) was used. The adsorption of lysozyme $1 \mu\text{mol}\cdot\text{L}^{-1}$ on mixed zwitterionic/anionic PC/PG SUVs was calculated ($T = 20 \text{ }^\circ\text{C}$, $\text{pH } 7.0$, $I = 0.015 \text{ mol}\cdot\text{L}^{-1}$). Protein adsorption increased with anionic PG content in PC/PG mixtures, as expected for cationic lysozyme-anionic PG electrostatic interaction for $z_L = -0.1, -0.2$ and -0.4 e.u. The z_p^+ , $\Gamma = \Gamma_{\text{exp}}$ and ν were obtained for lysozyme binding to PC/PG at various ν/v compositions. For adsorption on all PC/PG there was high surface coverage; the calculation of ν did not converge for fixed z_L . As ad-molecule is cationic $z_L^{\text{eff}} > z_L$ can be expected after adsorption; z_L^{eff} was treated as a fitting parameter and increased until ν convergence. For every experimental point a pair (z_p^+ , Γ) was obtained. The $z_p^+ = 4.8\text{-}5.1$ e.u. is lower than lysozyme physical charge at $\text{pH } 7.0$, which can be understood if one considers that lysozyme z_p^+ should decay because of the presence of counterions in electrolyte solution [29]. Overall $\langle z_p^+ \rangle$ values decay as anionic PG content increases, in agreement with experimental fact that in mixed anionic/zwitterionic SUVs, anionic phospholipid is asymmetrically located in the inner leaflet of bilayer [30-39]. On increasing PG content from 0% to 40%, $\langle \Gamma \rangle = \langle \Gamma_{\text{exp}} \rangle$ augments from 1.07×10^5 to $6.35 \times 10^5 \text{ L}\cdot\text{mol}^{-1}$, as expected for cationic lysozyme-anionic PG electrostatic interaction. Despite $\langle z_p^+ \rangle$ decayed $\langle \nu \rangle = 1.60$ e.u. stayed constant with PG content. The adsorption of lysozyme ($\text{pH } 7.0$) on PC/PG shows that protein adsorption increases with PG content in PC/PG, as expected for cationic protein-anionic PG electrostatic interaction. The $z_L, z_p^+, \Delta \bar{G}_p^{o,A}, \Delta \bar{G}_p^{o,L}, \Gamma = \Gamma_{\text{exp}}$ and ν were obtained for protein-PC/PG binding. The ν convergence required to treat phospholipid charge as a fitting parameter. Lysozyme binding was demonstrated to alter the structure of anionic membrane lipid phase [40]. Strong experimental support for a hydrophobic component in

interaction was provided; in contrast cationic lysozyme-anionic SUV electrostatic interaction also occurs [41]. Experiments on mastoparan X-anionic SUV binding suggested farther penetration into bilayer, leading to a translation *via* membrane; practically no translocation does occur in zwitterionic SUVs [42]. Membrane mimetic compounds, *e.g.*, geminis, caused membrane disruption [43-45]. There is a change of effective charge number: $z_p^+ < q$.

3.2 Binding Interface of Myoglobin into Lipid Bilayer

Myoglobin charges are 14.0 and 0.0 e.u. at $\text{pHs } 4.0$ and 7.0 corresponding to a pI of 6.9. Its binding curves were analyzed using partition equilibrium model with z_p^+ as adjustable parameter, assuming $\epsilon_L = 20$ and that the protein was solvated; a globular shape for myoglobin ($R_p = 22.6 \text{ \AA}$) was used. The adsorption of myoglobin $1 \mu\text{mol}\cdot\text{L}^{-1}$ on PC/PG SUVs ($T = 20 \text{ }^\circ\text{C}$, $\text{pH } 4.0$, $I = 0.015 \text{ mol}\cdot\text{L}^{-1}$) shows that surface coverage increases with anionic PG content in PC/PG, as expected for cationic myoglobin-anionic PG electrostatic interaction. The adsorption of myoglobin $1 \mu\text{mol}\cdot\text{L}^{-1}$ at $\text{pH } 4.0$ on PC/PG ($T = 20 \text{ }^\circ\text{C}$, $I = 0.015 \text{ mol}\cdot\text{L}^{-1}$) revealed that protein adsorption increased with anionic PG content in PC/PG, as expected for cationic protein-anionic PG electrostatic interaction. The $z_L, z_p^+, \Delta \bar{G}_p^{o,A}, \Delta \bar{G}_p^{o,L}, \Gamma = \Gamma_{\text{exp}}$ and ν were obtained for protein-PC/PG binding at various compositions. For PC/PG phospholipid charge was treated as a fitting parameter and optimized to $z_L = 0.00$ e.u. The $\langle z_p^+ \rangle$ decayed as PG content increased. The diminution was in agreement with anionic phospholipid asymmetric location in the inner leaflet of the bilayer. On increasing PG content from 0% to 40% $\langle \Gamma \rangle = \langle \Gamma_{\text{exp}} \rangle$ increased from 0.85×10^5 to $3.43 \times 10^5 \text{ L}\cdot\text{mol}^{-1}$, as expected for cationic myoglobin-anionic PG electrostatic interaction. Despite $\langle z_p^+ \rangle$ decay $\langle \nu \rangle = 1.69$ e.u. stayed constant with PG content.

3.3 Binding Interface of BSA into Lipid Bilayer

The BSA charges are 15.0, -9.0 and -33.5 e.u. at

pHs 4.0, 7.0 and 9.0, respectively, corresponding to a pI of 5.5. Its binding curves were analyzed using partition equilibrium model with z_p^+ as adjustable parameter, assuming $\epsilon_L = 20$ and that protein was solvated; a BSA globular shape ($R_p = 31.5 \text{ \AA}$) was used. The adsorption of BSA $1 \mu\text{mol}\cdot\text{L}^{-1}$ on PC SUVs ($T = 20 \text{ }^\circ\text{C}$, pH 7.0, Fig. 1) shows that surface coverage decays with increasing ionic strength I . The z_p^+ , $\Gamma = \Gamma_{\text{exp}}$ and ν are calculated for BSA binding to PC SUVs at various salt concentrations. For moderate ionic strengths $\langle z_p^+ \rangle$ drops as ionic strength increases as expected, because of the partial screening of counterions in electrolyte solution. The BSA formal electrostatic charge at pH 7.0 is negative while z_p^+ is calculated positive. As there exist three domains in BSA with calculated net charges of -5.0 , -4.0 and 0.0 e.u. for a total charge of -9.0 e.u., adsorption on PC SUVs is expected from neutral domain III. In the whole range of ionic strength $\langle z_p^+ \rangle$ slightly increases, $\langle I \rangle = \langle \Gamma_{\text{exp}} \rangle$ strongly decays from 0.84×10^5 to $0.61 \times 10^5 \text{ L}\cdot\text{mol}^{-1}$ and $\langle \nu \rangle$ strongly increases from 2.13 to 4.91 e.u. The adsorption of BSA $1 \mu\text{mol}\cdot\text{L}^{-1}$ on mixed PC/SA (90:10) SUVs is calculated ($T = 20 \text{ }^\circ\text{C}$, pH 7.0, $I = 0.025 \text{ mol}\cdot\text{L}^{-1}$). Surface coverage on PC/SA is lower than the one on PC. The z_p^+ , $\Gamma = \Gamma_{\text{exp}}$ and ν are computed for BSA binding to PC/SA (90:10). Mean averages are $\langle z_p^+ \rangle = 6.95$ e.u., $\langle I \rangle = \langle \Gamma_{\text{exp}} \rangle = 0.84 \times 10^5 \text{ L}\cdot\text{mol}^{-1}$ and $\langle \nu \rangle = 2.13$ e.u. The z_L was optimized to 0.00 e.u. A real plateau for isotherm was not always observed. Observations fit well with view that

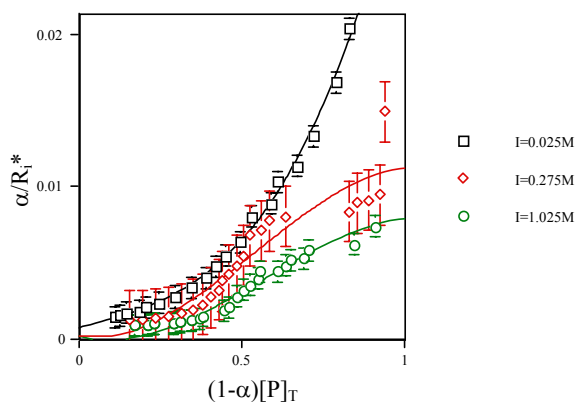


Fig. 1 Influence of ionic strength on the adsorption of BSA-PC at $T = 20 \text{ }^\circ\text{C}$ and pH 7.0.

hydrophobicity is predominant driving force for anionic ligand binding, but assisted by electrostatic interactions between phosphate headgroup and basic amino-acid residues. Since binding of BSA to vesicles suggests local, not global negative domain this may occur at $\text{pH} < \text{pI}$.

3.4 General Discussion of Three Proteins Binding Interfaces

For a given binding isotherm ν stayed constant and strongly smaller than z_p^+ . An effective charge, smaller than the one expected from the number of ionizable groups, was described for peptides [46-49]. Partition equilibrium model, in combination with Gouy-Chapman formalism, provides an expression for theoretical isotherms, which depend on adjustable parameters (Γ , ν). Theoretical isotherms look qualitatively similar to the ones obtained by thermodynamic approach. The $\Gamma_{\text{theoretical}}$ for both proteins are of the same order of magnitude as the ones derived from fitting, meaning that for each isotherm z_p^+ originates $\Gamma_{\text{theoretical}}$ similar to the one obtained from initial slope. Some calculations did not converge for fixed z_L because Gouy-Chapman model is limited to low coverages, but high surface concentration of cationic ad-molecules would cause z_L to become less negative; computations converged allowing z_L to be a fitting parameter. For $z_L = -1$ e.u. extrapolated $z_{L,\text{lysozyme}} = z_{L,\text{myoglobin}} = 0$ e.u. For $z_L = -1$ e.u. extrapolated $\langle z_p^+ \rangle_{\text{lysozyme}} = 4.8 < \langle z_p^+ \rangle_{\text{myoglobin}} = 5.3$ e.u. because of the greater q of the latter. For $z_L = -1$ e.u. extrapolated $\Delta \bar{G}_{p,\text{lysozyme}}^{o,A} = -50 \times 10^4 > \Delta \bar{G}_{p,\text{myoglobin}}^{o,A} = -61 \times 10^4 \text{ J}\cdot\text{mol}^{-1}$ because of the greater q of the latter. For $z_L = -1$ e.u. extrapolated $\Delta \bar{G}_{p,\text{lysozyme}}^{o,L} = -60 \times 10^4 > \Delta \bar{G}_{p,\text{myoglobin}}^{o,L} = -65 \times 10^4 \text{ J}\cdot\text{mol}^{-1}$ because of the greater q of the latter. For $z_L = -1$ e.u. from $\ln \Gamma$ -extrapolation $\langle I \rangle_{\text{lysozyme}} = \langle \Gamma_{\text{exp}} \rangle = 6 \times 10^5 < \langle I \rangle_{\text{myoglobin}} = \langle \Gamma_{\text{exp}} \rangle = 7.0 \times 10^5 \text{ L}\cdot\text{mol}^{-1}$ because of the lower $\Delta \bar{G}_p^{o,A}$ and $\Delta \bar{G}_p^{o,L}$ and greater $\langle z_p^+ \rangle$ and q of the latter. Relatively great errors in $\langle I \rangle = \langle \Gamma_{\text{exp}} \rangle$ were consistent with the fact that in mixed anionic/zwitterionic SUVs, anionic

phospholipid is asymmetrically located in the inner leaflet of bilayer, in experiments and molecular dynamics simulations. For $z_L = -1$ e.u. extrapolated $\langle v \rangle_{\text{lysozyme}} = 1.6 < \langle v \rangle_{\text{myoglobin}} = 1.68$ e.u. because of the greater q of the latter. Lysozyme (pH 7) showed a significant electrostatic selectivity for anionic SUVs (PC < PG), especially at low ionic strength, as can be expected for cationic protein-anionic SUVs, meaning that electrostatic interaction dominates over hydrophobic one. Electrostatic selectivity PC < PG is in agreement with FRET studies, between the cationic SP-B of pulmonary surfactant and anionic phospholipids [50-52]. In contrast the selectivity of myoglobin (pH 4, low PG content and saline concentration) was PG < PC, confirming that myoglobin-vesicle interaction is dominated by hydrophobic interaction at low PG content, in agreement with cationic SP-C-anionic phospholipid FRETs. The fact that the order, measured for the adsorptions of lysozyme-myoglobin with each SUV, be the opposite to one another suggests that the sum of the respective adsorption energies will be approximately equal for each protein, in accordance with suggestion above that protein activity depends on ability to adsorb with electrostatic and hydrophobic interactions. The comparative analysis of effective SUV charge z_L^{eff} with physical charge z_L , for lysozyme- and myoglobin-PC/PG adsorptions, showed that $z_L^{\text{eff}} = 0.00$ e.u. stays constant for zwitterionic PC, which predicts for both proteins zero z_L^{eff} extrapolation for $z_L = -1$ e.u. The $z_L^{\text{eff}} - z_L$ difference increased 0.417 e.u. because of high surface coverages. The examination of effective protein charge $z_{p,\text{eff}}^+$ with SUV z_L , for the adsorption of lysozyme- and myoglobin-PC/PG, showed that $z_{p,\text{eff}}^+$ increased with z_L for PC/PG as PC/PG < PC because anionic PG provides greater screening. The $z_{p,\text{eff}}^+$ change caused by PG content is lower for lysozyme than for myoglobin because of the greater q of the latter, which predicts a greater $z_{p,\text{eff}}^+$ extrapolation for $z_L = -1$ e.u. The study of protein molar free energy in aqueous phase $\Delta \bar{G}_p^{o,A}$ with

SUV z_L , for lysozyme- and myoglobin-PC/PG adsorptions, showed that $\Delta \bar{G}_p^{o,A}$ decays with z_L as PC < PC/PG because anionic PG drops $z_{p,\text{eff}}^+$, destabilizing protein-water electrostatic interaction responsible for protein hydration. The $\Delta \bar{G}_p^{o,A}$ change is greater for myoglobin because of its greater q , which predicted a lower $\Delta \bar{G}_p^{o,A}$ extrapolation for $z_L = -1$ e.u. The investigation of protein molar free energy in lipid phase $\Delta \bar{G}_p^{o,L}$ with SUV z_L , for lysozyme- and myoglobin-PC/PG adsorptions, showed that $\Delta \bar{G}_p^{o,L}$ decayed with z_L as PC < PC/PG because anionic PG dropped $z_{p,\text{eff}}^+$, destabilizing protein-SUV electrostatic interaction responsible for protein solvation. The $\Delta \bar{G}_p^{o,L}$ change was greater for myoglobin because of its greater q , which predicted a lower $\Delta \bar{G}_p^{o,L}$ extrapolation for $z_L = -1$ e.u. The variation of the logarithm of theoretical partition coefficient $\ln \Gamma$ with SUV z_L , for lysozyme- and myoglobin-PC/PG adsorptions (Fig. 2), shows above parabolic lines representing ideal Gouy-Chapman model [Eq. (11)], data deviations indicating effective charge increment $z_{L,\text{eff}} > z_L$, in agreement with the fact that in mixed anionic/zwitterionic SUVs, anionic phospholipid is asymmetrically located in the inner leaflet of bilayer, in experiments and molecular dynamics simulations. The $\ln \Gamma$ change is greater for myoglobin because of its greater $\Delta \bar{G}_p^{o,A}$, $\Delta \bar{G}_p^{o,L}$, $z_{p,\text{eff}}^+$ changes and q .

Comparing $\ln \Gamma$ vs. SUV z_L , for lysozyme- and myoglobin-PC/PG adsorptions, the greater absolute slope for myoglobin predicted a greater Γ extrapolation

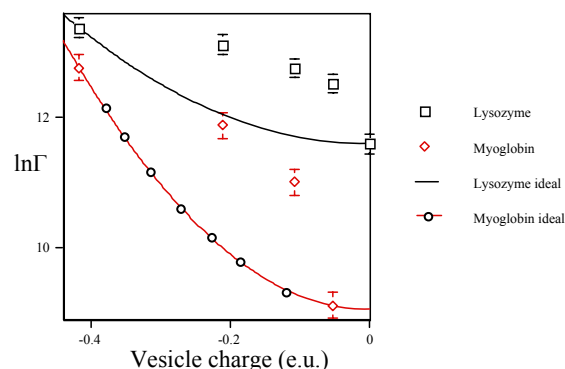


Fig. 2 Effect of vesicle charge on $\ln \Gamma$ for the adsorption of lysozyme (pH 7.0)- and myoglobin (pH 4.0)-PC/PG.

for $z_L = -1$ e.u. Trends were different from the ones of ideal Gouy-Chapman model. In the variation of effective interfacial charge ν_{eff} with SUV z_L for the adsorption of lysozyme- and myoglobin-PC/PG, ν_{eff} stayed constant with z_L for PC/PG because PG does not change z_L^{eff} . The ν_{eff} was lower for lysozyme (1.604 e.u.) than for myoglobin (1.686 e.u.), because of the greater $z_{p,\text{eff}}^+$ and q of the latter, which predicted a greater ν_{eff} extrapolation for $z_L = -1$ e.u. The correlation matrix \mathbf{R} of lysozyme-myoglobin/PC/PG and BSA/PC/SA associations, with regard to physicochemical properties $\{\langle z_p^+ \rangle, \Delta \bar{G}_p^{o,A}, \Delta \bar{G}_p^{o,L}, \langle I \rangle, \langle v \rangle\}$, was calculated with our program GraphCor [53-55]. Partial correlation diagram contained 66 high ($|r| \geq 0.75$) correlations. The CA was applied to associations *via* our program, which was written using IMSL subroutine CLINK [56]. *Single- and complete-linkage hierarchical CAs* performed a binary taxonomy of data, which allowed building the *dendrogram* of systems giving classes: {lysozyme/PC/PG 80/20, 60/40}, {lysozyme/PC/PG 95/5, 90/10, myoglobin/PC/PG 60/40}, {myoglobin/PC/PG 95/5, BSA/PC, BSA/PC/SA 90/10} and {lysozyme/PC, myoglobin/PC, myoglobin/PC/PG 90/10, 80/20}. Radial tree grouped them into the same classes. Program SplitsTree revealed conflicting relations between quartets lysozyme/PC-myoglobin/PC-myoglobin/PC/PG 90/10-myoglobin/PC/PG 80/20 and lysozyme/PC/PG 95/5-lysozyme/PC/PG 90/10-lysozyme/PC/PG 80/20-myoglobin/PC/PG 60/40 [57]. In association PCA factor F_1 explained 99.9% of variance, F_{1-2} 100.0% and classes were equal [58]. The correlation matrix \mathbf{R} of properties showed that partial correlation diagram contained eight high, one medium ($0.25 \leq |r| < 0.50$) and one low ($|r| \leq 0.25$) correlations. Both CAs allowed building physicochemical property dendrogram, which divided classes: $\{\langle v \rangle\}$, $\{\langle I \rangle\}$ and $\{\langle z_p^+ \rangle, \Delta \bar{G}_p^{o,A}, \Delta \bar{G}_p^{o,L}\}$. Radial tree grouped them into equivalent classes. Splits graph revealed conflicting relations between pairs $\Delta \bar{G}_p^{o,A} - \Delta \bar{G}_p^{o,L}$. In PCA F_1 explained 86% of variance, F_{1-2} 98%, F_{1-3} 100% and

the classes were matching.

Forms adopted by adsorption isotherms from diluted lysozyme-BSA solutions are *sigmoid*. The initial part of curves expresses the little affinity of SUVs for protein, with the adsorption of the first protein molecule to SUVs, which favours protein-protein attraction, the progressive adsorption of additional protein molecules to the first one is induced. The inflection point is related to protein multilayer formation, which requires the orientation of the first layer to place the second one. Saturation is not reached in our experiments because the formation of triple protein complexes is not probable. In contrast the number of SUV adsorption places in which protein could locate is limited: protein concentration in a monolayer increases until certain limit in which all adsorption places are occupied; behaviour is related with the zone of high protein concentrations. Fig. 3 shows Scatchard B/F - B plot for lysozyme- and BSA- (pH 7.0), and myoglobin- (pH 4.0) -PC SUV binding. Myoglobin upwardly concave curve indicates that for a given B/F , corresponding B is lower than the one expected for ideal simple model suggesting negatively cooperative binding; in contrast lysozyme-BSA downward concavity denotes that for a given B/F , resultant B is greater than the one expected for ideal model signifying positive cooperativity, in agreement with a model proposed by Sánchez-Muñoz et al. for BSA-biomaterial adsorption [59]. When BSA concentration adsorbed on biomaterial particles increases,

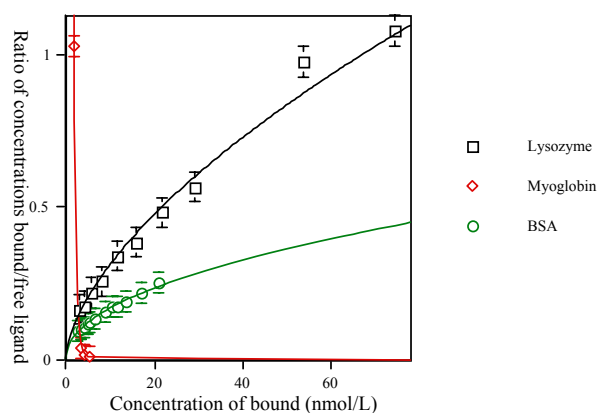


Fig. 3 Scatchard plot of lysozyme-, myoglobin- and bovine serum albumin-PC.

biomaterial zeta potential is less negative until BSA adsorption layer on their surface will be structured. Biomaterial particle-BSA interaction is mediated by (1) electrokinetic forces, especially dispersion ones caused by the movement of electrons in BSA molecules when they approach to biomaterial particles, and (2) electrostatic forces, especially orientation ones given when polar molecules (BSA) adsorb on surfaces that contain constant electrostatic charges. Induction forces also appear, which are present when dipolar moments exist in adsorbed BSA molecules and are caused by biomaterial surface charge. All forces are attractive and, approaching BSA to biomaterial particles, are balanced for repulsion forces that increase quickly to short distances. Adsorption interactions are mediated for orientation and dispersion electrostatic forces. The BSA has an interaction of orientation normal to biomaterial surfaces. The schematic simplified model of BSA double layer represents interaction between BSA as dipole moment and an isolated anion from biomaterial surface as charge. During BSA adsorption to biomaterial surfaces and depending on their structure and properties, the part that remains free to the bulk of solution could be able to interact with other protein molecules. They assumed that formed biomaterial-BSA complex could be simulated by porous layer model.

Hill $\log P_B/(1-P_B)-\log F$ plots were calculated for the binding of lysozyme-BSA (pH 7.0) and myoglobin (pH 4.0) to PC SUVs. Slopes represented Hill coefficient $h = 1.749, 0.402$ and 1.598 for lysozyme, myoglobin and BSA, respectively (Table 1). The PC binds myoglobin with a cooperativity constant $h = 0.402$, indicating that binding affinity is reduced by 2.5-fold when PC is pre-bound to myoglobin. It is postulated that conformational changes that occur because of PC presence regulates cooperativity. The $h < 1$ means that protein-lipid binding shows negative cooperativity, in partial agreement with the classical work of reversible myoglobin- O_2 binding in aqueous solution, with non-positive cooperativity. Negative

cooperativity was previously observed in cationic peptides (DNC-)melittin-zwitterionic PC SUVs binding, with coefficient $h = 0.888$ and 0.909 . Hill coefficient reflects negative cooperativity of melittin and monodomain myoglobin. In contrast for lysozyme and BSA $h > 1$ (positive cooperativity), in agreement with previous results for lysozyme-thyroglobulin [60] and BSA-biomaterials and -yeast protoplasm [61]. Hill coefficient reflects subunit cooperativity of bidomain lysozyme and tridomain BSA, in concordance with the classical cooperative reversible binding of tetrameric haemoglobin to O_2 in aqueous solution ($h = 2.8$).

Fig. 4 displays Hill plots for cationic lysozyme-mixed zwitterionic/anionic PC/PG SUV binding. Slopes are Hill coefficient $h = 1.749, 1.248, 1.194, 1.097$ and 0.894 for lysozyme-PC and -PC/PG 95:5, 90:10, 80:20 and 60:40, respectively. For the former four $h > 1$; however for the latter $h < 1$, meaning that for lesser anionic SUVs electrostatic attraction between ad-protein dipoles dominates over electrostatic repulsion between cationic ad-proteins.

Fig. 5 presents Hill plots for cationic lysozyme-mixed zwitterionic/anionic PC/PG 90:10 binding; Hill coefficients $h = 1.194, 2.095, 2.214$ and 2.827 for $I = 0.015, 0.025, 0.055$ and $0.105 \text{ mol}\cdot\text{L}^{-1}$, respectively. For all $h > 1$ increasing with ionic strength, meaning that electrostatic repulsion between cationic proteins decays with increasing salt effect, and electrostatic attraction between ad-protein dipoles dominates over electrostatic repulsion between ad-protein charges.

Fig. 6 exhibits Hill plots for cationic lysozyme-SUV binding; Hill coefficients $h = 1.749, 1.935, 1.751, 1.769$ and 2.022 for PC, PS, PI, PG and CL SUVs, respectively. For all $h > 1$, which is smaller for zwitterionic PC than for monoanionic PS, PI and PG than for partially dianionic CL, meaning that with increasing SUV anionic character, protein-protein electrostatic repulsion is decreasingly important vs. protein-SUV attraction, and electrostatic attraction between ad-protein dipoles dominates over electrostatic

Table 1 pH, peptide q and lipid z_L physical charges, maximum concentration of bound ligand and Hill coefficient for the binding of protein to phospholipid vesicles.^a

System	pH	q (e.u.)	z_L (e.u.)	B_{max} (nmol·L ⁻¹)	h	System	pH	q (e.u.)	z_L (e.u.)	B_{max} (nmol·L ⁻¹)	h
Lysozyme/PC ^b	7.0	8.0	0.00	107.7	1.749	Myoglobin/PC/PG 90:10 ^f	4.0	14.0	-0.10	6.6	0.658
Lysozyme/PC/PG 95:5 ^b	7.0	8.0	-0.05	171.7	1.248	Myoglobin/PC/PG 90:10 ^h	4.0	14.0	-0.10	18.0	1.333
Lysozyme/PC/PG 90:10 ^b	7.0	8.0	-0.10	303.6	1.194	Myoglobin/PC/PG 90:10 ⁱ	4.0	14.0	-0.10	54.3	1.511
Lysozyme/PC/PG 80:20 ^b	7.0	8.0	-0.20	136.0	1.097	Myoglobin/PC/PG 90:10 ^j	4.0	14.0	-0.10	10.4	1.340
Lysozyme/PC/PG 60:40 ^b	7.0	8.0	-0.40	383.6	0.894	Myoglobin/PC/PG 90:10 ^k	4.0	14.0	-0.10	7.5	1.477
Lysozyme/PC/PG 90:10 ^c	7.0	8.0	-0.10	250.8	2.095	Myoglobin/PC/PG 90:10 ^l	4.0	14.0	-0.10	43.5	1.716
Lysozyme/PC/PG 90:10 ^d	7.0	8.0	-0.10	238.2	2.214	Myoglobin/PS ^f	4.0	14.0	-0.11	8.3	0.591
Lysozyme/PC/PG 90:10 ^e	7.0	8.0	-0.10	123.8	2.827	Myoglobin/PI ^f	4.0	14.0	-1.00	4.4	0.886
Lysozyme/PS ^b	7.0	8.0	-1.00	127.4	1.935	Myoglobin/PG ^f	4.0	14.0	-1.00	10.5	0.986
Lysozyme/PI ^b	7.0	8.0	-1.00	119.8	1.751	Myoglobin/CL ^f	4.0	14.0	-1.00	8.6	2.039
Lysozyme/PG ^b	7.0	8.0	-1.00	6.9	1.769	Myoglobin/PC ^f	4.0	14.0	0.00	6.2	0.402
Lysozyme/CL ^b	7.0	8.0	-1.24	168.0	2.022	Myoglobin/PC ^b	7.0	0.0	0.00	26.2	0.936
Lysozyme/PC ^f	4.0	12.0	0.00	41.1	2.823	Myoglobin/PC ^g	9.0	-4.0	0.00	8.5	1.007
Lysozyme/PC ^b	7.0	8.0	0.00	107.7	1.749	Myoglobin/PC/PG 90:10 ^f	4.0	14.0	-0.10	6.6	0.658
Lysozyme/PC ^g	9.0	6.0	0.00	68.9	1.452	Myoglobin/PC/PG 90:10 ^b	7.0	0.0	-0.10	21.6	1.042
Lysozyme/PC/PG 90:10 ^f	4.0	12.0	-0.10	50.0	0.934	Myoglobin/PC/PG 90:10 ^g	9.0	-4.0	-0.10	6.2	2.032
Lysozyme/PC/PG 90:10 ^b	7.0	8.0	-0.10	303.6	1.194	BSA/PC ^c	7.0	-9.0	0.00	34.4	1.598
Lysozyme/PC/PG 90:10 ^g	9.0	6.0	-0.10	186.3	1.256	BSA/PC ^m	7.0	-9.0	0.00	40.8	1.643
Myoglobin/PC ^f	4.0	14.0	0.00	6.2	0.402	BSA/PC ⁿ	7.0	-9.0	0.00	15.8	2.041
Myoglobin/PC/PG 95:5 ^f	4.0	14.0	-0.05	2.2	0.516	BSA/PC ^o	7.0	-9.0	0.00	9.0	2.228
Myoglobin/PC/PG 90:10 ^f	4.0	14.0	-0.10	6.6	0.658	BSA/PC/SA 90:10 ^c	7.0	-9.0	-0.10	41.1	1.529
Myoglobin/PC/PG 80:20 ^f	4.0	14.0	-0.20	8.7	0.745	DNC-melittin/PC ^p	7.0	6.0	0.00	82.4	0.888
Myoglobin/PC/PG 60:40 ^f	4.0	14.0	-0.40	21.2	0.994	Melittin/PC ^p	7.0	6.0	0.00	96.4	0.909

^a In all calculations ϵ_L was 20.0 and it was considered that the protein is solvated in both phases.

^b pH 7.0, $I = 0.015$ M, $T = 20.0$ °C. ^c pH 7.0, $I = 0.025$ M, $T = 20.0$ °C. ^d pH 7.0, $I = 0.055$ M, $T = 20.0$ °C.

^e pH 7.0, $I = 0.105$ M, $T = 20.0$ °C. ^f pH 4.0, $I = 0.015$ M, $T = 20.0$ °C. ^g pH 9.0, $I = 0.015$ M, $T = 20.0$ °C.

^h pH 4.0, $I = 0.020$ M, $T = 20.0$ °C. ⁱ pH 4.0, $I = 0.025$ M, $T = 20.0$ °C. ^j pH 4.0, $I = 0.040$ M, $T = 20.0$ °C.

^k pH 4.0, $I = 0.055$ M, $T = 20.0$ °C. ^l pH 4.0, $I = 0.105$ M, $T = 20.0$ °C. ^m pH 7.0, $I = 0.125$ M, $T = 20.0$ °C.

ⁿ pH 7.0, $I = 0.275$ M, $T = 20.0$ °C. ^o pH 7.0, $I = 1.025$ M, $T = 20.0$ °C. ^p pH 7.0, $I = 0.030$ M, $T = 23.0$ °C.

repulsion between ad-protein charges.

Fig. 7 reveals Hill plots for cationic lysozyme-zwitterionic PC SUV binding at pHs 4.0, 7.0 and 9.0 with coefficient $h = 2.823$, 1.749 and 1.452, respectively. For all $h > 1$, which decays denoting that with increasing pH and dropping protein cationic character, protein-SUV attraction is decreasingly important vs. protein-protein electrostatic repulsion, and electrostatic repulsion between ad-protein charges dominates over electrostatic attraction between ad-protein dipoles.

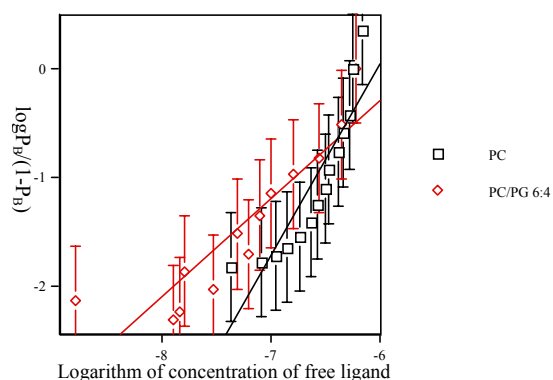


Fig. 4 Hill plot of lysozyme-PC and -PC/PG 60:40; $B_{max} = 107.7$ and 383.6 nmol·L⁻¹.

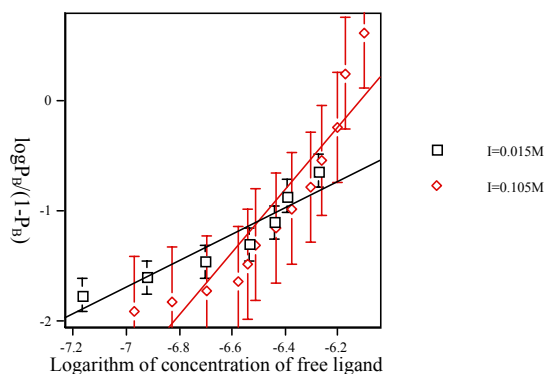


Fig. 5 Hill plot of lysozyme-PC/PG 90:10 at $I = 0.015$ and 0.105 M; $B_{\max} = 303.6$ and 123.8 nmol·L⁻¹.

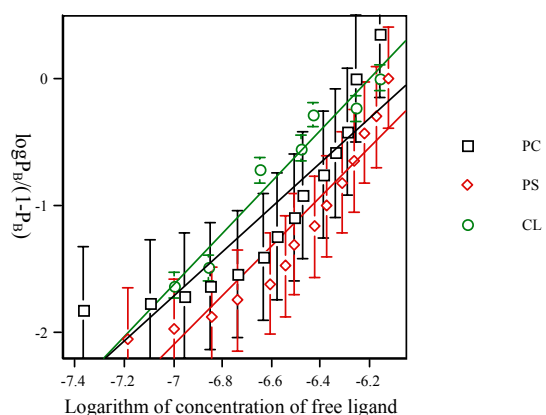


Fig. 6 Hill plot of lysozyme-PC, -PS and -CL with $B_{\max} = 107.7$, 127.4 and 168.0 nmol·L⁻¹.

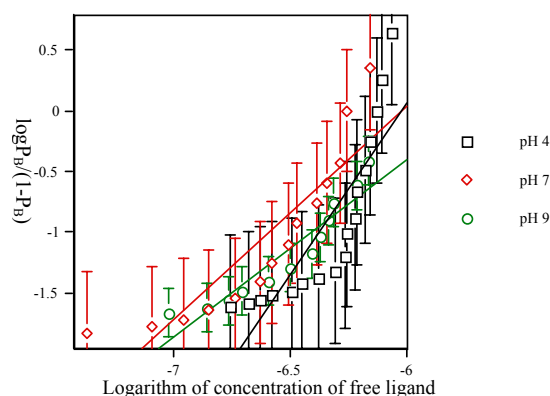


Fig. 7 Hill plot of lysozyme-PC at pHs 4.0, 7.0 and 9.0; $B_{\max} = 41.1$, 107.7 and 68.9 nmol·L⁻¹.

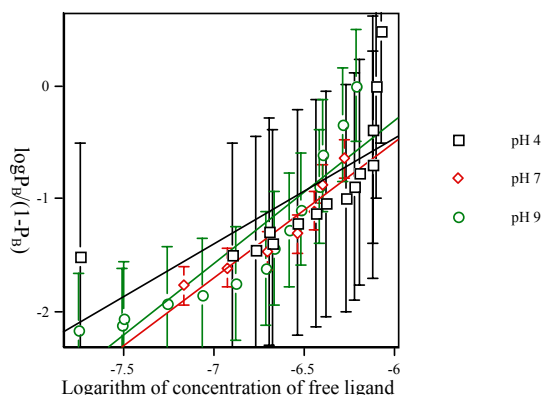


Fig. 8 Hill plot of lysozyme-PC/PG 90:10 at pHs 4.0, 7.0 and 9.0; $B_{\max} = 50.0$, 303.6 and 186.3 nmol·L⁻¹.

Fig. 8 illustrates Hill plots for cationic lysozyme-mixed zwitterionic/anionic PC/PG 90:10 SUVs at pHs 4.0, 7.0 and 9.0 with coefficient $h = 0.934$, 1.194 and 1.256 , respectively, which increases meaning that with increasing pH and decaying protein cationic character, electrostatic attraction between ad-protein dipoles dominates over electrostatic repulsion between ad-protein charges.

Fig. 9 shows Hill plots for cationic myoglobin-mixed zwitterionic/anionic PC/PG SUVs at pH 4.0; Hill coefficient $h = 0.402$, 0.516 , 0.658 , 0.745 and 0.994 for PC and PC/PG 95:5, 90:10, 80:20 and 60:40, respectively. All $h < 1$ meaning that for mixed zwitterionic/anionic SUVs, electrostatic repulsion between cationic ad-proteins dominates over electrostatic attraction between ad-protein dipoles. Negative cooperativity decays with increasing PG.

Fig. 10 displays Hill plots for cationic myoglobin-mixed zwitterionic/anionic PC/PG 90:10 SUV binding

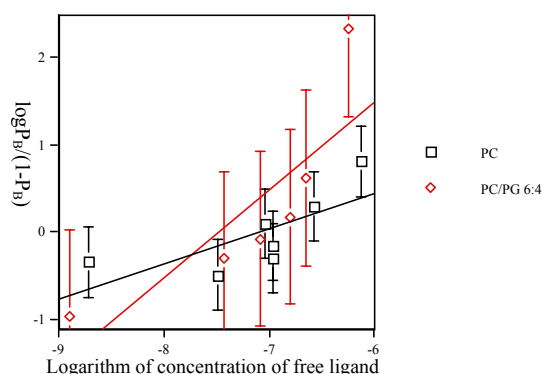


Fig. 9 Hill plot of myoglobin-PC and -PC/PG 60:40; $B_{\max} = 6.2$ and 21.2 nmol·L⁻¹.

at pH 4.0; Hill coefficient $h = 0.658$, 1.333 , 1.511 , 1.340 , 1.477 and 1.716 for $I = 0.015$, 0.020 , 0.025 , 0.040 , 0.055 and 0.105 mol·L⁻¹, respectively. For anionic enough SUVs $h > 1$, which increases with ionic strength, meaning that electrostatic repulsion between cationic proteins decays with increasing salt effect, and electrostatic attraction between ad-protein dipoles dominates over electrostatic repulsion between

178 Binding of Mono, Bi and Tridomain Proteins to Zwitterionic and Anionic Vesicles: Asymmetric Location of Anionic Phospholipids in Mixed Zwitterionic/Anionic Vesicles and Cooperative Binding

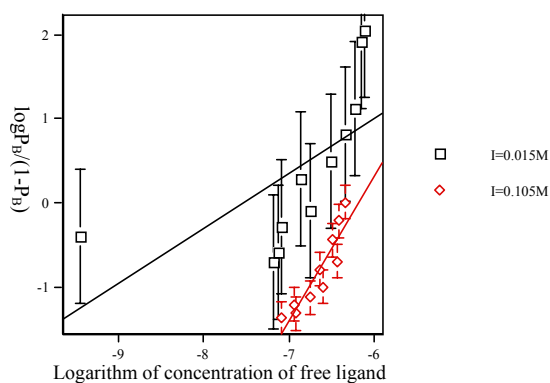


Fig. 10 Hill plot of myoglobin-PC/PG 90:10 at $I = 0.015$ and 0.105 M; $B_{\max} = 6.6$ and 43.5 nmol·L⁻¹.

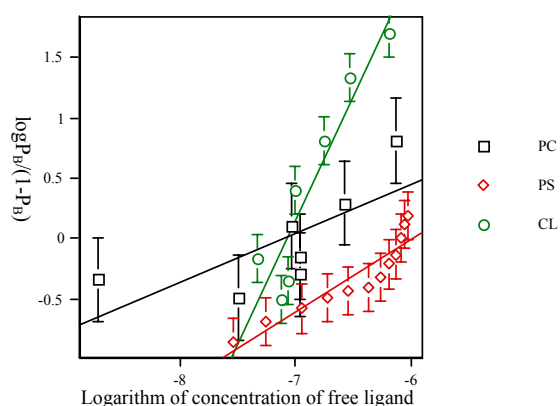


Fig. 11 Hill plot of myoglobin-PC, -PS and -CL with $B_{\max} = 6.2$, 8.3 and 8.6 nmol·L⁻¹.

ad-protein charges.

Fig. 11 illustrates Hill plots for cationic myoglobin-SUV binding at pH 4.0; Hill coefficient $h = 0.402$, 0.591 , 0.886 , 0.986 and 2.039 for PC, PS, PI, PG and CL SUVs, respectively, which results smaller for zwitterionic PC than for partially monoanionic PS than for monoanionic PI-PG-CL, meaning that with increasing SUV anionic character, protein-protein electrostatic repulsion is decreasingly important vs. protein-SUV attraction, and electrostatic attraction between ad-protein dipoles dominates over electrostatic repulsion between ad-protein charges.

Fig. 12 depicts Hill plots for myoglobin-zwitterionic PC SUV binding at pHs 4.0, 7.0 and 9.0 showing coefficient $h = 0.402$, 0.936 and 1.007 , respectively, which increases, meaning that with increasing pH and decaying protein cationic character, protein-protein electrostatic repulsion is decreasingly important vs. protein-SUV attraction, and electrostatic attraction

between ad-protein dipoles dominates over electrostatic repulsion between ad-protein charges.

Fig. 13 exhibits Hill plots for myoglobin-mixed zwitterionic/anionic PC/PG 90:10 SUV binding at pHs 4.0, 7.0 and 9.0 with coefficient $h = 0.658$, 1.042 and 2.032 , respectively, which increases, meaning that with increasing pH and decaying protein cationic character, protein-protein electrostatic repulsion is decreasingly important against protein-SUV attraction, and electrostatic attraction between ad-protein dipoles dominates over electrostatic repulsion between ad-protein charges.

Fig. 14 reveals Hill plots for anionic BSA-zwitterionic PC SUV binding at pH 7.0; Hill coefficient $h = 1.598$, 1.643 , 2.041 and 2.228 for $I = 0.025$, 0.125 , 0.275 and 1.025 mol·L⁻¹, respectively. For all systems $h > 1$, which increases with ionic strength, meaning that electrostatic repulsion between cationic ad-proteins

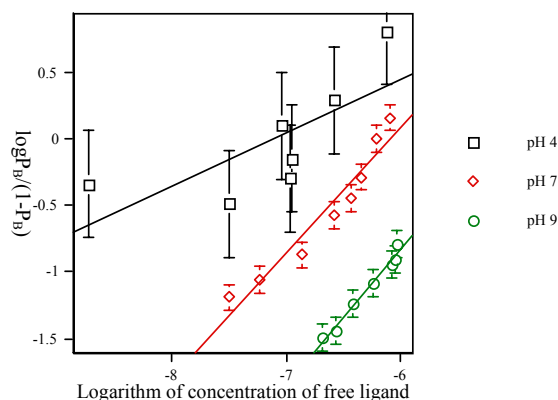


Fig. 12 Hill plot of myoglobin-PC at pHs 4.0, 7.0 and 9.0; $B_{\max} = 6.2$, 26.2 and 8.5 nmol·L⁻¹.

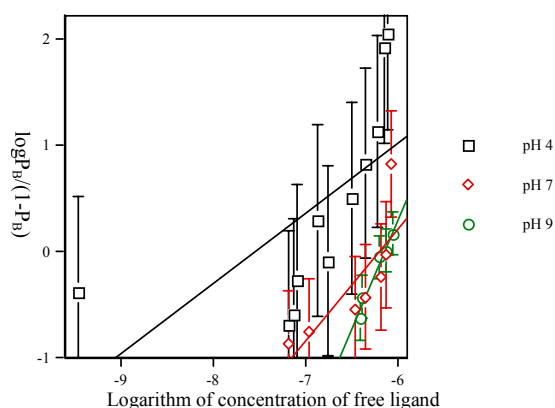


Fig. 13 Hill plot of myoglobin-PC/PG 90:10 at pHs 4.0, 7.0 and 9.0; $B_{\max} = 6.6$, 21.6 and 6.2 nmol·L⁻¹.

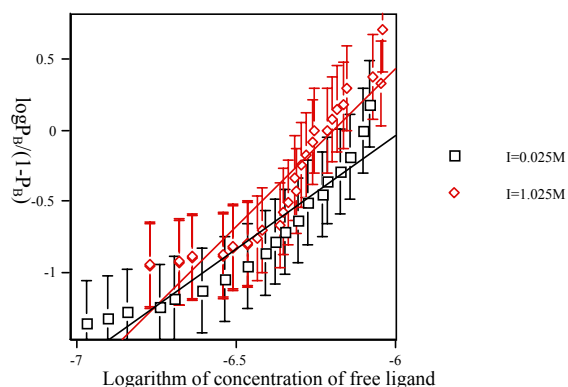


Fig. 14 Hill plot of BSA-PC at $I = 0.025$ and 1.025 M with $B_{\max} = 34.4$ and 9.0 $\text{nmol}\cdot\text{L}^{-1}$.

decreases with increasing salt effect, and electrostatic attraction between ad-protein dipoles dominates over electrostatic repulsion between ad-protein charges.

Fig. 15 illustrates Hill plots for anionic BSA-zwitterionic PC and -mixed zwitterionic/anionic PC/SA 90:10 SUV binding, with coefficient $h = 1.598$ and 1.529 for PC and PC/SA 90:10, respectively. For both systems $h > 1$, which decays with increasing SUV anionic character meaning that for low-anionic SUVs, electrostatic attraction between ad-protein dipoles dominates over electrostatic repulsion between cationic ad-proteins.

4. Conclusions

The present results allow for the following conclusions.

(1) Maximum binding occurred at protein isoelectric point, suggesting complementary electrostatic-driven adsorption, which is the driving force for asymmetry creation: high electrolyte concentrations prevent it. It showed moderate cooperativity because of protein-protein interaction. For monovalent ions Gouy-Chapman model is correct; however for multivalent ions it is semi-quantitative. The γ was obtained as: $\ln\gamma \propto \nu \sinh^{-1}(\nu)$; as $\Gamma \propto \gamma$ at constant ν , $\ln\Gamma \propto \ln\gamma \propto z_L \cdot \sinh^{-1}(z_L) \approx z_L^2$ is expected. For lysozyme- and myoglobin-mixed zwitterionic/anionic vesicle adsorptions, deviations from ideal model indicated asymmetric location of anionic phospholipid

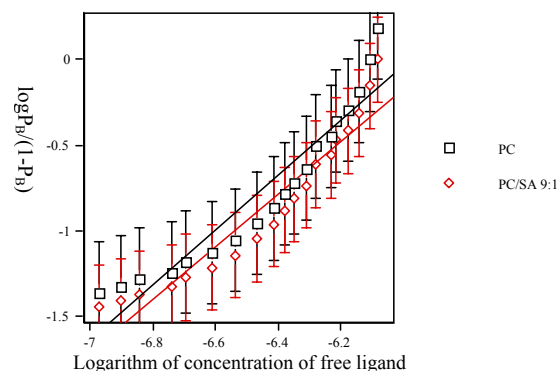


Fig. 15 BSA-PC and -PC/SA 90:10 with $B_{\max} = 34.4$ and 41.1 $\text{nmol}\cdot\text{L}^{-1}$, respectively.

in the inner leaflet, in agreement with experiments and molecular dynamics simulations.

(2) Some quali/quantitative differences for protein and vesicle effects were analyzed. Myoglobin and (DNC-)melittin association to vesicles can be described by a simple model, incorporating water-membrane partition equilibrium, modulated by membrane electrostatic charging as protein accumulates at interface. Induced surface potential counteracts further protein association, which is difficult because the repulsion of like charges becomes dominant. In contrast lysozyme and albumin binding to vesicles follow a model of positive cooperativity, which represents interaction between protein considered as dipole moment and anionic phospholipid headgroups as isolated anion. Hill coefficient reflects the subunit cooperativity of bi and tridomain proteins.

(3) Charge effect on protein binding showed that for lysozyme-anionic enough vesicles and myoglobin, electrostatic repulsion between cationic ad-proteins dominates over electrostatic attraction between ad-protein dipoles. Cooperativity increases with ionic strength.

Acknowledgments

The authors dedicate this manuscript to Prof. Dr. Agustín Campos, who was greatly interested in this research and would have loved to see its conclusion.

References

- [1] P.F. Devaux, R. Morris, Transmembrane asymmetry and lateral domains in biological membranes, *Traffic* 5 (2004) 241-246.
- [2] A. Seiyama, Virtual cooperativity in myoglobin oxygen saturation curve in skeletal muscle *in vivo*, *Dyn. Med.* 5 (3) (2006) 1-8.
- [3] F. Torrens, A. Campos, C. Abad, Binding of vinyl polymers to anionic model membranes, *Cell. Mol. Biol.* 49 (2003) 991-998.
- [4] F. Torrens, C. Abad, A. Codoñer, R. García-Lopera, A. Campos, Interaction of polyelectrolytes with oppositely charged micelles studied by fluorescence and liquid chromatography, *Eur. Polym. J.* 41 (2005) 1439-1452.
- [5] F. Torrens, G. Castellano, A. Campos, C. Abad, Negatively cooperative binding of melittin to neutral phospholipid vesicles, *J. Mol. Struct.* 834-836 (2007) 216-228.
- [6] F. Torrens, G. Castellano, A. Campos, C. Abad, Binding of water-soluble, globular proteins to anionic model membranes, *J. Mol. Struct.* 924-926 (2009) 274-284.
- [7] F. Torrens, G. Castellano, Comparative analysis of the electrostatics of the binding of cationic proteins to vesicles: Asymmetric location of anionic phospholipids, *Anal. Chim. Acta* 654 (2009) 2-10.
- [8] F. Torrens, G. Castellano, Improvement of charge-transfer indices for multifunctional amino acids: Application to lysozyme, *SAR QSAR Environ. Res.* 19 (2008) 643-654.
- [9] F. Torrens, G. Castellano, Topological charge-transfer indices: From small molecules to proteins, *Curr. Proteomics* 6 (2009) 204-213.
- [10] N.A. Williams, N.D. Weiner, Interactions of small polypeptides with dimyristoylphosphatidylcholine monolayers: Effect of size and hydrophobicity, *Int. J. Pharm.* 50 (1989) 261-266.
- [11] Y. Kato, T. Kitamura, T. Hashimoto, High-performance hydrophobic interaction chromatography of proteins, *J. Chromatogr. A* 266 (1983) 49-54.
- [12] M.L. Heinitz, L. Kennedy, W. Kopaciewicz, F.E. Regnier, Chromatography of proteins on hydrophobic interaction and ion-exchange chromatographic matrices: Mobile phase contributions to selectivity, *J. Chromatogr. A* 443 (1988) 173-182.
- [13] C. Tanford, The interpretation of hydrogen ion titration curves of proteins, *Adv. Protein Chem.* 17 (1962) 69-165.
- [14] W.S. Singleton, M.S. Gray, M.L. Brown, J.C. White, Chromatographically homogeneous lecithin from egg phospholipids, *J. Am. Oil Chem. Soc.* 42 (1965) 53-56.
- [15] J.C. Dittmer, M.A. Wells, Quantitative and qualitative analysis of lipids and lipid components, *Methods Enzymol.* 14 (1969) 482-530.
- [16] J.R. Harris, A negative staining study of natural and synthetic L- α -lysophosphatidylcholine micelles, macromolecular aggregates and crystals, *Micron Microsc. Acta* 17 (1986) 289-305.
- [17] E. Pérez-Payá, I. Porcar, C.M. Gómez, A. Campos, C. Abad, Binding of basic amphipathic peptides to neutral phospholipid membranes: A thermodynamic study applied to dansyl-labeled melittin and substance P analogues, *Biopolymers* 42 (1997) 169-181.
- [18] E. Pérez-Payá, J. Dufourcq, L. Braco, C. Abad, Structural characterisation of the natural membrane-bound state of melittin: A fluorescence study of a dansylated analogue, *Biochim. Biophys. Acta* 1329 (1997) 223-236.
- [19] J. Pedrós, C.M. Gómez, A. Campos, C. Abad, A fluorescence spectroscopy study of the interaction of monocationic quinine with phospholipid vesicles, Effect of ionic strength and lipid composition, *Spectrochim. Acta Part A* 53 (1997) 2219-2228.
- [20] C.M. Gómez, A. Codoñer, A. Campos, C. Abad, Binding of a fluorescent dansylcadaverine-substance P analogue to negatively charged phospholipid membranes, *Int. J. Biol. Macromol.* 27 (2000) 291-299.
- [21] C. Tanford, J.A. Reynolds, Characterization of membrane proteins in detergent solutions, *Biochim. Biophys. Acta* 457 (1976) 133-170.
- [22] J.O'M. Bockris, A.K.N. Reddy, *Modern Electrochemistry*, Vol. 1, New York: Plenum, 1970, p. 45.
- [23] I. Tuñón, E. Silla, J.L. Pascual-Ahuir, Continuum-uniform approach calculations of the solubility of hydrocarbons in water, *Chem. Phys. Lett.* 203 (1993) 289-294.
- [24] G. Schwarz, G. Beschiaschvili, Thermodynamic and kinetic studies on the association of melittin with a phospholipid bilayer, *Biochim. Biophys. Acta* 979 (1989) 82-90.
- [25] S. Stankowski, Surface charging by large multivalent molecules, Extending the standard Gouy-Chapman treatment, *Biophys. J.* 60 (1991) 341-351.
- [26] G. Scatchard, The attractions of proteins for small molecules and ions, *Ann. N.Y. Acad. Sci.* 51 (1949) 660-672.
- [27] J.D. McGhee, P.H. von Hippel, Theoretical aspects of DNA-protein interactions: Co-operative and non-co-operative binding of large ligands to a one-dimensional homogeneous lattice, *J. Mol. Biol.* 86 (1974) 469-489.
- [28] A.V. Hill, The combinations of haemoglobin with oxygen and with carbon monoxide, *Biochem. J.* 7 (1913) 471-480.
- [29] E. Pérez-Payá, L. Braco, A. Campos, V. Soria, C. Abad, Solution properties of polyelectrolytes: IV, Use of a new hydrophilic size-exclusion chromatographic packing for the separation of anionic and cationic polyions, *J. Chromatogr. A* 461 (1989) 229-242.
- [30] M.S. Bretscher, The proteins of erythrocyte membranes: Where are they?, *Biochem. J.* 122 (5) (1971) 40.

- [31] S.E. Gordesky, G.V. Marinetti, The asymmetric arrangement of phospholipids in the human erythrocyte membrane, *Biochem. Biophys. Res. Commun.* 50 (1973) 1027-1031.
- [32] R.F.A. Zwaal, B. Roelofsen, C.M. Colley, Localization of red cell membrane constituents, *Biochim. Biophys. Acta* 300 (1973) 159-182.
- [33] E.M. Bruckheimer, A.J. Schroit, Membrane phospholipid asymmetry: host response to the externalization of phosphatidylserine, *J. Leukoc. Biol.* 59 (1996) 784-788.
- [34] V. Fadok, D. Bratton, D. Rose, A. Pearson, R. Ezekewitz, P. Henson, A receptor for phosphatidylserine-specific clearance of apoptotic cells, *Nature (London)* 405 (2000) 85-90.
- [35] N.M. Okely, M.H. Gelb, A designed probe for acidic phospholipids reveals the unique enriched anionic character of the cytosolic face of the mammalian plasma membrane, *J. Biol. Chem.* 279 (2004) 21833-21840.
- [36] F.F. Rossetti, M. Textor, I. Reviakine, Asymmetric distribution of phosphatidyl serine in supported phospholipid bilayers on titanium dioxide, *Langmuir* 22 (2006) 3467-3473.
- [37] J.J. López Cascales, A study by molecular dynamics simulation of the effect of the ionic strength on the properties of a model DPPC/DPPS asymmetric membrane, *J. Argent. Chem. Soc.* 94 (2006) 157-168.
- [38] A.A. Gurtovenko, I. Vattulainen, Lipid transmembrane asymmetry and intrinsic membrane potential: Two sides of the same coin, *J. Am. Chem. Soc.* 129 (2007) 5358-5359.
- [39] A.A. Gurtovenko, I. Vattulainen, Membrane potential and electrostatics of phospholipid bilayers with asymmetric transmembrane distribution of anionic lipids, *J. Phys. Chem. B* 112 (2008) 4629-4634.
- [40] T. Gulik-Krzywicki, E. Shechter, V. Luzzati, M. Faure, Interactions of proteins and lipids: Structure and polymorphism of protein-lipid-water phases, *Nature (London)* 223 (1969) 1116-1121.
- [41] H.K. Kimelberg, D. Papahadjopoulos, Phospholipid-protein interactions: Membrane permeability correlated with monolayer "penetration", *Biochim. Biophys. Acta* 233 (1971) 805-809.
- [42] A. Arbuzova, G. Schwarz, Pore-forming action of mastoparan peptides on liposomes: A quantitative analysis, *Biochim. Biophys. Acta* 1420 (1999) 139-152.
- [43] L. Massi, F. Guittard, R. Levy, Y. Duccini, S. Gèribaldi, Preparation and antimicrobial behaviour of gemini fluorosurfactants, *Eur. J. Med. Chem.* 38 (2003) 519-523.
- [44] M.C. Murguía, L.M. Machuca, M.C. Lurá, M.I. Cabrera, R.J. Grau, Synthesis and properties of novel antifungal gemini compounds derived from *N*-acetyl diethanolamines, *J. Surfact. Deterg.* 11 (2008) 223-230.
- [45] M.C. Murguía, V.A. Vaillard, V.G. Sánchez, J. di Conza, R.J. Grau, Synthesis, surface-active properties, and antimicrobial activities of new double-chain gemini surfactants, *J. Oleo Sci.* 57 (2008) 301-308.
- [46] G. Beschiaschvili, J. Seelig, Melittin binding to mixed phosphatidylglycerol/phosphatidylcholine membranes, *Biochemistry* 29 (1990) 52-58.
- [47] S.T. Swanson, D. Roise, Binding of a mitochondrial presequence to natural and artificial membranes: Role of surface potential, *Biochemistry* 31 (1992) 5746-5751.
- [48] G. Schwarz, U. Blochmann, Association of the wasp venom peptide mastoparan with electrically neutral lipid vesicles: Salt effects on partitioning and conformational state, *FEBS Lett.* 318 (1993) 172-176.
- [49] J. Seelig, S. Nebel, P. Ganz, C. Bruns, Electrostatic and nonpolar peptide-membrane interactions, Lipid binding and functional properties of somatostatin analogues of charge $z = +1$ to $z = +3$, *Biochemistry* 32 (1993) 9714-9721.
- [50] J. Pérez-Gil, K.M.W. Keough, Interfacial properties of surfactant proteins, *Biochim. Biophys. Acta* 1408 (1998) 203-217.
- [51] J. Pérez-Gil, Lipid-protein interactions of hydrophobic proteins SP-B and SP-C in lung surfactant assembly and dynamics, *Pediatr. Pathol. Mol. Med.* 20 (2001) 445-469.
- [52] A.G. Serrano, J. Pérez-Gil, Protein-lipid interactions and surface activity in the pulmonary surfactant system, *Chem. Phys. Lipids* 141 (2006) 105-118.
- [53] F. Torrens, G. Castellano, Periodic classification of local anaesthetics (procaine analogues), *Int. J. Mol. Sci.* 7 (2006) 12-34.
- [54] G. Castellano, F. Torrens, Local anaesthetics classified using chemical structural indicators, *Nereis* 2 (2009) 7-17.
- [55] F. Torrens, G. Castellano, Table of periodic properties of human immunodeficiency virus inhibitors, *Int. J. Comput. Intelligence Bioinf. Syst. Biol.* 1 (2010) 246-273.
- [56] Integrated Mathematical Statistical Library (IMSL), IMSL, Houston, 1989.
- [57] R.D.M. Page, TreeView: An application to display phylogenetic trees on personal computers, *Comput. Appl. Biosci.* 12 (1996) 357-358.
- [58] D.H. Huson, SplitsTree: Analyzing and visualizing evolutionary data, *Bioinformatics* 14 (1998) 68-73.
- [59] O.L. Sánchez-Muñoz, E.G. Nordström, E. Prèrez-Hernández, Electrophoretic and thermodynamic properties for biomaterial particles with Bovine Serum Albumin adsorption, *Biomed. Mater. Eng.* 13 (2003) 147-158.
- [60] A.B. Rawitch, G. Weber, The reversible association of lysozyme and thyroglobulin, *J. Biol. Chem.* 247 (1972) 680-685.
- [61] M. Matsukata, M. Nishino, J.P. Gong, Y. Osada, Y. Sakurai, T. Okano, Adsorption of bovine serum albumin to yeast protoplast, *Colloids Surf. B* 13 (1999) 203-211.

Photosynthetic Excitation Pressure Causes Violaxanthin De-epoxidation in Aging Cabbage (*Brassica Oleracea* L.) Leaves

Amarendra Narayan Misra¹, Dariusz Latowski² and Kazimierz Strzałka²

1. Department of Biosciences and Biotechnology, School of Biotechnology, Fakir Mohan University, Balasore 756019, India

2. Faculty of Biochemistry, Biophysics and Biotechnology, Jagiellonian University, Krakow 30-387, Poland

Received: June 09, 2010 / Accepted: September 02, 2010 / Published: March 30, 2011.

Abstract: The purpose of the present studies was analysis of the age induced changes in photochemical efficiency and xanthophylls cycle pigments of the primary cabbage (*Brassica oleracea* L. cv. Capitata f. alba) leaves. Photochemical efficiency of photosystem II (PS II) was studied by a pulse amplitude modulated chlorophyll fluorescence apparatus, chlorophyll concentration was analysis spectrophotometrically and xanthophyll cycle pigments were estimated by high-pressure liquid chromatography (HPLC). Leaf senescence was accompanied with a decrease both in chlorophylls concentration, the photochemical efficiency and rate constant for PS II photochemistry whereas non-photochemical parameters increased. Excitation pressure (1-qP) which is a measure of relative lumen acidification increased by 1.2× in aging leaves. The maximum quantum yield of PS II showed no significant change. The level of de-epoxidised xanthophylls increased but the concentration of mono- and di-epoxy xanthophylls decreased in aging leaves. A linear relationship between the excitation pressure and the de-epoxidation state of the xanthophyll cycle pigments and lutein, during the onset of senescence suggests that excitation pressure can be used as a sensor for monitoring the onset of senescence as well for the de-epoxidation state of the xanthophylls responsible for non-photochemical quenching in stressed leaves.

Key words: Cabbage (*Brassica oleracea* L.), violaxanthin cycle, excitation pressure, senescence, photosynthetic parameters.

Abbreviations: Ax, antheraxanthin; Car, carotenes; Chl *a* and *b*, chlorophyll *a* and chlorophyll *b*; DES, de-epoxidation state of violaxanthin; F_m, maximal fluorescence level in the dark; F_m' , maximal fluorescence in the light; F_o, minimal fluorescence level in the dark; F_o' , minimal fluorescence in the light; F_s, actual fluorescence level; F_v, variable fluorescence level in the dark; F_v/F_m, photochemical efficiency of PS II under dark adapted state; F_v'/F_m' , quantum yield of PSII electron transport.

Q_A, primary quinone acceptor in PSII; L, lutein; Lx, Lutein-5, 6-epoxide; NPQ, non-photochemical quenching; PAR, photosynthetic active radiation; q_N, rate constant for non-photochemical quenching; q_P, rate constant for photochemical quenching; Vx, violaxanthin; VDE, violaxanthin de-epoxidase; Zx, zeaxanthin.

Leaf aging and senescence are used interchangeably in this study.

1. Introduction

Leaves develop from leaf primordia, undergo phases of several patterns formation during development to maturity, and after a productive photosynthetic period, leaf cells enter the phase of senescence otherwise

known as aging [1-3]. Leaf senescence is the most remarkable developmental event in plant life. There is an ordered metabolic shift from anabolism to catabolism, and sequential degradation of cellular structures [1-3]. Leaf senescence in higher plants is a type of apoptosis [1-3].

One of the important questions is how the senescence process is regulated in an orderly manner in leaves [1-3]. The useful and convenient senescence

Corresponding author: Kazimierz Strzałka, Ph.D., Prof., research fields: plant biochemistry, biochemistry and biophysics of photosynthesis. E-mail: kazimierzstrzalka@gmail.com.

markers so far used widely are the changes in photosynthetic efficiency starting from primary photochemistry to carbon fixation [4]. Leaf yellowing or the loss of chlorophyll (Chl) is an external manifestation of leaf senescence [5-8]. This leads to an array of biochemical, biophysical and molecular changes in the chloroplasts resulting in the disassembly of the photosynthetic apparatus and concomitant decrease in the photosynthetic performance [4, 5]. The loss of PS II activity during leaf senescence is extensively studied leading to characterization of the site of damage in the electron transfer chain from water to the electron acceptors of PS II [4-8].

Senescing leaves efficiently adjust composition of their photosynthetic components to prevailing light environment [9]. They act as shade leaves, which have lower Rubisco content relative to their Chl level than the sun leaves [9]. The unshaded leaves showed a slower decrease in Chl and F_v/F_m than in the carboxylation activity [10]. These indicate that the stromal activity decreased faster than the thylakoid activity including light harvesting. Under conditions of lower activity of Calvin-Benson cycle, plants tend to absorb light beyond their competence for photosynthesis, and the electron transport components between PS I and PS II are reduced. This state of the thylakoid membrane is known as excitation pressure, which determines the redox state of plastoquinone pool [11]. The redox states of the electron transport components in thylakoid membranes affect several processes in plants including photosynthetic gene expression [12]. Chloroplasts developing under high excitation pressure are sun-type [13]. Therefore, it is likely that PSII excitation pressure during the leaf development affects photosynthetic activity of the leaf. However, it has not been investigated whether PS II excitation pressure also works as a sensor of changes in light environment during leaf aging/senescence.

When light is excessive, in all vascular plants and some species of algae, two de-epoxidised pigments are formed. One of them is completely epoxide free,

zeaxanthin (Zx) and another, monoepoxide antheraxanthin (Ax). These pigments are formed by de-epoxidation of violaxanthin (Vx) and they all are involved in a photoprotective process whereby excess absorbed excitation energy is dissipated thermally in the light-harvesting antennae of PSII. This process is called xanthophyll or violaxanthin cycle [14-17]. Vx is converted to Zx via Ax in a reaction catalyzed by the enzyme violaxanthin de-epoxidase (VDE) when the luminal pH decreases as a consequence of the light reactions, producing a higher proton gradient than can be utilized in CO₂ fixation [18, 19]. Such changes in the xanthophyll pool were also reported in some types of stress and stress tolerance mechanisms of plants [20, 21]. The retention of Zx plus Ax in photoinhibited leaves often correlates closely with sustained low PSII efficiencies measured as the F_v/F_m [22]. Such correlations have led to the suggestion that Zx plus Ax may be engaged for thermal energy dissipation under these conditions and may therefore be involved in the reduced PSII efficiencies observed.

Identification and characterization of the processes that regulate leaf senescence is crucial for the understanding of the underlying phenomena of leaf senescence and plant life cycle. Deciphering the mechanism of leaf senescence could facilitate the biotechnological applications to enhance plant productivity, post-harvest technology and stress adaptation [1, 3].

In the present study the authors followed the ontogenic changes of cabbage (*Brassica oleracea* L.) leaves, and the excitation pressure and the violaxanthin cycle pigments as sensors for leaf aging were investigated.

2. Experiment

Cabbage (*Brassica oleracea* L. cv. Capitata f. alba) seedlings were grown in hydroponic cultures, supplied with Hoagland nutrient solution under white light intensity of (PAR) 125 $\mu\text{mol photons} \cdot (\text{m}^{-2} \cdot \text{s}^{-1})$, 10 h light period, 60-70% RH and temperature of 24 ± 2 °C

as described by Misra et al. [21]. Age induced changes in photochemical efficiency and pigments of the first (primary leaf) were monitored from 7 day to 16 day at 3 day intervals.

Photochemical efficiency of photosystem II (PS II) was studied by a pulse amplitude modulated chlorophyll fluorescence apparatus (PAM 101 with data acquisition software DQ, Walz, Germany) as described by Schreiber et al. [23]. The initial level of chlorophyll fluorescence (F_o) was measured with a dim red light modulated at 600 Hz. Saturating light intensity for F_m and F_m' was 4,500 $\mu\text{mol photons (m}^{-2}\cdot\text{s}^{-1})$, and was 800 msec in duration, which was sufficient to achieve a stable maximum fluorescence yield. The maximal or optimal quantum yield of PS II photochemistry was calculated as $F_v/F_m = (F_m - F_o)/F_m$. The actual or effective quantum yield of PS II photochemistry (Φ_{II}) was measured in leaves illuminated with white light produced by a Schott light source (KL 1500) as $(F_m' - F_s)/F_m'$, where F_s is the steady state fluorescence level and F_m' is the maximal fluorescence level in the light. The non-photochemical quenching of chlorophyll fluorescence (NPQ) was calculated as $[(F_m/F_m') - 1]$ according to Bilger and Björkman [24]. To determine the rate constant of photoinactivation of PSII in the photochemical (qP) and non-photochemical (qN) quenching following calculation according to Genty et al. [25] was done: $qP = (F_m' - F_s)/(F_m' - F_o) = \text{redox state of PS II with higher values indicating greater proportion of open or oxidised reaction center and } qN = (1 - F_v'/F_v) = qN = (F_v - F_v')/F_v$ nonphotochemical quenching $NPQ = (F_m' - F_m)/(F_m)$ were also analysed.

Total chlorophyll content was estimated spectrophotometrically in 80% aqueous acetone extract as described by Arnon [26] (1949). Xanthophyll cycle pigments were estimated by high-pressure liquid chromatography (HPLC, Jasco, Japan) method as described by Latowski et al. [27]. The de-epoxidation state was calculated from the equation $[\% (Z_x + 0.5A_x) / (V_x + A_x + Z_x)]$. Xanthophyll pigments were

extracted from leaf samples, treated frozen in liquid nitrogen by solvent A containing: acetonitrile:methanol:water (36:4:1) using mortar and pestle, centrifuged for 10 min at $10,000 \times g$ in Microfuge Type 320. Supernatant was loaded to column (with 20 microliter loop volume, column: Nucleosil Gel 250 \times 4 m, 5 micrometer, TEKNOCROMA, Barcelona, Spain) and separated in solvent A with flow rate 0.7 mL/min, and after retention time of Z_x solvent was changed to methanol: ethyl acetate (340: 160) and rate of flow was 2 mL/min. The pigments detection was at 440 nm (Detecting light source: UV-970 Jasco, Tokyo, Japan). Peak area measurements were performed using a program Borwin Chromatography Software, Version 1.20, JMBS Developments, Le Fontanil, France. The maximum level of de-epoxidation state was measured for 1 h under saturating light ($2,000 \mu\text{mol}\cdot(\text{m}^{-2}\cdot\text{s}^{-1})$) condition [28-31].

3. Results

The cabbage leaves showed a gradual decrease in the Chl content from 7th day until 16th days of seedling growth (Fig. 1). Decrease in Chl content was already previously used as a base of the external manifestation of leaf aging [4, 6, 32]. Therefore the period from 7th day through 16 days of seedling growth was considered as leaf aging time and the changes in photosynthetic parameters and violaxanthin cycle pigments of these leaves were studied during that time.

The photosynthetic parameters under the dark adapted and light adapted state of aging cabbage leaves were analyzed by PAM Chl fluorescence measurements. During leaf aging the maximal fluorescence (F_m) decreased by 8% and minimal fluorescence (F_o) increased by 7% (Fig. 2).

This resulted in a decrease in the maximum quantum yield of PS II or the photochemical efficiency of PS II under dark adapted state, $F_v/F_m = [(F_m - F_o)/F_m]$ (Fig. 3A). The actual fluorescence quenching under light adapted state (qP and Φ_{II}) also showed a sharp decrease in the

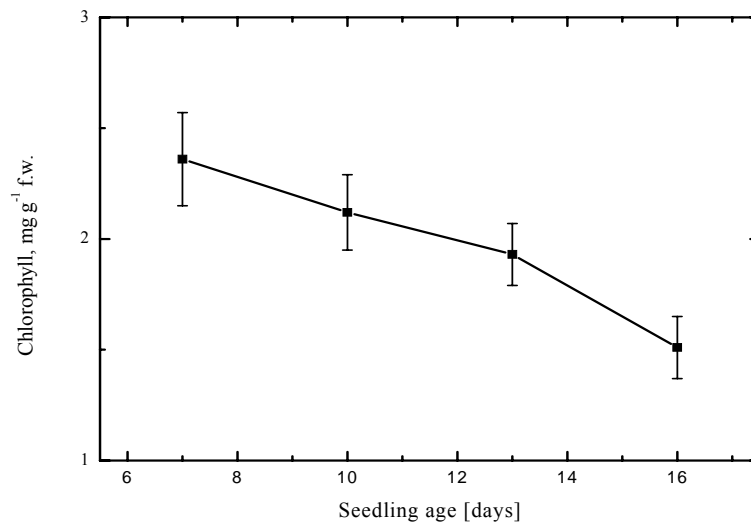


Fig. 1 Age induced changes in the total Chl content of cabbage (*Brassica oleracia* L.) leaves.

Each data point is an average (mean \pm SD, n = 3) of 3 separate experiments with 5 leaves each. The bars represent standard deviation of the mean. The same with Figs. 2 and 3.

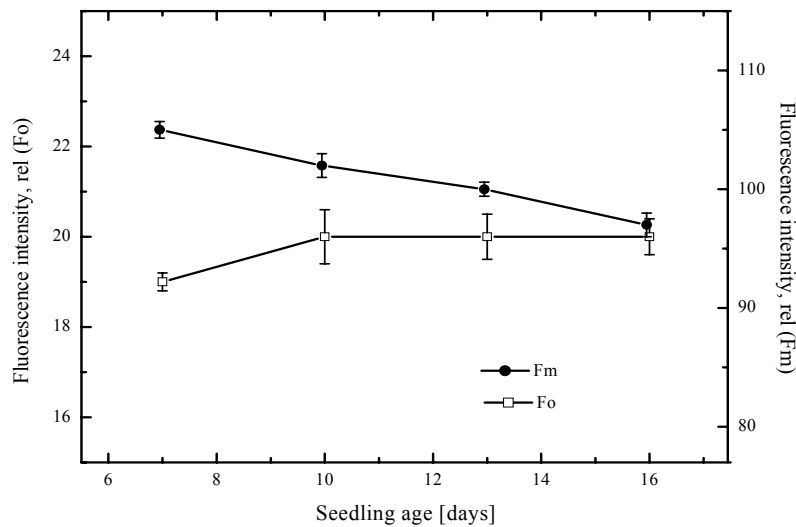


Fig. 2 Age induced changes in the fluorescence intensity Fo and Fm of cabbage (*Brassica oleracia* L.) leaves.

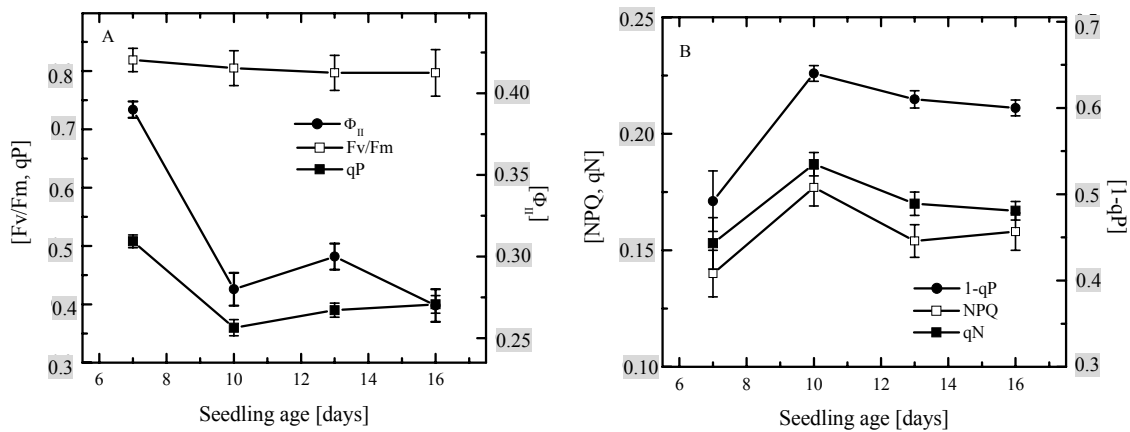


Fig. 3 Age induced changes in the photochemical (A) and non-photochemical (B) quenching parameters of cabbage (*Brassica oleracia* L.) leaves.

initial phase of leaf aging at 10 day (Fig. 3A). The photochemical efficiency of PS II (Φ II) in the light adapted state decreased by 31% and the rate constant for the photochemistry of PS II (qP) decreased by 21% (Fig. 3A). The parameter qP is a reflection of the redox state of Q_A in the light. A decrease in the qP indicates that Q_A becomes more reduced, and therefore the balance between reduction and re-oxidation of Q_A shifts towards reduction. This may either be due to a higher excitation rate of PS II or to a slower outflow of electrons towards the Calvin-Benson cycle. In contrast, the non-photochemical parameters of Chl fluorescence viz. rate constant for non-photochemical quenching (qN) and non-photochemical quenching (NPQ) as well as energy dissipation through non-photochemical means increased in aging leaves (Fig. 3B). On 16 day, the values for qN increased by 9% and that for NPQ increase by 13% of 7 day values (Fig. 3B). The excitation pressure (1-qP) which is a measure of the relative amount of the lumen acidification increased to 1.2x in aging leaves (Fig. 3B).

Analysis of the amount of the violaxanthin cycle pigments also showed a gradual and significant ($P < 0.5$) change during leaf aging (Fig. 4). The amount of Vx and Ax decreased but the amount of Zx increased about 2.5x in the aging leaves (Fig. 4A). The de-epoxidation state of xanthophyll cycle pigments

increased gradually and a 13 day onwards it reached 1.5x that of 7day old seedlings (Fig. 4B).

Lutein is most abundant comprising of 30-60% of total xanthophylls pigments and plays a structural role in LHC [18, 19, 33, 34]. Like violaxanthin cycle pigments, L undergoes epoxidation and de-epoxidation in the thylakoid membranes of cabbage primary leaves and it is also regulated by the redox state of the thylakoid [18, 19, 33, 34]. During leaf aging the level of L (the de-epoxide form) increased gradually and the amount of lutein-5,6-epoxide (Lx) decreased, leading to a gradual increase in the de-epoxidation state of L (Fig. 5).

The de-epoxidation of xanthophyll cycle pigments is regulated by the enzyme de-epoxidase and is well characterized [34, 35]. The epoxidation and de-epoxidation in plants is regulated by lumen acidification [19]. As the excitation pressure of photosynthetic PSII reactions are a measure of the redox state of quinone pool and the lumen acidification [11, 36], the relationship between the de-epoxidation state of violaxanthin cycle pigments [% (Zx + 0.5Ax)/(Vx + Ax + Zx)] and de-epoxidised Lx [%L/(L+Lx)] with that of excitation pressure (1-qP) as depicted in Fig. 6 were analysed. The de-epoxidation of xanthophyll pigments showed a saturation kinetics with excitation pressure (Figs. 6A and 6C), which

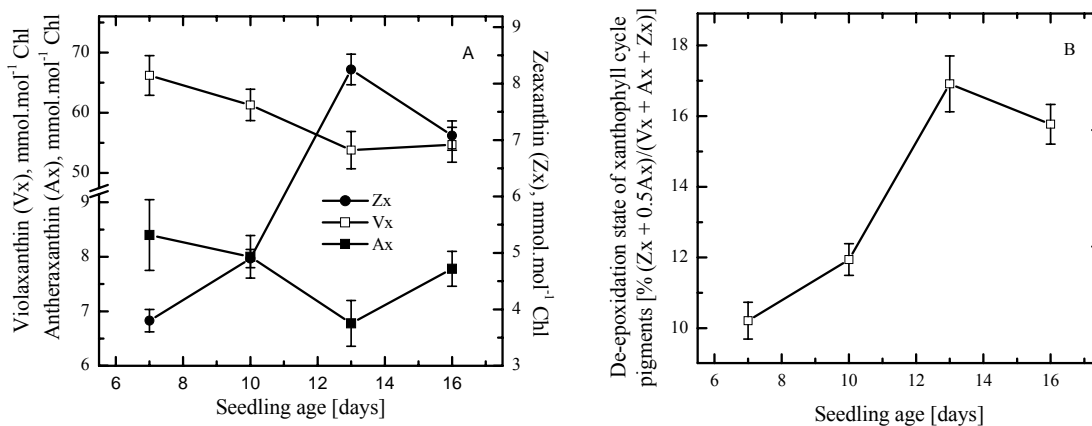


Fig. 4 Age induced changes in the xanthophylls cycle pigments (A) and their de-epoxidation state [% (Zx + 0.5Ax)/(Vx + Ax + Zx)] (B) in cabbage (*Brassica oleracea* L.) leaves with the seedling age.

Each data point is an average of 2 separate experiments. The same with Fig. 5.

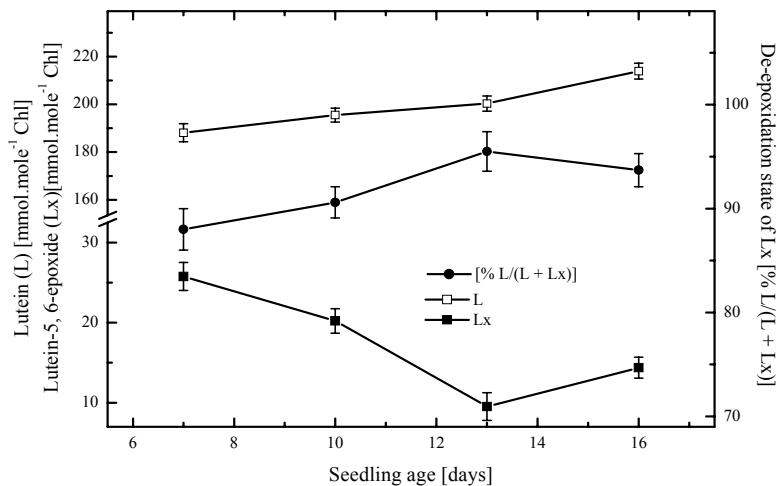


Fig. 5 Age induced changes in the lutein (L) and lutein-5, 6-epoxide (Lx) pigments of cabbage (*Brassica oleracea* L.) leaves. The de-epoxidation state of Lx as percent of total lutein [%L/(L+Lx)] (closed circles) is shown.

suggests that at lower de-epoxidation states, the excitation pressure could become linearly related or regulated proportionately by the regulation of quenching of excess dissipative energy by xanthophylls in aging leaves. However, after a critical concentration of the de-epoxidised xanthophylls can maintain the excitation pressure in aging leaves probably regulating the energy quenching to their maximum limit (Figs. 6A and 6C). The increase in the excitation pressure or the lumen acidification during aging of brassica leaves, de-epoxidation of xanthophyll pigments continued linearly (Figs. 6B and 6D).

This suggests that the de-epoxidase enzyme activity continues progressively during leaf aging in brassica and the substrates either violaxanthin or lutein epoxide cycle pigments do not become limiting during the leaf aging. There was a need to invoke thermal energy dissipation associated with xanthophyll pigments [13] in aging cabbage leaves due to an increase in the redox pressure.

4. Discussion

The changes in photosynthetic parameters and xanthophyll cycle pigments of aging cabbage leaves from 7 day through 16 days of seedling growth were studied. The initial fluorescence F_0 gradually increased and maximal fluorescence F_m gradually decreased

leading to a decrease in photochemical efficiency of PS II under dark adapted state, $F_v/F_m = [(F_m - F_0)/F_m]$ (Figs. 3 and 4). The increase in the F_0 is reported in the heat stressed leaves, in which increase of this parameter is attributed to a combination of processes such as (i) dissociation of light-harvesting complex II (LHC II) from the PSII complex and accumulation of inactive RCs of PS II [37, 38], (ii) reduction of Q_A in the dark [38], (iii) enhanced back electron transfer from Q_B to Q_A [39], and/or (iv) heat induced monomerization of LHC II trimers [40]. This might also be the reason for the increase in F_0 in aging cabbage leaves.

Moreover, a sharp decrease of q_P and Φ_{II} was observed in the initial phase of cabbage leaf aging at 10 day (Fig. 3). The parameter q_P is a reflection of the redox state of Q_A in the light [11, 25] and the decrease of the value of this parameter indicates that Q_A becomes more reduced, and therefore the balance between reduction and re-oxidation of Q_A shifts towards reduction. This may either be due to a higher excitation rate of PS II or to a slower outflow of electrons towards the Calvin-Benson cycle [11]. The non-photochemical quenching of Chl fluorescence, q_N and NPQ, and the excitation pressure measured as $(1-q_P)$ increased significantly in aging leaves (Fig. 3). The aging induced inhibition of PS II photochemical

efficiency with a subsequent decrease in the quantum efficiency of light energy utilisation by PS II and charge separation of primary charge pairs in PS II [4, 6, 7] could lead to the absorption of light beyond their competence for photosynthesis. Excess light absorbed by the light-harvesting chlorophyll-protein complexes, LHCs of PS II, is dissipated as heat through various non-photo chemical processes commonly known as qN or NPQ [11, 35]. A decrease in the photochemical utilisation of absorbed quanta and increase in the dissipation of excess light as heat is reported in the aging leaves [4, 5]. The redox states of the electron transport components and the excitation pressure thylakoid membranes affect several processes in plants including photosynthetic gene expression [12]. Huner et al. [13] reported that chloroplasts developing under high excitation pressure are sun-type. However, it has

not been investigated whether PS II excitation pressure also works as a sensor of changes for structure/function relationship during leaf aging/senescence.

The de-epoxidised xanthophyll cycle pigments Zx and Ax are formed from Vx (epoxide form) when light is excessive, and they are involved in a photoprotective process whereby excess absorbed excitation energy is dissipated thermally in the light-harvesting antennae of PSII [14-16]. The retention of de-epoxidised Zx plus Ax in photoinhibited leaves often correlates closely with sustained low PSII efficiencies measured as the F_v/F_m [22]. Such correlations have led to the suggestion that Zx plus Ax may be engaged for thermal energy dissipation under these conditions and may therefore be involved in the reduced PSII efficiencies observed. Presumably, photo-transformation of Vx and binding of protons to the LHCs act synergistically to

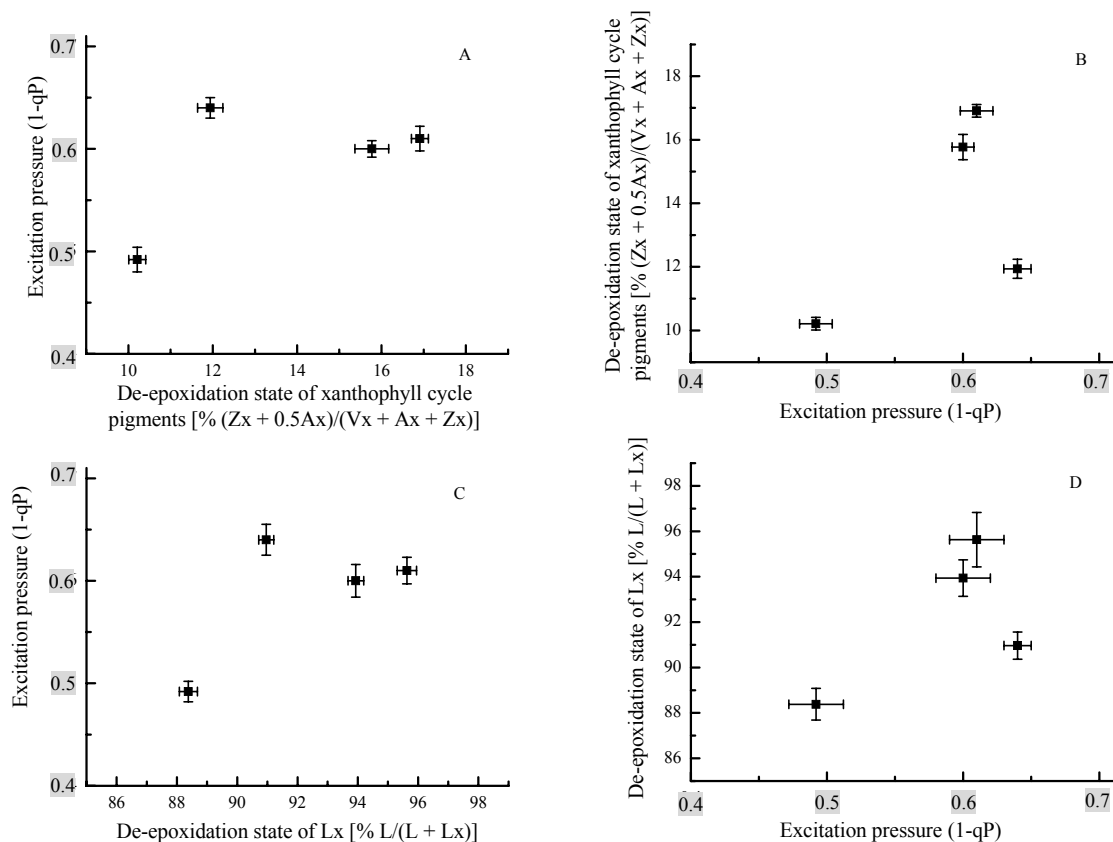


Fig. 6 Analysis of the relationship between de-epoxidation state of xanthophyll cycle pigments (A, B) and de-epoxidation state of lutein-5,6-epoxide (Lx) (C, D) with photosynthetic excitation pressure. The saturation kinetics (A, C) and linear relationship between the excitation pressure and de-epoxidation states (B, D) at the onset of senescence is a clear-cut indication of the sensory mechanism in lumen acidification and xanthophyll pigments de-epoxidation in brassica leaves.

induce a conformational change, that is necessary for thermal energy dissipation. However, *npq* mutants defective in heat dissipation processes in *Arabidopsis* and *Chlamydomonas* suggest that during long-term adaptation of plants to high light, other protective processes can compensate for these defects [28]. In such a case plants adapted to stressful environment, where they dissipate heat under stress, might play both NPQ dependent and NPQ independent processes. Also the xanthophyll cycle pigment dynamics may be altered as per the NPQ related processes.

The increase in the level of de-epoxidised xanthophylls (Zx and L) with an increase in NPQ in aging leaves might signify protective function of these xanthophylls during leaf aging (Figs. 3-6). This corroborates with the findings described for the photoinhibited leaves [33] and leaves from stress sensitive plants [41]. The de-epoxidation of Vx to Zx is mediated by the reductant ascorbate [35, 42] proposed that the size of the Vx fraction available for de-epoxidation is related to the redox state of the PQ pool. The more the reduced PQ pool the greater Vx availability for de-epoxidation. A gradual and significant decrease in Vx in the aging cabbage (*Brassica oleracea* L.) leaves (Fig. 4A) clearly demonstrates the fact that it is sensing the increased reduction of the PQ pool *in vivo* through the increase in the excitation pressure (1-qP) (Fig. 3B). The steady state level of Vx and Zx do not only depends on the availability of Vx for de-epoxidation, but also on the ratio of epoxidation to de-epoxidation at each light intensity. The reverse reactions are catalyzed by an epoxidase [42]. The back reaction rate is decreased with the increased light intensity [42]. A faster decrease in the PS I activity [32] and RUBISCO activity [4] compared to that of PSII activity in aging leaves could also lead to a decrease in the production of NADPH and the increased excitation pressure (Fig. 3B) can facilitate lumen acidification in aging brassica leaves. This could lead to the increase in the de-epoxidation of xanthophylls pigments in aging

leaves. Increase in the xanthophyll cycle pigments was also reported under natural senescence of *Pistacia* leaves [38], white clover [39] and in wheat leaves [43, 44] in the late stage of senescence. But in this study it is shown that de-epoxidation of xanthophyll pigments (Figs. 4 and 6) starts with the onset of leaf aging or senescence as measured by a decrease in Chl content (Fig. 1).

5. Conclusion

It is concluded from this study that (i) PS II excitation pressure also works as a sensor of changes in light environment during leaf aging/senescence; (ii) there is a significant change in the xanthophyll cycle pigments in aging/senescent leaves growing under low light conditions, also. So excitation pressure and/or the xanthophyll cycle pigments can act as sensors for cabbage leaf aging. The linear relationship between the excitation pressure and the de-epoxidation state of the xanthophyll cycle pigments, during the onset of senescence states that excitation pressure can be used as a sensor for monitoring the onset of senescence as well for the de-epoxidation state of the xanthophylls responsible for non-photochemical quenching in stressed leaves.

Acknowledgments

This work was supported by the Polish Ministry of Science and Higher Education (project No. 50/N-DFG/2007/0). The financial support of INSA-PAS collaborative exchange visit program (INSA award No. IA/PAS-2/2001-2002) and UGC-MRP No.36-302/2008(SR) to ANM is gratefully acknowledged.

References

- [1] P.O. Lim, H.R. Woo, H.G. Nam, Leaf senescence, *Annu. Rev. Plant Physiol. Plant Mol. Biol.* 58 (2007) 115-136.
- [2] H. Thomas, H. Ougham, P. Canter, I. Donnison, What stay-green mutants tell us about nitrogen remobilisation in leaf senescence, *J. Exp. Bot.* 53 (2002) 801-808.
- [3] A. Wingler, C. Masclaux-Daubresse, A.M. Fischer, Sugars,

190 **Photosynthetic Excitation Pressure Causes Violaxanthin De-epoxidation in Aging Cabbage (*Brassica Oleracea* L.) Leaves**

- senescence, and ageing in plants and heterotrophic organisms, *J. Exp. Bot.* 60 (2009) 1063-1066.
- [4] F. Dilnawaz, P. Mahapatra, M. Misra, N.K. Ramaswamy, A.N. Misra, The distinctive pattern of photosystem 2 activity, photosynthetic pigment accumulation and ribulose-1,5-bisphosphate carboxylase/oxygenase content of chloroplasts along the axis of primary wheat leaf lamina, *Photosynthetica* 39 (2001) 557-563.
- [5] A.K. Biswal, F. Dilnawaz, K.A.V. David, N.K. Ramaswamy, A.N. Misra, Increase in the intensity of thermoluminescence Q-band during leaf aging is due to a block in the electron transfer from Q_A to Q_B, *Luminescence* 16 (2001) 309-313.
- [6] A.N. Misra, U.C. Biswal, Effect of phytohormone of chlorophyll degradation of chloroplast *in vivo* and *in vitro*, *Protoplasma* 105 (1980) 1-8.
- [7] A.N. Misra, U.C. Biswal, Changes in photosynthetic pigments during aging of attached and detached leaves, and of isolated chloroplasts, *Photosynthetica* 15 (1981) 75-79.
- [8] A.N. Misra, M. Misra, Effect of temperature on senescing rice leaves, I. Photoelectron transport activity of chloroplasts, *Plant Sci.* 46 (1986) 1-4.
- [9] I. Terashima, K. Hirotsuka, Comparative ecophysiology of leaf and canopy photosynthesis, *Plant Cell Environ.* 18 (1995) 1111-1128.
- [10] K. Ono, Y. Nishi, A. Watanabe I. Terashima, Possible mechanism of adaptive leaf senescence, *Plant Biol.* 3 (2001) 234-243.
- [11] C. Miyake, K. Amako, N. Shiraishi, T. Sugimoto, Acclimation of tobacco leaves to high light intensity drives the plastoquinone oxidation system-relationship among the fraction of open PSII centers, non-photochemical quenching of Chl fluorescence and the maximum quantum yield of PSII in the dark, *Plant Cell Physiol.* 50 (2009) 730-743.
- [12] A.N. Misra, A.K. Biswal, Thylakoid membrane protein kinase activity as a signal transduction pathway in chloroplasts, *Photosynthetica* 38 (2001) 323-332.
- [13] N.P.A. Huner, G. Oquist F. Sarhan, Energy balance and acclimation to light and cold, *Trends in Plant Sci.* 3 (1998) 224-230.
- [14] B. Demmig-Adams, W.W.III. Adams, The role of xanthophyll cycle carotenoids in the protection of photosynthesis, *Trends in Plant Science* 1 (1996) 21-26.
- [15] M. Eskling, P.O. Arvidsson, H.E. Akerlund, The xanthophyll cycle, its regulation and components, *Physiol. Plant* 100 (1997) 806-816.
- [16] A.M. Gilmore, Mechanistic aspects of xanthophyll cycle-dependent photoprotection in higher plant chloroplasts and leaves, *Physiol. Plant* 99 (1997) 197-209.
- [17] B. Demmig-Adams, W.W.III. Adams, U. Heber, S. Neimanis, K. Winter, A. Krüger, et al., Inhibition of zeaxanthin formation and of rapid changes in radiationless energy dissipation by dithiothreitol in spinach leaves and chloroplasts, *Plant Physiol.* 92 (1990) 293-301.
- [18] D. Latowski, J. Grzyb, K. Strzałka, The xanthophyll cycle-molecular mechanism and physiological significance, *Acta Physiol. Plant* 26 (2004) 197-212.
- [19] P. Jahns, D. Latowski, K. Strzałka, Mechanism and regulation of the violaxanthin cycle: The role of antenna proteins and membrane lipids, *Biochim. Biophys. Acta* 1787 (2009) 3-14.
- [20] K. Strzałka, A. Kostecka-Gugala, D. Latowski, Carotenoids and environmental stress in plants: Significance of carotenoid-mediated modulation of membrane physical properties, *Russian J. Plant Physiol.* 50 (2003) 168-173.
- [21] A.N. Misra, D. Latowski, K. Strzałka, The xanthophyll cycle activity in kidney bean and cabbage leaves under salinity stress, *Russian J. Plant Physiol.* 53 (2006) 102-109.
- [22] B. Demmig-Adams, D.L. Moeller, B.A. Logan, W.W.III. Adams, Positive correlation between levels of retained zeaxanthin + antheraxanthin and degree of photoinhibition in shade leaves of *Schefflera arboricola* (Hayata), Merrill. *Planta* 205 (1998) 367-374.
- [23] U.U. Schreiber, U. Schliwa W. Bilger, Continuous recording of photochemical and non-photochemical chlorophyll fluorescence quenching with a new type of modulation fluorometer, *Photosynth. Res.* 10 (1986) 51-62.
- [24] W. Bilger, O. Björkman, Role of the xanthophyll cycle in photoprotection elucidated by measurements of light-induced absorbance changes, fluorescence and photosynthesis in leaves of *Hedera canariensis*, *Photosynth. Res.* 25 (1990) 173-185.
- [25] B. Genty, J. Harbinson, J.M. Briantais N.R. Baker, The relationship between non-photochemical quenching of chlorophyll fluorescence and the rate of photosystem 2 photochemistry in leaves, *Photosynth. Res.* 25 (1989) 249-257.
- [26] D.I. Arnon, Copper enzyme in isolated chloroplasts, Polyphenol oxidase in *Beta vulgaris*, *Plant Physiol.* 24 (1949) 1-15.
- [27] D. Latowski, J. Kruk, K. Burda, M. Skrzynecka-Jaskier, A. Kostecka-Gugala, K. Strzałka, Kinetics of violaxanthin de-epoxidation by violaxanthin de-epoxidase, a xanthophyll cycle enzyme, is regulated by membrane fluidity in model lipid bilayers, *Eur. J. Biochem.* 269 (2002) 4656-4665.

- [28] B. Demmig, K. Winter, A. Kruger F.C. Czygan, Photoinhibition and zeaxanthin formation in intact leaves, *Plant Physiol.* 84 (1987) 218-224.
- [29] S.S. Theyer, O. Björkmann, Leaf xanthophylls content and composition in sun and shade determined by HPLC, *Photosynth. Res.* 23 (1990) 331-343.
- [30] A.M. Gilmore, H.Y. Yamamoto, Linear models relating xanthophylls and lumen acidity to non-photochemical fluorescence quenching, Evidence that antheraxanthin explains zeaxanthin independent quenching, *Photosynth. Res.* 35 (1991) 67-78.
- [31] A. Farber, A.J. Young, A.V. Ruban, P. Horton, P. Jahns, Dynamics of xanthophylls cycle activity in different antenna subcomplexes in photosynthetic membranes of higher plants, The relationship between Zeaxanthin conversion and non-photochemical fluorescence quenching, *Plant Physiol.* 115 (1997) 1609-1618.
- [32] A.N. Misra, U.C. Biswal, Differential changes in electron transport properties of chloroplasts during aging of attached and detached leaves, and of isolated chloroplasts, *Plant Cell Environ.* 5 (1982) 27-30.
- [33] W. Kühlbrandt, D.N. Wang, Y. Fujiyoshi, Atomic model of plant light-harvesting complex by electron crystallography, *Nature* 367 (1994) 614-621.
- [34] B.J. Pogson, K.K. Niyogi, O. Bjorkman, D. Penna, Altered xanthophylls compositions adversely affect chlorophyll accumulation and non-photochemical quenching in *Arabidopsis* mutants, *Proc. Nat. Acad. Sci. USA* 95 (1998) 13324-13329.
- [35] C. Neubauer, H.E. Yamamoto, Membrane barriers and mehlner peroxidase reaction limit the ascorbate availability for violaxanthin de-epoxidase activity in intact chloroplasts, *Photosynth. Res.* 39 (1994) 137-147.
- [36] P. Muller, X.P. Li, K.K. Niyogi, Non-photochemical quenching, a response to excess light energy, *Plant Physiol.* 125 (2001) 1558-1566.
- [37] Y. Yamane, Y. Kashino, H. Koike, K. Satoh, Increases in the fluorescence F_o level and reversible inhibition of Photosystem 2 reaction center by high-temperature treatments in higher plants, *Photosynth. Res.* 52 (1997) 57-64.
- [38] Y. Yamane, T. Shikanai, Y. Kashino, H. Koike, K. Satoh, Reduction of Q_A in the dark: Another cause of fluorescence F_o increases by high temperatures in higher plants, *Photosynth. Res.* 63 (2000) 23-34.
- [39] R. Kouřil, D. Lazár, P. Ilić, J. Skotnica, P. Krchňák, J. Nauš, High-temperature induced chlorophyll fluorescence rise in plants at 40-50 °C: Experimental and theoretical approach, *Photosynth. Res.* 81 (2004) 49-66.
- [40] G. Garab, Z. Cseh, L. Kovács, S. Rajagopal, Z. Várkonyi, M. Wentworth, et al., Light-induced trimer to monomer transition in the main light-harvesting antenna complex of plants: Thermo-optic mechanism, *Biochemistry* 41 (2002) 15121-15129.
- [41] M. Spundova, K. Strzałka, J. Naus, Xanthophyll cycle activity in detached barley leaves senescing under dark and light, *Photosynthetica* 43 (2005) 117-124.
- [42] D. Siefertman, H.E. Yamamoto, Properties of NADPH and oxygen dependent zeaxanthin epoxidation of isolated chloroplasts, *Arch. Biochem. Biophys.* 171 (1962) 70-77.
- [43] C.M. Lu, Q.T. Lu, J.H. Zhang, T.Y. Kuang, Characterization of photosynthetic pigment composition, photosystem II photochemistry and thermal energy dissipation during leaf senescence of wheat plants in the field, *J. Exp. Bot.* 52 (2001) 1805-1810.
- [44] C.M. Lu, Q.T. Lu, J.H. Zhang, T.Y. Kuang, Xanthophyll cycle, light energy dissipation and photosystem II down-regulation in senescent leaves of wheat plants grown in the field, *Aust. J. Plant Physiol.* 28 (2001) 1023-1030.

Gene Expression Profiles in Porcine Tissues of Liver and Kidney

Tatiana Glazko¹, Nataliya Khlopova¹, Scott Fahrenkrug², John Garbe² and Valeriy Glazko¹

1. Department of Animal Science, Russian State Agrarian University-MTAA, Moscow 127550, Russia

2. Department of Animal Science, University of Minnesota, St. Paul, MN 55108, USA

Received: April 12, 2010 / Accepted: June 21, 2010 / Published: March 30, 2011.

Abstract: Microarray technologies are widely used all over the world for the gene expression analysis in various tissues, but still this technology has some limitations. The problem of eliminated reproducibility of the results, obtained in different laboratories using different platforms, is very relevant nowadays. For revelation of problems of microarrays, the comparative analysis of hepatic and renal gene expression profiles (GEP) was carried out by using swine protein annotated oligonucleotide microarrays (SPAM). Revealed differences in GEP between kidney and liver of pigs were correlated with functional and histological distinctions of these organs. It was shown that sources of errors in the comparative analysis of organ-specific GEP could be connected to the cross hybridization of one probe to transcripts (cDNA of mRNA) of different genes and to individual variability in gene expression between animals, related with the changeability of influences of exo- and endogenous regulation factors.

Key words: Oligonucleotide microarrays, gene expression, cross hybridization, individual variability.

Abbreviations: GEP: gene expression profiles, SPAM: swine protein annotated oligonucleotide microarray, FGB: fibrinogen beta chain precursor, FGG: fibrinogen gamma chain precursor, VTN: vitronectin precursor, F2: prothrombin precursor, PLG: plasminogen precursor, ApoC3, Apo-E, ApoA-I: apolipoprotein precursors, AGP2: alpha-1-acid glycoprotein 2 precursor, PRBP: Plasma retinol-binding protein precursor, FHR2: complement factor H-related protein 2 precursor, TMEM8: Transmembrane protein 8 precursor, PAI2: Plasminogen activator inhibitor 2 precursor, ST7: suppression of tumorigenicity 7 isoform b, AGAP1: Centaurin-gamma 2, NAGA: Alpha-N-acetylgalactosaminidase precursor, CLU: Clusterin precursor, TNFRSF19: Tumor necrosis factor receptor superfamily member 19 precursor, NMDA: Glutamate [NMDA] receptor subunit epsilon 2 precursor, KLHL1: Kelch-like protein 1, hERV1, ALR: Augmenter of liver regeneration, HAPLN2: Hyaluronan and proteoglycan link protein 2 precursor, AHSG: Alpha-2-HS-glycoprotein precursor, TrpRS: Tryptophanyl-tRNA synthetase.

1. Introduction

Gene expression profile (GEP) is a genetic-biochemical basis of physiological function of each organ of mammals; it allows identifying the differentially expressed (DE) genes involved in specific biological processes such as disease or response to environmental stimulus. The possibility to reveal genetic-biochemical bases of various diseases and, accordingly, to develop methods of their

correction, is really relevant with necessity to collect the data about physiological “norm” of such profiles in different organs. Such data can be used for consideration of interrelations between changes in expression of “critical” genes and phenotypic variability of various morpho-physiological characteristics of animals.

Thereupon, the comparative analysis of GEP across two pig organs: liver, and kidney were carried out and analyzed in the present research. Liver and kidney have the common traits in early stages of histogenesis and belong to the central organs of detoxification, maintenance of a blood biochemical homeostasis. For

Corresponding author: Tatiana T. Glazko, Ph.D., Prof., research fields: genomics, cell biology. E-mail: vglazko@yahoo.com.

today there are a considerable quantity of works on gene expression profiling in different tissues and organs. However, till now there is an actual question of incomplete reproducibility of gene expression profiles results received in different laboratories [1, 2]. Nonrepeatability in composition of the gene expression profiles may have various reasons connected with the human error [3], cross hybridization of microarray probes with cDNA, mRNA of different genes [4-6], influences of some external are organs regulatory factors. Discrepancies in gene expression profiles can be caused by individual features of animals (a condition of nervous and hormonal systems, enzyme activity and etc.) [7]. Usually the analysis of GEP excludes the genes with individual differences in expression between the investigated animals or making this differences averaged by pooling the samples [8, 9]. In order to find out the possible reasons of such variability we carried out the analysis of the interrelationships between genes, which expression showed the essential differences in transcription level in liver and kidney among six Landrace pigs.

2. Materials and Methods

Tissues of liver and kidney, heart and thymus were collected from six Landrace gilts at the age of six months. RNA was extracted, cDNA synthesized and aliquots of dye-labeled cDNA samples were used for all hybridizations at the University of Minnesota (UMN) under the supervision of professor S. Fahrenkrug. The analysis of hybridization intensity of dye-labeled cDNA was carried out on Swine Protein Annotated Oligonucleotide Microarray comprising of 19980 70-mer oligonucleotide probes targeting 15204 unique genes, about 76% of the genes in ENSEMBL annotation of the pig genome. The cDNA and fluorescence dye hybridization steps were accomplished by a modification to the 3DNA array 350 kit protocol (Genisphere Inc., Hatfield, PA). The hybridized microarrays were scanned on GSI Lumonics ScanArray 5000 laser scanner (GSI

Lumonics, Watertown, MA) and converted into TIFF images using ScanArray Express software. The image data were extracted using BlueFuse for microarrays (BlueGnome, Cambridge, UK) and statistical data processing was carried out with "Statistica" Software.

The method is based on competitive hybridization of nucleotide sequences, preliminary labeled with fluorescent dyes cy3 and cy5 with microarray probes, creating thereby the certain relation of cy3-cDNA to cy5-cDNA in each array spot. Later the numeric data, characterized by standard units of fluorescence for each spot was obtained by the relation definition $cy3/cy5$, carried out by microarray scanning.

All the distinctions in the signals of hybridization intensity in present research were estimated separately for each microarray.

3. Results and Discussion

According to the above state, liver expression profiles were compared with kidney expression profiles. At the total analysis of 600 liver genes, with the maximum distinctions in intensity of hybridization between liver cDNA and kidney cDNA, 12 genes were found out with more than one probe in microarray. The obtained data allowed comparing hybridization intensity of various sites of the same gene with microarray probes separately for each animal. Two basic groups of genes were allocated by results of digitized signal strength estimations of these 12 genes. The first group of genes had the least distinctions between signal strength of hybridization of various sites cDNA of same mRNA with microarray probes (up to 4500 standard units of a luminescence), and the second group of genes had the greatest distinctions (more than 10000 standard units of a luminescence).

The first group of genes with the least differences in hybridization signal of various sites of the same gene included following genes: Apolipoprotein A-II precursor, C4b-binding protein alpha chain precursor (C4bp), dermokine isoform beta, Glutathione S-transferase A5-5, Glutathione S-transferase Mu 2,

multiple substrate lipid kinase; the second group with the greatest differences between signals of hybridization of various sites of the same gene was presented by two genes – Alpha-1-antichymotrypsin precursor (ACT), Fibrinogen alpha chain precursor. Observable differences were reproduced in independent experiments for all investigated animals.

Among GEP in kidney for 600 genes, with the maximum distinction in intensity of hybridization between kidney cDNA and liver cDNA 9 genes were allocated with more than one probe to different sites of the same gene on the microarray. These 9 genes were subdivided into 3 groups depending on difference in hybridization intensity between probes corresponding to one gene. Groups with differences in hybridization signal between gene sites up to 4500, 4500-10000 and above 10000. The first group (with differences up to 4500 standard units of a luminescence) included CDNA FLJ12547 fis, clone NT2RM4000634 and Translationally-controlled tumor protein (TCTP) (p23). The group of genes, which internal sites of hybridization differed more than on 10000 standard units of a luminescence, consisted of the genes coding ATP synthase a chain, Chromogranin A precursor (CgA), Pituitary secretory protein I (SP-I) and Ubiquitin.

It was possible to expect that one of the reasons in differences in intensity of hybridization of different cDNA sites of same transcript were caused by the fact that nucleotide sequence of microarray probe was simultaneously complementary to cDNAs of different mRNAs (Fig. 1) [4]. It was obvious that possibility of such “cross” hybridization of microarray probes with homologous transcript sequences of different genes was necessary for considering at the statistical analysis of GEP as it could be a source of essential errors at revealing of “critical” genes in organ-specific transcriptome.

To check up this assumption, the search of homology sites to nucleotide sequences of microarray probes reproducing distinctions in signals of hybridization

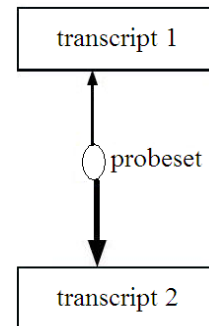


Fig. 1 The TPT (transcript-probe-transcript) motif of multiple targeting.

intensity with different sites of the same gene was executed by means of program BLASTn in a sus scrofa EST databank presented in NCBI (Table 1).

Alpha-1-antichymotrypsin precursor (ACT) (SERPINA3-2) – is a member of a huge family. ACT is a retarding agent of serine proteinase, which has received the name - SERine Proteinase INhibitors (Serpins). This family includes the genes coding classical retarding agents of serine proteinases, such as an alpha-1-antitripsin and an alpha-1-antihemotripsin, protein C depressor, kallistatins and non-abscopal serpins, such as globulins, connecting corticosteroids and thyroxin. Many serpins, in particular, antitrypsin and antihemotripsin, participate in the metabolic cascades connected with blood coagulation. Non-abscopal serpins participate in transport of hormones, and also carry out function of chaperones. The length of gene SERPINA3-2 includes approximately 9.0 thousand bp, consists of five exons and four introns. The coding sequence of SERPINA3-2 cDNA has 86% of identity with the SERPINA3-1. Gene SERPINA3-2 is charted on distal end of a short shoulder of a pigs chromosome # 7 (7q), in a serpins gene cluster, including gene PI1 (SERPINA1), PI2, PI3, PI4 (gene paralog SERPINA3), PO1A and PO1B [10].

The search of a homology sites in a Sus scrofa EST database (refseq_rna) for 70 nucleotides, which were used as microarray probes for the analysis of GEP, allowed obtaining the following data. The most expressed differences in hybridization signal have been found out for three probes identifying cDNA of gene

Table 1 Homology sites to nucleotide sequences of microarray probes reproducing distinctions in signals of hybridization intensity with different sites of the same gene.

Gene	Probe	Homology sites of the microarray probes to cDNAs of different genes
Alpha-1-antichymotrypsin precursor (SERPINA3-2)	1st probe	SERPINA3-2: 84% (1027 - 1096); SERPINA3-1: 86%; SERPINA3-3: 81% (1045 - 1114); SERPINA3-6: 81% (772 - 841); LOC100153899: 100% (1096 - 1165); LOC100156752: 100% (753 - 822); LOC100156325: 80% (1096 - 1165)
	2nd probe	SERPINA3-2: 89% (1082 - 1150); SERPINA3-6: 89% (809 - 877)
	3rd probe	SERPINA3-2: 100% (1194 - 1263); SERPINA3-2: 89% (1295 - 1328)
Fibrinogen alpha chain precursor A	1st probe	gb:FD606208.1: 100% (535 - 604), 80% (509 - 563)
	2nd probe	100% (209 - 278)
ATP synthase a chain	1st probe	100% (191 - 260) (377 - 446); 100% (124 to 55)
	2nd probe	100% + chain and - chain
	3rd probe	100% + chain
Chromogranin A precursor	1st probe	100% (120 - 189; 300 - 369; 592 - 661), 100% (193 - 124)
	2nd probe	100% (31 - 100; 85 - 154; 120 - 189; 195 - 264)
Ubiquitin	1st probe	100% (149 - 218); (399 - 330)
	2nd probe	100% (177 - 246; 405 - 474; 630 - 699)
	3rd probe	100% (83 - 152)
	4th probe	100% (138 - 207; 367 - 435; 593 - 661)

SERPINA3-2 in total cDNA of a pig's liver. The full homology for the first probe (100%) was found out in two transcripts: LOC100153899 (positions 1096 - 1165) and LOC100156752 (positions 753 - 822), which in a database are presented as cDNA's with similarity to transcripts of a gene SERPINA3-2. The partial homology (with 14 mono- and dinucleotides discrepancies) was observed with cDNA of LOC100156325 from a position 1096 to 1165. cDNA of a gene SERPINA3-2 had inside homology site from a position 1027 to 1096 with 11 mono- and dinucleotides discrepancies (84% of a homology). The partial homology of a microarray probe (13 discrepancies, 81% of a homology) were revealed in cDNA of a gene SERPINA3-3, from a position 1045 to 1114, and also with cDNA of SERPINA3-6 (13 discrepancies, 81% of a homology) from a position 772 to 841. High level of coincidence (89%) was found out for the second probe with cDNA site of LOC100155540 (SERPINA3-6, from a position 809 to 877) and cDNA of a gene SERPINA3-2 (from a position 1082 to 1150). For the third probe almost full homology (with one discrepancy) was observed with a cDNA of a gene SERPINA3-2 (position 1194-1263),

and also partial homology with the site of 35 nucleotides (with four discrepancies) from a position 1295 to 1328.

The obtained data testifies that for the first probe the quantity of a homology sites both inside of the cDNA transcript, and between cDNA of the genes SERPINA3-2, SERPINA3-3, SERPINA3-6 was much more than for the second probe. Only the third probe had homology sites to cDNA of a gene SERPINA3-2. That could lead to the observable differences in hybridization signal of this cDNA with different probes.

The fibrinogen molecule consists of fibrinopeptide A and a set of subunits (alpha, beta, gamma), connected in one molecule through sulphide bonds. Formation of fibrin happens after chipping off a fibrinopeptide A from alpha chain of fibrinogen that induces polymerization of fibrin [11].

For finding out the activity of a fibrinopeptide A transcription in liver the search of homology sequences in two probes of this gene was executed. The following data was obtained. Homologous sequences for the first probe were not revealed in a refseq_ma database (*Sus scrofa*), but some sequences carried to cDNA of fibrinopeptide A mRNA were revealed in EST

database. cDNA of this gene was characterized by one strongly pronounced feature - except 70 nucleotides of full homology to the first probe, cDNA included partially blocking the same sequence in length about 55 nucleotides (with more than 80 % a homology). For example, in cDNA gb:FD606208.1 the full homology was observed from a position 535 to 604; the second site of a partial homology was located between a position 509 and 563, (44 of 55 nucleotides, 80% of a homology). Presence of such internal repetitions in cDNA to the same probe could create complexities during hybridization because of a competition of internal homologous cDNA sites for the same probe. The homologous sequence to the second probe (100% homology) was observed for cDNA of this gene between positions 209 - 278. That is, two probes for the cDNA of a gene fibrinopeptide A differed in localization on mRNA, and also, one probe had a site of additional internal homology (55 nucleotides) that could cause differences in hybridization intensity between probes.

The analysis of homology sites for the three probes corresponding to cDNA of a gene ATP synthase a chain allowed obtaining the following data.

ATP synthase – is a membrane-connected enzyme complex combining synthesis/hydrolysis of ATP with transport of protons through a membrane. There are two parts - complex ATP synthase/hydrolase including five subunits (alpha, beta, gamma, delta, epsilon) and transmembrane component (F0), consisting at least of three subunits (A-C) which are coded with mitochondrion DNA (A-G, F6, F8). Subunit A (or Subunit 6) is a key component of ATPase and defines transmembrane proton transport.

In connection with a key role of ATPases in power supply of endocellular fundamental biochemical processes, they can be considered as the most ancient enzymes. Their occurrence in evolution preceded occurrence of photosynthesis and cytochromes of a respiratory chain. ATPases remains highly conservative enzymes in all live organisms: ATPases

founded in thylakoids of chloroplasts in eucariotic mitochondrial membranes keep high nucleotide and aminoacid similarity with ATPases in a plasmatic membrane of bacteria. Special conservatism was found out in subunits that are most essential for catalytic function of enzyme [12].

Search in EST database had allowed to find out a considerable quantity of sequences, homologous to probe No.1 of ATP synthase a chain - F0 - F6. The full homology to the same cDNA fragment for the probe No.1 were found out both in transcript of a plus chain (position 191-260; 377-446), and in transcript of a minus chain (position 124-55). For probe No.2 sites of a full homology were observed in cDNA of a plus chain, both in direct sequence, and in complimentary variant, and also in a minus chain. For the probe No.3 some sites of a full homology were revealed for cDNA of a plus chain. Thus, probes to cDNA of subunit A of ATP synthase transmembrane site differ by quantity of homologous sequences in cDNA transcripts both in a plus, and in a minus chain of mitochondrial DNA. It is necessary to notice that homology sites to all three probes were found out in a database of clones of sequenced nucleotide sequences of different pig's chromosomes.

The Chromogranin A precursor (CgA) concerns to granins (chromogranin/sekretogranin) superfamily. Its derivatives include vasostatin 1, vasostatin II; EA-92; ES-43; pancreastatin; SS-18; WA-8; WE-14; LF-19; AL-11; GV-19; GR-44; ER-37 [13]. Chromogranin A and its derivatives participate in regulation of calcium and glucose metabolism, condition of cardiovascular systems and in some other functions [14]. Homology sites to the probe No.1 were observed simultaneously in different positions - at the beginning (120 -189; 300 - 369), closer to the end (592 - 661) of a plus chain, and also in cDNA of a minus chain (direct sequence 193 - 124). Blocked sites of homology for the probe No.2 were found out in a plus chain (31-100; 85-154; 120-189; 195-264), and also the partial homology with cDNA of proteins participated in maintenance of

spermatozoon's mobility.

The expressed differences in the signals of hybridization intensity were also found out to the probes of ubiquitin. Ubiquitin family and ubiquitin-similar proteins includes the genes that provide protein proteolysis and are the part of the cascade of the co-operating proteins, that participate in consecutive stages of a cellular cycle regulation. A number of members of this family belong to modifiers of the various proteins which are carrying out a wide spectrum of various functions. Ubiquitination of proteins is usually accompanied by linkage of final ubiquitin domain (C) with lysine of protein-substratum [15, 16].

Search of homology sites to DNA probes in EST database allowed obtaining the following data. Homology sites to the probe No.1 were revealed in cDNA of a minus chain (position 399-330) and in a plus chain (position 149-218); for the probe No.2 - in three sites of a plus chain (positions 177-246; 405-474; 630-699); for the probe No.3 - one site of a homology in a plus chain (83-152); for the probe No.4 - three sites of a homology in a plus chain (138-207; 367-435; 593-661). It is visible that probes differ in quantity of homologous sites in cDNA, and some of them partially block each other.

By results of the executed analysis it is visible that all considered cases of reproduced differences between hybridization intensity of different microarray probes with cDNA of liver and kidney genes were typical for the genes belonging to supergene families. For the all cases the expressed differences between probes were observed to cDNA of the same gene by quantity of homology fragments, on presence of sites of a homology for cDNA of other genes, including paralogs, and also on presence/absence of homologous sequences in cDNA of a plus and a minus mRNA chains. The obtained data is well coordinated with the assumption that "cross" hybridization can be a source of errors at the comparative estimation of expression intensity of various genes, especially essential for the

genes belonging to supergene families.

The total comparative analysis of 19980 probes hybridized with cDNA of 15204 structural pig genes presented on the microarray allowed revealing 20 liver-specific genes, differing on the level of hybridization intensity between liver and kidney cDNA for more than on 10000 standard units of a luminescence, and 40 kidney-specific genes which expression was essentially above in kidney than in liver. More than half of kidney-specific genes (26) were the genes coding transport proteins or signal transducers of plasmatic or mitochondrial membrane, representing the receptor signaling pathways directly participating in ionic exchange between extracellular space and cytoplasm, and also between cytoplasm and internal mitochondrial matrix. Products of the 10 genes were involved in regulation of transcription and the ubiquitin-dependent cascade, 3 genes coded proteins of ribosomes and 1 gene – dynactin complex subunit, directly participating in the control of cytokinesis. In general, the basic differences in profiles of gene expression between kidney and liver had appeared connected with the genes supervising inter- and an intracellular ionic exchange, and also mechanisms of cellular division. It would be coordinated well with dominating participation of kidneys in maintenance of ionic balance in blood of mammals, in comparison with a liver, and also with known differences of mitochondrial morphology in liver and kidneys, the lowered activity of cytokinesis in a liver (polyploidy of hepatocytes). Thus, the revealed differences in profiles of gene expression in kidney and liver corresponded to functional and histological distinguishes between these organs.

The analysis of 600 genes allowed forming two groups of the genes distinguished by hybridization intensity between liver and kidney on microarray probes for more than on 20000 standard units of the luminescence in investigated pigs. The first group included genes with the same contribution in gene expression profiles in different animals ("constitutive"

genes) and the second group joined the genes with varied expression levels in different animals ("variable" genes). A total of 24 genes (FGB, FGG, VTN, F2, PLG, ApoC3, Apo-E, ApoA-I, AGP2, PRBP, FHR2, TMEM8, PAI2, ST7, AGAP1, NAGA, CLU, TNFRSF19, NMDA (Grin2b), KLHL1, hERV1, ALR, HAPLN2, AHSG, TrpRS) with the significant individual variability in expression were revealed. The individual animal variability in gene expression correlated between liver and kidney in 11 (FGG, VTN, F2, PLG, ApoC3, PRBP, CFHR2, NAGA, Grin2b, HAPLN2, AHSG, VTN) of these 24 genes ($r > 0.96$; $P < 0.05$). That allowed to assume the presence of common regulatory factors for both organs for these 11 genes. 24 variable genes were subdivided into groups with inner statistically significant correlations in individual variability of gene expression.

As a rule, genes in individual groups with the interconnected expression belonged to the general metabolic way. Totally 8 groups were allocated - 6 genes

(FGB, FGG, VTN, F2, PAI2, PLG) which products participated in formation of a blood clot [17-20]; 6 genes (ApoC3, Apo-E, ApoA-I, AGP2, PRBP, FHR2) - in transport and a lipid metabolism [20-25]; 5 genes (TMEM8, PAI2, ST7, AGAP1, NAGA) represented markers of blood cells and lysosomes [20, 26-28]; products of 3 genes (CLU, TNFRSF19, PLG) participated in programmed cell death [28-30] and four groups of 2 genes which products participated in Ca^{2+} transport (Grin2b, KLHL1) [31, 32], in intercellular matrix creation (HAPLN2, AHSG) [20], reflected the mitochondrion functional activity (ALR, TrpRS) [33, 34] and the glucocorticoid hormone depended genes (FGB, ALR, VTN) [17, 20, 35] (Table 2).

The obtained data testifies that revealed individual variability of a gene expression between different animals is co-ordinated and basically defined on distinctions between animals in regulation of separate biochemical ways by exogenous and endogenous factors. Besides, individual differences between animals

Table 2 Correlation coefficients between different genes among all animals, $P < 0.05$. Diagonal presents correlation coefficient of this gene between kidney and liver among all animals, $P < 0.05$.

1. Group of the genes which products participate in system of a fibrillation and formation of a blood clot							2. Group of a substrate-dependent genes						
	FGB	FGG	VTN	F2	PAI2	PLG		ApoC3	APOE	ApoA1	AGP2	PRBP	CFHR2
FGB	-	1.00	0.97	0.98	0.96	1.00	ApoC3	1.00	0.99	0.97	-	-	1.00
FGG	1.00	0.97	0.99	0.99	-	0.99	APOE	0.99	-	-	-	0.98	0.99
VTN	0.97	0.99	0.98	0.97	-	0.98	APOA1	0.97	-	-	-	-	-
F2	0.98	0.99	0.97	-	-	1.00	AGP2	-	-	-	-	-	-
PAI2	0.96	-	-	-	-	-	PRBP	-	0.98	-	-	0.97	0.96
PLG	1.00	0.99	0.98	1.00	-	1.00	CFHR2	1.00	0.99	-	-	0.96	1.00
3. Group of genes - markers of blood cells and lysosomes							4. Group of genes, participating in apoptosis and receptors to tumor necrosis factors						
	TMEM8A	PAI2	ST7	AGAP1	NAGA		CLU	PLG	TNFRSF19				
TMEM8	-	-	-	0.99	-	CLU	-	0.95	-				
PAI2	-	-	-	-	1.00	PLG	0.95	1.00	0.99				
ST7	-	-	-	-	-	TNFRSF19	-	0.99	-				
AGAP1	0.99	-	-	-	-								
NAGA	-	1.00	-	-	0.96								
5. Group of genes, that controls a stream of Ca^{2+} through a superficial membrane							6. Group of mitochondrial genes						
	Grin2b	KLHL1					TrpRS	ALR					
Grin2b	1.00	0.99				TrpRS	-	0.97					
KLHL1	0.99	-				ALR	0.97	-					
7. Group of genes of extracellular matrix							8. The group of hormone-dependent genes						
	HAPLN2	AHSG					FGB	ALR	VTN				
HAPLN2	0.97	0.98				FGB	-	0.97	0.97				
AHSG	0.98	1.00				ALR	0.97	-	1.00				
						VTN	0.97	1.00	0.98				

in the expression of genes which products mark leukocytes, can be caused by the different maintenance of blood cells in the initial samples of organs at sampling time.

Our analysis testifies that the basic sources of errors and contradictions in estimation of organ-specific GEP are the following:

(1) Extended sequences of a nucleotide homology in different genes, leading to cross hybridization of one probe with cDNAs of mRNA of the genes having the common ancestry or the common functional domains;

(2) Individual variability of gene groups belonging to the general metabolic ways, is regulated by exogenous and endogenous factors which influence can vary between different animals;

(3) Individual differences between animals in number of blood cells in initial tissue samples taken for the analysis of the gene expression profiles.

References

- [1] G. Parmigiani, E.S. Garrett-Mayer, R. Anbazhagan, E. Gabrielson, A cross-study comparison of gene expression studies for the molecular classification of lung cancer, *Clinical Cancer Research* 10 (2004) 2922-2927.
- [2] S. Draghici, P. Khatri, A.C. Eklund, Z. Szallasi, Reliability and reproducibility issues in DNA microarray measurements, *Trends Genet* 22 (2006) 101-109.
- [3] D. Murphy, Gene expression studies using microarrays: Principles, problems, and prospects, *Advan. Physiol.* 26 (2002) 256-270.
- [4] M.J. Okoniewski, C.J. Miller, Hybridization interactions between probesets in short oligo microarrays lead to spurious correlations, *BMC Bioinformatics* 7 (2006) 276-290.
- [5] Y.A. Chen, C.C. Chou, X. Lu, E.H. Slate, K. Peck, W. Xu, et al., A multivariate prediction model for microarray cross-hybridization, *BMC Bioinformatics* 7 (2006) 101.
- [6] C. Wu, R. Carta, L. Zhang, Sequence dependence of cross-hybridization on short oligo microarrays, *Nucleic Acids Res.* 33 (2005) e84.
- [7] M. Sultan, I. Piccini, D. Balzereit, R. Herwig, N.G. Saran, H. Lehrach, et al., Gene expression variation in Down's syndrome mice allows prioritization of candidate genes, *Genome Biol.* 8 (2007) 91.
- [8] S.D. Zhang, T.W. Gant, Effect of pooling samples on the efficiency of comparative studies using microarrays, *Bioinformatics* 21 (2005) 4378-4383.
- [9] M.I. Dorrell, E. Aguilar, C. Weber, M. Friedlander, Global gene expression analysis of the developing postnatal mouse retina, *Investigative Ophthalmology and Visual Science* 45 (2004) 1009-1019.
- [10] A. Stratil, L.J. Peelman, M. Mattheeuws, P.V. Poucke, G. Reiner, H. Geldermann, A novel porcine gene, alpha-1-antichymotrypsin 2 (SERPINA3-2): Sequence, genomic organization, polymorphism and mapping, *Gene* 292 (2002) 113-119.
- [11] M.W. Mosesson, Fibrinogen and fibrin structure and functions, *J. Thromb Haemost* 3 (2005) 1894-1904.
- [12] A. Blair, L. Ngo, J. Park, I.T. Paulsen, M.H. Jr. Saier, Phylogenetic analyses of the homologous transmembrane channel-forming proteins of the F0F1-ATPases of bacteria, chloroplasts and mitochondria, *Microbiology* 142 (1996) 17-32.
- [13] W.B. Huttner, H.H. Gerdes, P. Rosa, The granin (chromogranin/secretogranin) family, *Trends Biochem. Sci.* 16 (1991) 27-30.
- [14] K.B. Helle, A. Corti, M.H. Metz-Boutigue, B. Tota, The endocrine role for chromogranin A: A prohormone for peptides with regulatory properties, *Cell Mol Life Sci* 64 (2007) 2863-2886.
- [15] J. Xu, J. Zhang, L. Wang, J. Zhou, H. Huang, J. Wu, et al., Solution structure of Urm1 and its implications for the origin of protein modifiers, *Proc. Natl. Acad. Sci. USA* 103 (2006) 11625-11630.
- [16] M. Nei, I.B. Rogozin, H. Piontkivska, Purifying selection and birth-and-death evolution in the ubiquitin gene family, *Proc. Natl. Acad. Sci. USA* 97 (2000) 10866-10871.
- [17] T. Minh-Doan, N. Simpson-Haidaris, P.J. Simpson-Haidaris, Cell type-specific regulation of fibrinogen expression in lung epithelial cells by dexamethasone and interleukin-1 β , *American Journal Respiratory Cell Molecular Biology* 22 (2000) 209-217.
- [18] O.B. Ekmekci, H. Ekmekci, Vitronectin in atherosclerotic disease, *International Journal of Clinical Chemistry and Diagnostic Laboratory Medicine* 368 (2006) 77-83.
- [19] P. Carmeliet, D. Collen, Genetic analysis of the plasminogen and coagulation system in mice, *Haemostasis* 26 (1996) 132-153.
- [20] The UniProt database available online at: www.uniprot.org.
- [21] M. Sundaram, S. Zhong, M.B. Khalil, P.H. Links, Y. Zhao, J. Iqbal, et al., Expression of apolipoprotein C-III in McA-RH7777 cells enhances VLDL assembly and secretion under lipid-rich conditions, *Journal of Lipid Research* 21 (2009) 150-161.
- [22] A.R. Mensenkamp, M.C. Jong, H. Goor, M.J.A. Luyn, V. Bloks, R. Havinga, et al., Apolipoprotein E participates in the regulation of very low density lipoprotein-triglyceride secretion by the liver, *The Journal of Biological Chemistry* 274 (1999) 35711-35718.

- [23] J. Chen, C. Song, R.N. Redinger, Effects of dietary cholesterol on hepatic production of lipids and lipoproteins in isolated hamster liver, *Hepatology* 24 (1996) 424-434.
- [24] P.J. Ojala, M. Hermansson, M. Tolvanen, K. Polvinen, T. Hirvonen, U. Impola, et al., Identification of alpha-1 acid glycoprotein as a lysophospholipid binding protein: A complementary role to albumin in the scavenging of lysophosphatidylcholine, *Biochemistry* 45 (2006) 14021-14031.
- [25] C. Redondo, M. Vouropoulou, J. Evans, J. Findlay, Identification of the retinol-binding protein (RBP) interaction site and functional state of RBPs for the membrane receptor, *The FASEB Journal* 22 (2008) 1043-1054.
- [26] A. Wohlwend, D. Belin, J.D. Vassalli, Plasminogen activator-specific inhibitors produced by human monocytes/macrophages, *Journal of Experimental Medicine* 165 (1987) 320-339.
- [27] T. Kanzaki, A.M. Wang, R.J. Desnick, Lysosomal alpha-N-acetylgalactosaminidase deficiency, the enzymatic defect in angiokeratoma corporis diffusum with glycopeptiduria, *The Journal of Clinical Investigation* 88 (1991) 701-711.
- [28] The NextBio database available online at: www.nextbio.com.
- [29] S.E. Jones, C. Jomary, Clusterin, *The International Journal of Biochemistry and Cell Biology* 34 (2002) 427-431.
- [30] The Gene Cards database available online at: www.genecards.org.
- [31] Y. Liu, J. Zhang, Recent development in NMDA receptors, *Chinese Medical Journal* 113 (2000) 948-956.
- [32] K.A. Aromolaran, K.A. Benzow, M.D. Koob, E.S. Piedras-Rentería, The Kelch-like protein 1 modulates P/Q-type calcium current density, *Neuroscience* 145 (2007) 841-850.
- [33] R. Jørgensen, T.M. Sogaard, A.B. Rossing, P.M. Martensen, J. Justesen, Identification and characterization of human mitochondrial tryptophanyl-tRNA synthetase, *The Journal of Biological Chemistry* 275 (2000) 16820-16826.
- [34] C. Thirunavukkarasu, L.F. Wang, S.A. Harvey, S.C. Watkins, J.R. Chaillet, J. Prelich, et al., Augmenter of liver regeneration: an important intracellular survival factor for hepatocytes, *Journal of Hepatology* 48 (2008) 578-588.
- [35] H. Sugimoto, C. Yang, V.S. LeBleu, M.A. Soubasakos, M. Giraldo, M. Zeisberg, et al., BMP-7 functions as a novel hormone to facilitate liver regeneration, *The FASEB Journal* 21 (2007) 256-264.

Antiproliferative Activity of *Kappaphycus Alvarezii* Extract on Three Cancer Cell Lines (NCIH 460, HCT 116 and U 251)

Madhavarani Alwarsamy and Ramanibai Ravichandran

Department of Zoology, University of Madras, Guindy Campus, Chennai 25, India

Received: April 19, 2010 / Accepted: June 21, 2010 / Published: March 30, 2011.

Abstract: The methanolic extract of red seaweed *Kappaphycus alvarezii* was evaluated against three different cancer cell lines to study for its antiproliferative effect. Lung cancer cell line (NCIH 460), Colon cancer cell line (HCT 116) and Glial cell carcinoma (U 251) are the three selected cell lines investigated in this study. Different concentrations of methanol extract (0.01, 0.10, 1.00, 10.00 and 100.00 $\mu\text{g/mL}$ respectively) of *Kappaphycus alvarezii* were prepared and screened by quantitative MTT (Microculture Tetrazolium) (3-(4, 5-dimethylthiazol)-2, 5-diphenyltetrazolium bromide) assay. MTT assay are the colorimetric assay which was applied to assess the viability and proliferation of cancer cells to determine the cytotoxicity of methanol extract of *K. alvarezii*. The MTT test is based on the enzymatic reduction of the tetrazolium salt (MTT) to formazon crystals exclusively in living metabolically active cells developed purple color complex which was directly proportional to the viability of cells. To elucidate the in-vitro anticancer activity the Lethal Concentration (LC_{50}), Growth Inhibition (GI_{50}) and Total Growth Inhibition (TGI) of the extract were investigated individually for each cancer cell line. Analysis of the extract has shown good cytotoxicity in all tested cancer cell lines, with an IC_{50} of 55 $\mu\text{g/mL}$ against NCIH460 and U251, 65 $\mu\text{g/mL}$ for HCT116 respectively. GI_{50} was found to be 5 $\mu\text{g/mL}$ for NCIH 460 and 10 $\mu\text{g/mL}$ for HCT 116 and U251 cell lines. TGI was 19 $\mu\text{g/mL}$ for NCIH 460, 29 $\mu\text{g/mL}$ for HCT 116 and 25 $\mu\text{g/mL}$ for U 251 cell lines. The cytotoxicity of the extract were significantly high in Lung Cancer Cell line (NCIH 460) when compared to Colon Cancer Cell line (HCT 116) and Glial Cell Carcinoma (U251) in the following order NCIH 460 > HCT 116 > U251.

Key words: *Kappaphycus alvarezii*, cytotoxicity, MTT assay.

1. Introduction

Cancer is the second leading cause of death next to heart diseases. Lung cancer is the leading cause of cancer death reported in developing countries. Nearly 85% of lung cancer is caused by smoking [1]. Colon cancer is the second most common cause of cancer death in men and women. Nearly one million people every year affected by colorectal cancer [2]. Whereas, 10,000 Americans were diagnosed for malignant Gliomas [3].

A large number of marine flora and fauna were reported to possess a wide range of interesting

biological properties. Seaweeds are the marine algae which have been used as sea vegetables, cattle fodder, herbal medicines and fertilizers in Asia, Pacific and Mediterranean regions for centuries. The total global seaweed production in the year 2004 was more than 15 million metric tones [4] and it is the excellent sources of polysaccharides, minerals, proteins and Vitamins [5]. It is said that 100 g of seaweed provides more than the daily requirements of Vitamin A, Vitamin B2 and Vitamin B12 and two-thirds of Vitamin C in human [6]. It helps in preventing constipation, colon cancer, cardiovascular diseases and obesity as well [7]. Many people around the world use seaweeds for food and medicine. Seaweeds are already marketed worldwide as a dietary supplement and as alternative medicines.

Corresponding author: Ramanibai Ravichandran, Ph.D., Prof., research field: biomonitor. E-mail: rramani8@hotmail.com.

The antibacterial, antiviral and cytotoxic activity of red and brown seaweeds from black sea was reported earlier [8].

Kappaphycus alvarezii is one of the red seaweed which is economically important species that has been extensively cultivated in more than 20 countries as an edible species and as source of carrageenan. Kappa carrageenan has been used for medicinal purposes and as a homogenizer in milk products, toothpaste and gellies [9]. It is highly grazed, found to be the primary food item in gut contents of common herbivorous fishes provide habitat for the diverse invertebrate population and reef fishes. It has been previously reported for its antioxidant potential and free radical scavenging activity [10, 11]. In the present study, the cytotoxic effect of the methanolic extract of *K. alvarezii* was studied in Lung cancer cell line (NCIH 460), Colon Cancer Cell line (HCT 116) and Glial Cell Carcinoma (U 251) cell lines.

2. Experiment

2.1 Seaweed Material

Red seaweed *K. alvarezii* used in this study was collected freshly from Mandapam Coast Rameswaram, Tamilnadu. Algal samples were washed thoroughly to remove the sand particles and epiphytes. It was shade dried at room temperature in the laboratory. The pulverized and moisture free samples were used for further experiments.

2.2 Preparation of Seaweed Extracts

The seaweed *K. alvarezii* extract was prepared as indicated in previous studies with slight modifications [11]. The pulverized moisture free sample (20.0 g) was extracted with 200 mL of methanol as solvent for several times. Filtrate was condensed in a rotary evaporator at 40 rpm to remove excess solvent and stored as such. This solvent extract was used to determine the cytotoxicity through MTT assay. All the experiments were conducted in triplicates.

2.3 Chemicals

Dulbecco's Modified Eagle Medium (DMEM) (Sigma), 10% Fetal Bovine Serum (FBS) (Gibco). All other chemicals used in this study were of analytical grade.

2.4 Cell Line Maintenance

The cell lines namely HCT 116, NCIH 460 and U251 were obtained from National Centre for Cell Science (NCCS), Pune. The cells were cultured in DMEM medium supplemented with 10% FBS with 100 U/mL of penicillin and 100 U/mL streptomycin. Cells were maintained in a humidified atmosphere of 5% CO₂ incubator at 37 °C until the confluency stage was attained. The medium was replaced for every two days and maintained strictly in accordance with standard methods [12]. The cells were dissociated with trypsin phosphate versenal glucose in phosphate buffered saline. The stock cultures were grown in 25 cm² tissue culture flasks. The experiments were commenced after confluency was attained.

2.5 MTT Assay

The Microculture Tetrazolium Assay (MTT) was carried out as described by Anne Monks, et al. (1991) [13]. Cell viability was observed and cytotoxic index LC₅₀, GI₅₀ and TGI₅₀ were calculated. NCIH 460 cells (2.5×10^4 cells/mL) were seeded in seven columns of 96 well microplates and incubated for 24 hrs (37 °C, 5% CO₂ air humidified). Then 20 µL of prepared concentrations (0.01, 0.10, 1.00, 10.00, 100.00 µg/mL) of extract was added to each column and incubated for next 48 hrs in the same condition. The untreated cells incubated for 48 hrs are specified for control. To evaluate cell survival, 20 µL of MTT solution (5 mg/mL in Phosphate buffer solution) was added to each well and incubated for four hours. After four hours, carefully the supernatant was removed leaving formazan crystals. 150 µL of DMSO was added to each well. The crystals were dissolved and the absorbance was read at 570 nm. The same procedure was carried

out for HCT 116 cells and U 251 as well. The percentage of growth was calculated by the following formula:

$$\text{Percentage growth \%} = \frac{(T-T_0)}{(C-T_0)} \times 100 \quad (1)$$

(when $T > T_0$)

Where, T = cells treated with compounds for 48 hrs; T_0 = untreated cells assayed before compound addition, and C = untreated cells incubated for 48 hrs specified for control.

3. Results and Discussion

The MTT cell proliferation assay offered a quantitative and convenient method for evaluating cell population response to external factors. This spectrometric procedure can detect even slight change in the cell metabolism, making it much more sensitive than Trypan Blue staining. Recent studies indicates the reduction of tetrazolium salts now recognized as a safe, alternative to radioactive testing [14].

The dietary seaweed contained macrophage activating polysaccharide was confirmed and active against intraperitoneally implanted Lewis Lung Carcinoma (LLC) and Spontaneous AKRT Cell Leukemia [15]. The Fucans extracted from brown seaweed *Ascophyllum nodosum* inhibited CCl 39 Fibroblast cells about 85% and Human Colon adenocarcinoma COLO DM 320 proliferation by 50% [16]. It had been reported that the aqueous extract of brown seaweed *Sargassum kjellmanianum* was effective in the *in vivo* growth inhibition of the implanted sarcoma -180 cells [17].

Powdered tissues from 46 species of air dried marine seaweeds were screened for antitumor activity. Appreciable inhibition of *Ehrlich carcinoma* was found for fucoidan preparations from *Undaria pinnatifida* and *Sargassum ringgoldianum* for carrageenan and porphyrins [18].

Based on the anticancerous activities of several seaweeds studied earlier, the present investigation aimed to evaluate the cytotoxicity of methanolic extract of *K. alvarezii*, one of the red seaweed against

NCIH 460, HCT 116 and U251 cell lines. GI_{50} , TGI_{50} and LC_{50} concentration of the extract were obtained from the graph plotted against concentration ($\mu\text{g/mL}$) of the extract along 'X' axis and percentage of growth (%) along 'Y' axis (Figs. 1-3). Cell viability was found decreased in cancer cell lines with increasing concentration of methanol extract of *K. alvarezii* (Tables 1-3). The lowest concentration of about 5 $\mu\text{g/mL}$ extract has inhibited 50% cell growth in Lung Cancer Cell line (NCIH 460), whereas GI_{50} recorded in HCT 116 and U 251 cell lines were 10 $\mu\text{g/mL}$ concentration of the extract. Evaluation of Lethal concentration (LC_{50}) indicated that the extract was lethal to both NCIH 460 and U251 cell line at 55 $\mu\text{g/mL}$

Table 1 Concentration ($\mu\text{g/mL}$) of the extract and its percent growth (%) on NCIH 460 cell line.

S.No.	NCIH 460 (Lung Cancer Cell line)	
	Concentration in μg of the extract	% Growth
1	0.01	96.14
2	0.1	90.76
3	1	85.52
4	10	25.75
5	100	- 77.99

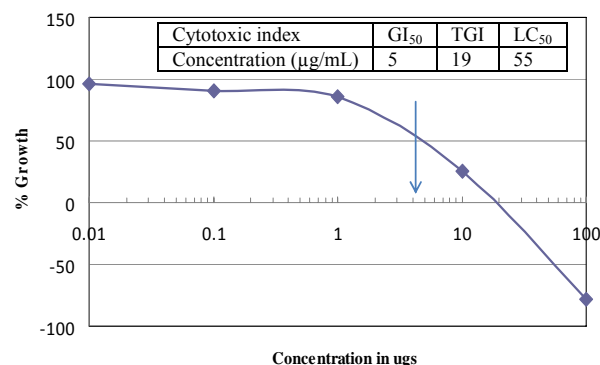


Fig. 1 Growth inhibition of methanolic extract of *Kappaphycus alvarezii* on NCIH 460 cell line.

Table 2 Concentration ($\mu\text{g/mL}$) of the extract and its percent growth (%) on HCT 116 cell line.

S.No.	HCT116 (Colon Cancer Cell line)	
	Concentration in μg s of the extract	% Growth
1	0.01	87.11
2	0.1	74.38
3	1	79.71
4	10	50.19
5	100	- 80.55

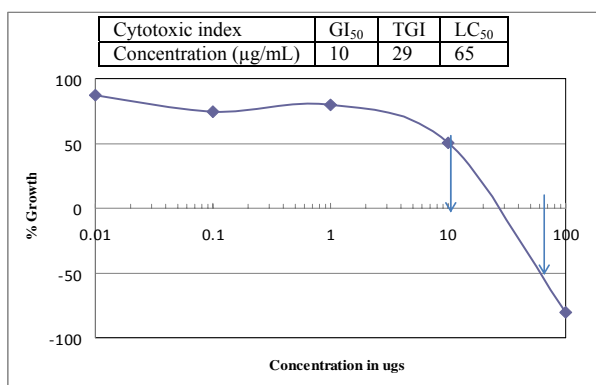


Fig. 2 Growth inhibition of methanolic extract of *Kappaphycus alvarezii* on HCT 116 cell line.

Table 3 Concentration (µg/mL) of the extract and its percent growth (%) on U251 cell line.

S.No.	U251 (Glioma Cell line)	
	Concentration in µg of the extract	% Growth
1	0.01	92.12
2	0.1	92.84
3	1	91.7
4	10	51.13
5	100	- 87.88

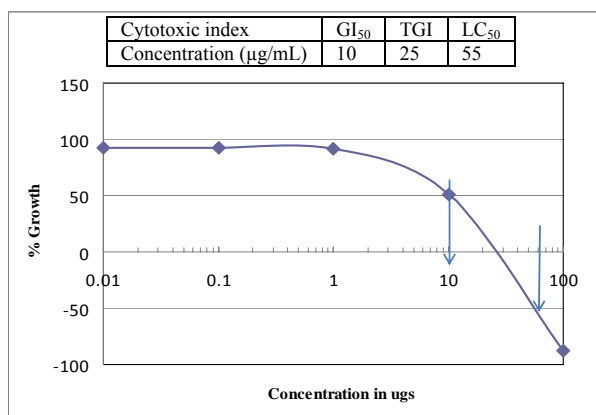


Fig. 3 Growth inhibition of methanolic extract of *Kappaphycus alvarezii* on U251 cell line.

concentration. 100% cell growth was obstructed in NCIH 460 cell line at 19 µg/mL concentration. In case of HCT 116 and U 251, Total Growth inhibition (TGI) was noticed at 29 and 25 µg/mL concentration of the extract respectively. The decrease in cell growth may be due to cell necrosis or cell apoptosis. From these results it was evident that the methanolic extract of *K. alvarezii* exhibited more potent cell growth inhibitory activity in Lung Cancer Cell line (NCIH 460)

compared to Colon Cancer Cell line (HCT 116) and Glial Cell Carcinoma (U 251).

4. Conclusion

Many synthetic drugs used for cancer treatment are producing serious side effects. Nowadays researchers have concentrate on novel drugs from plant origin to reduce side effects. Seaweeds are the marine algae found to be rich in nutrients including antioxidants and various remarkable properties. Certain brown seaweeds are exhibiting excellent anticancer activity especially the Fucoidan, the active compound isolated from *Laminaria* which has been widely studied for its oncological importance. In the present investigation we selected the red seaweed *K. alvarezii* as one of the prime material to work on. The methanolic extract of *K. alvarezii* exhibited good cytotoxicity in Lung cancer cell line (NCIH 460) compared to Colon cancer cell line (HCT 116) and Glial Cell Carcinoma (U 251). Since this is a preliminary study, further detailed investigations are to be carried out to isolate active compounds from *K. alvarezii* and to be observed in-vitro and later in *in vivo* animal models.

Acknowledgment

The authors thanked University of Madras (UPE) for the support to carry out the research work.

References

- [1] N. Gray, A global approach to tobacco smoking ‘Lung Cancer’, Biomed. Central 39 (2) (2003) 113-117.
- [2] S. Huerta, E.J. Goulet, E.H. Livingston, Colon cancer and apoptosis, The American Journal of Surgery 191 (4) (2006) 517- 526.
- [3] A.N. Mamelak, D.B. Jacoby, Targeted delivery of antitumoral therapy to glioma and other malignancies with synthetic chlorotoxin (TM-601), Expert Opin. Drug Drliv. 4 (2) (2007) 175-186.
- [4] FAO, Year Book of Fisheries Statistics, Food and Agricultural Organization of the United Nations, Rome, 2006, p. 98.
- [5] D. Wilson, Rhodophyta, Red algae version, Mar. 24, 2000, available online at: <http://tolweb.org/Rhodophyta/2381/2000.03.24>.

- [6] V.I. Chapman, D.I. Chapman, *Seaweeds and Their Uses* (3rd ed.), Chapman and Hall, London, 1980.
- [7] J. Ortiz, N. Romero, P. Robert, J. Araya, J. Lopez-Hernandez, C. Bozzo, et al., Dietary fiber, amino acid, fatty acid and tocopherol contents of the edible seaweeds *Ulva lactuca* and *Durvillaea antarctica*, *Food Chemistry* 99 (1) (2006) 98-104.
- [8] Z. Kamenarska, J. Serkedjeva, H. Najdenski, K. Stefanov, I. Tsvetkova, S. Dimitrova-Konaklieva, et al., Antibacterial, antiviral, and cytotoxic activities of some red and brown seaweeds from the Black Sea, *Botanica Marina* 52 (1) (2009) 80-86.
- [9] I.A. Abbott, *Marine Red Algae of the Hawaiian Islands*, Bishop Museum Press, Honolulu, Hawaii, 1999.
- [10] P. Ganesan, S.K. Chanini, N. bhasker, Antioxidant properties of methanol extract and its solvent fractions obtained from selected Indian red seaweeds, *Bioresource Technology* 99 (8) (2008) 2717-2723.
- [11] K.K. Suresh, K. Ganesan, R.P.V. Subbu, Antioxidant potential of solvent extracts of *Kappaphycus alvarezii* (Doty) Doty- An edible seaweed, *Food Chemistry* 107 (2007) 289-295.
- [12] J. Carmichale, W.G. De Graff, A.F. Gazdar, J.D. Mina, J.B. Mitchell, Evaluation of a tetrazolium based semiautomated colorimetric assay: Assessment of chemosensitivity testing, *Cancer Res.* 47 (1987) 936-942.
- [13] A. Monks, D. Scudiero, P. Skehan, R. Shoemaker, K. Paull, D. Vistica, et al., Feasibility of a high-flux anticancer drug screen using a diverse panel of cultured human tumor cell lines, *JNCL* 83 (11) (1991) 757-766.
- [14] A.A. Van De Loosdrecht, R.H. Beelen, G.J. Ossenkoppele, M.G. Broekhoven, M. Langenhuijsen, A tetrazolium-based colorimetric MTT assay to quantitate human monocyte mediated cytotoxicity against leukemic cells from cell lines and patients with acute myeloid leukemia, *J. Immunol. Methods* 174 (1-2) (1994) 311-320.
- [15] E. Furusawa, S. Furusawa, Anticancer potential of vivanatural, a dietary seaweed extract on Lewis lung carcinoma in comparison with chemical immunomodulators and on cyclosporine accelerated AKR leukemia, *Oncology* 46 (1989) 343-349.
- [16] M. Ellouli, C. Boisson Vidal, P. Durand, J. Jozefonvicz, Antitumor and antiproliferative effects of a fucan extracted from brown seaweed *Ascophyllum nodosum*, *Anticancer Res.* 13 (6A) (1993) 2011-2020.
- [17] I. Yamamoto, M. Takahashi, E. Tamura, H. Maruyama, H. Mori, Antitumor activity of edible marine red algae: Effect of crude fractions prepared from edible brown seaweeds against L-1210 leukemia, *Hydrobiologia* 116/117 (1984) 145-148.
- [18] H. Noda, H. Amano, K. Arashima, K. Nisizawa, Antitumor activity of marine algae, *Hydrobiologia* 204/205 (1990) 577-584.

Evaluation of Emmer Wheat Genetic Resources Aimed at Dietary Food Production

Zdeněk Stehno¹, Ivana Paulíčková², Jana Bradová¹, Petr Konvalina³, Ivana Capouchová⁴, Eva Mašková², Dana Gabrovská², Marie Holasová², Vlasta Fiedlerová², Renáta Winterová², Jarmila Ouhřabková² and Ladislav Dotlačil¹

1. Department of Gene Bank, Crop Research Institute, Praha 161 06, Czech Republic

2. Department of Nutritive Substances, Food Research Institute, Praha 102 31, Czech Republic

3. Faculty of Agriculture, University of South Bohemia, České Budějovice 370 05, Czech Republic

4. Faculty of Agrobiolgy, Food and Natural Resources, Czech University of Life Sciences, Praha 165 21, Czech Republic

Received: July 28, 2010 / Accepted: October 24, 2010 / Published: March 30, 2011.

Abstract: Emmer wheat cultivated by organic farmers is used as a component of some bio (organic) food products. Its positive influence on consumer health is caused by grain composition. With the aim of selecting varieties or landraces for their possible further use we tested selected emmer wheat accessions maintained in the Czech Gene Bank. In the set of 8 emmer wheat accessions, the main grain components, bread making characteristics and contents of health supporting chemical substances such as total dietary fibre content and its components, content of total polyphenols plus catechin and ferulic acid contents, vitamins of the B group and E plus total content of carotenoids were evaluated by standard methods. Tests of bread making quality confirmed a very well known fact that emmer wheat grain is much more suitable for other purposes as whole grain mixtures, cereal pure, etc. than for bread preparation. The results indicate the possibilities to select emmer wheat genotypes differing in grain composition and containing compounds with positive effects on human health. Among the tested emmer wheat accessions the Rudico variety had a complex of positive characteristics such as content of total dietary fibre, total polyphenol content with prevailing catechin and the highest amount of B group vitamins such as B1, B2, niacin, pantothenic acid and B6.

Key words: Emmer wheat, *Triticum diccocon*, grain quality, HMW glutenin subunits, polyphenols, vitamins, wheat genetic resources.

1. Introduction

Genus *Triticum* L. consists of over 30 different species with large interspecific variability. Some of them such as bread wheat (*Triticum aestivum* L.) and durum wheat (*T. durum* Desf.) play an important role in human nutrition. Other species are used for human consumption rarely or not at all. For example, spelta wheat (*T. spelta* L.) and emmer (*T. diccocon* Schrank) belong to the rarely used, so they were called as minor wheat species.

The number of accessions in wheat collections of genetic resources usually corresponds to crop

importance. The wheat collection in the Czech Gene Bank at the Crop Research Institute is comprised of 30 wheat species (passport data accessible at EVIGEZ – The Czech National Database of Plant Genetic Resources [1]). Among 10,691 accessions hexaploid bread, wheat is clearly the prevailing species (86.4%). The sub collection of hulled tetraploid emmer wheat (*T. diccocon* Schrank) contains 117 landraces and obsolete varieties. In addition to this set of cultivated emmer, there is a group of wild emmer *T. diccooides* (Körn. Ex Aschers. Graebn.) Schwiempf. containing 26 accessions.

Interest in minor wheat species has been increasing in the Czech Republic (CR) recently as it has in certain European countries like: Austria, Germany, Belgium,

Corresponding author: Zdeněk Stehno, head of the Gene Bank Department, research field: wheat genetic resources collection. E-mail: stehno@vurv.cz.

Italy and others, owing to the developments in and their extending of their organic farming systems. In the CR there are 2 registered varieties of winter spelt and one emmer variety is legally protected.

The varieties of emmer wheat are less demanding and more adaptable [2, 3]. Therefore, they are suitable for low-input or organic farming systems [4-6]. When grown in marginal areas, they provide a lower, but more stable harvest level [7] and they may contribute, as organic products, to a higher economic profit than other conventional varieties of cereals [8].

Increased interest in emmer wheat has stimulated research aiming at evaluation of a pre-selected set of emmer accessions for their food and dietary quality. Emmer wheat cultivated by organic farmers is used as a component of some bio (organic) food products. Its positive influence on consumer health is caused by grain composition. With the aim of selecting varieties or landraces for their possible further use we tested selected emmer wheat accessions which were maintained in the Czech Gene Bank.

2. Materials and Methods

A pre-selected set of 10 emmer wheat accessions is characterized by high molecular weight glutenin subunits (HMW-GSs). The electrophoretic patterns of HMW-GSs were determined by the one-dimensional sodium dodecyl sulphate polyacrylamide gel electrophoresis (SDS-PAGE), using the Laemmli buffer system [9]. The acrylamide/bisacrylamide concentration (T) and the cross linker (C) used were as follows: T = 10% and C = 2.60%. The particular alleles of HMW-GSs were identified according to a published catalogue [10].

With the aim of evaluating grain quality parameters, a set of 8 emmer landraces including a legally protected variety, Rudico, has been tested in field plot experiments in organic farming for two years. Average grain samples from 3 replications were analysed in the second year of evaluation to assess standard bread making quality characteristics as well as content of

dietary valuable compounds. For the analyses, the following methods were used:

(1) Crude protein content: The Kjeldahl Method according to ČSN ISO 1871;

(2) Wet gluten content and Gluten index (GI): on Glutomatic 2200 according to ČSN ISO 5531;

(3) Sedimentation index – The Zeleny Test: according to ČSN ISO 5529;

(4) Total dietary fibre (TDF): The enzyme – gravimetric method according to AOAC 991.42 using the enzyme set Bioquant (Merck), and filter machinery FIBERTEC (Scan Tec);

(5) The total polyphenol content: the sample was extracted with 80% ethanol under a reverse cooler in a temperature of 90 °C for 120 min. The extract was filtrated through a folded filter. Ten millilitres of distilled water, 2.5 mL of Folin-Ciocalteu reagent (FCR) and 7.5 mL of 20% bicarbonate dilution were added to an aliquot part of the extract. The content was mixed and filled to 50 mL by adding distilled water. After 2 hrs (max. coloration) the sample was measured spectrophotometrically (wave length $\lambda = 765$ nm). The calibrating curve was put together of 0.1-0.4 g·L⁻¹ concentrations of Gallic acid. The results are presented as Gallic acid equivalents (GAE) [g GAE·kg⁻¹] [11];

(6) The content of selected phenolic substances (catechin, epicatechin, ferulic acid, chlorogenic acid): RP – HPLC method – Summit system (DIONEX);

(7) Vitamin B1 (thiamine): isolation by acid and enzyme hydrolysis, oxidation of thiamine by potassium hexacyanoferrate in an alkalic environment to thiochrom, The RP – HPLC method;

(8) The Vitamin B2 (riboflavin) lumiflavin method according to ČSN 65 0054: isolation by acid and enzyme hydrolysis, transformation of riboflavin to lumiflavin, fluorescence method $\lambda_{ex} - 290$ nm – $\lambda_{em} - 330$ nm;

(9) The Niacin – *Lactobacillus plantarum* microbiological method ATCC 8014, ČSN 56 0051;

(10) The Pantothenic acid - *Lactobacillus plantarum* modified microbiological method ATCC 8014, ČSN

56 0051;

(11) The Vitamin B6 – *Saccharomyces uvarum* microbiological method ATCC 9080, ČSN 56 056;

(12) Vitamin E - sample saponification and extraction of unsaponifiable parts, HPLC method;

(13) Total carotenoids - sample saponification and extraction of unsaponifiable parts, spectrophotometric method, calculation based on absorbance of hexanol dilution under 445 nm using the extinction coefficient for β -carotene.

3. Results and Discussion

3.1 Polymorphism of HMW Glutenin Subunits

Selected emmer wheat accessions differed considerably in the polymorphisms of HMW-GSs. Out of the total of 10 studied emmer wheat landraces, 5 accessions [*T. dicoccon* (Ruzyně), Kahler Emmer, May-Emmer, Weisser Sommer and *T. dicoccon* (Tapioszele)] appeared to be homogeneous in the electrophoretic patterns of HMW-GSs; they were formed by a single glutenin line (Table 1).

3.2 Standard Bread Making Quality Characteristics Plus Content of Dietary Valuable Compounds

3.2.1 Crude Protein Content

All tested emmer accessions exceeded the check bread wheat variety Vlasta in crude protein and fat contents. The highest crude protein content (14.74%), measured by the Kjeldahl method was detected in the legally protected emmer variety Rudico. In total this parameter ranged from 14.39% to 11.99% (Table 2). A high content of crude protein in emmer wheat is described in Refs. [12, 13].

Also in the category of fat content, all emmer accessions (3.77-4.40%) overcame the Vlasta variety (by 2.76%). Fibre content was relatively variable with the check bread wheat variety nearly in the middle of the range of this parameter. The content of carbohydrates reflects reciprocally crude protein content.

Table 1 HMW Glutenin markers of emmer landraces and obsolete cultivars.

<i>T. dicoccon</i> landrace	Stat of origin	Glu lines	HMW-GSs ⁺		
			Glu-A1	Glu-B1	Glu-1D
<i>T. dicoccon</i> (Kroměříž)	(CZE)	A	1	7+8	-
		B	1	21	-
		C	1	6+7	-
<i>T. dicoccon</i> (Ruzyně)	(CZE)	A	1	7+8	-
Kahler Emmer	GER	A	1	7+8	-
May-Emmer	CHE	A	1	7+8	-
Weisser Sommer	GER	A	1	(7+8)	-
<i>T. dicoccon</i> (Tapioszele)	(HUN)	A	1	7+8	-
Krajova-Podbranc (Toman)	CSK	A	2*	21	-
		B	2*	6+9	-
Poering Jaarma (Nachitchevan.)	AZE	A	1	22	-
		B	1	7+8	-
		C	0	7+8	-
		D	2*	7+8	-
<i>T. dicoccon</i> (Balkan)	(GER)	A	2*	14+15	-
		B	0	14+15	-
<i>T. dicoccon</i> (Brno)	CSK	A	2*	6+8	-
		B	2*	21	-
Sandra (<i>T. aestivum</i>) - control	CSK	A	2*	7+8	3+12
		B	2*	7+9	3+12
		C	1	7+9	3+12

⁺) alleles of HMW-GSs identified 0, 1, 2*, etc. according to catalogue (Payne & Lawrence 1983) [11].

3.2.2 Wet Gluten Content and Gluten Index

The quality of wet gluten, characterised by gluten index (GI) which is evaluated by Glutomatic 2200, was very low in all emmer accessions (Table 3). Gluten of 3 landraces - *T. dicoccon* (Dagestan ASSR), *T. dicoccon* (Palestine) and *T. dicoccon* (Brno) – was completely flowable.

3.2.3 Sedimentation Index – The Zeleny Test

Zeleny Sedimentation, an important parameter of bread making quality, was very low and ranged from 6 mL [*T. dicoccon* (Dagestan ASSR)] to 19 mL (Rudico). Based on such results, the emmer wheat landraces can be considered potentially more suitable for other purposes than for the preparation of bread (e.g. for different grain mixtures, pure, etc.). The emmer wheat may be used in pasta production, as the grains contain the necessary weak gluten and high level of protein [13].

Table 2 Basic emmer grain components in comparison to bread wheat variety Vlasta. (Unit: %)

Genotype / variety	Dry matter	Crude protein content	Fat content	Fibre	Carbohydrates	Crude ash
Rudico	89.78	14.74	4.00	13.89	55.30	1.85
May-Emmer	89.23	13.35	3.77	9.18	61.03	1.90
Weisser Sommer	89.12	12.15	3.81	8.77	62.51	1.88
<i>T. dicoccon</i> (Dagestan)	89.25	11.99	3.83	8.68	62.99	1.76
<i>T. dicoccon</i> (Palestine)	89.37	13.91	4.10	8.90	60.44	2.02
<i>T. dicoccon</i> (Tapioszele)	89.27	13.10	4.40	10.59	59.20	1.98
<i>T. dicoccon</i> (Brno)	89.53	13.42	4.19	9.56	60.28	2.08
<i>T. dicoccon</i> (Tabor)	89.74	14.39	4.38	12.51	56.69	1.77
Vlasta (<i>T. aestivum</i> check)	89.09	11.59	2.76	11.13	62.23	1.38

Table 3 Bread making parameters of emmer accessions.

Genotype / variety	Wet gluten content (%)	Gluten Index	SDS-sedimentation (mL)	Zeleny sedimentation (mL)	Falling number (s)
Rudico	24.21	4	32	19	402
May-Emmer	28.06	6	37	10	337
Weisser Sommer	27.55	6	34	8	331
<i>T. dicoccon</i> (Dagestan)	*	*	11	6	386
<i>T. dicoccon</i> (Palestine)	*	*	17	9	379
<i>T. dicoccon</i> (Tapioszele)	30.2	9	18	11	421
<i>T. dicoccon</i> (Brno)	*	*	17	9	317
<i>T. dicoccon</i> (Tabor)	33.84	4	25	18	328
Vlasta (<i>T. aestivum</i> check)	26.69	65	-	36	-

*) totally flowable gluten.

On the other hand, emmer wheat is becoming a more and more popular crop in organic farming. With the aim of describing other compounds of emmer grain, we analysed them in greater detail.

3.2.4 Total Dietary Fibre Content and Its Components

The content of total dietary fibre (TDF) ranged from 8.68% to 13.89% in Rudico. The proportion between soluble and insoluble fractions of TDF in average was nearly 1 : 1 (5.3 : 4.8% soluble to insoluble fractions respectively), however there were differences among accessions (Table 4).

Differences among emmer accessions in the ratio between IDF and SDF reflect the opportunity to select suitable genotypes. The results obtained by D'Antuoni et al. [14] suggest that the native emmer genetic material may represent a source of high-value dietary fibre.

3.2.5 The Content of Total Polyphenols Plus Catechin and Feluric Acid Contents

Table 4 Total dietary fibre content (%) and its components in emmer grain.

Genotype / variety	TDF*	IDF**	SDF***
Rudico	13.89	7.01	5.88
May-Emmer	9.18	4.34	4.84
Weisser Sommer	8.77	5.02	3.75
<i>T. dicoccon</i> (Dagestan)	8.68	3.33	5.35
<i>T. dicoccon</i> (Palestine)	8.9	4.89	4.01
<i>T. dicoccon</i> (Tapioszele)	10.59	6.71	3.88
<i>T. dicoccon</i> (Brno)	9.56	4.85	4.71
<i>T. dicoccon</i> (Tabor)	12.51	6.56	5.95
Vlasta (<i>T. aestivum</i> check)	11.13	7.06	4.07

*) Total Dietary Fibre, **) Insoluble Dietary Fibre, ***) Soluble Dietary Fibre.

Differences in content of total polyphenols among emmer accessions were relatively deep; they ranged from 2.54 g GAE/kg DM (Weisser Sommer) to 3.55 g GAE/kg DM (Rudico) (Table 5). Five emmer accessions overcame the check bread wheat variety Vlasta in its content of total polyphenols. The highest content, 3.55 g GAE/kg DM, was detected in the Rudico variety. The

Table 5 Total polyphenols plus catechin and ferulic acid contents.

Genotype / variety	Total polyphenols (g GAE/kg DM)	Catechin (mg/100g DM)	Ferulic acid (mg/100g DM)
Rudico	3.55	149.5	2.2
May-Emmer	2.72	66.0	2.3
Weisser Sommer	2.54	57.5	2.5
<i>T. dicoccon</i> (Dagestan)	2.85	109.6	1.5
<i>T. dicoccon</i> (Palestine)	3.22	112.5	1.2
<i>T. dicoccon</i> (Tapioszele)	3.31	43.6	2.3
<i>T. dicoccon</i> (Brno)	3.40	66.8	1.2
<i>T. dicoccon</i> (Tabor)	3.50	78.6	1.1
Vlasta (<i>T. aestivum</i> check)	2.81	97.1	1.3

Table 6 Content of B group vitamins.

Genotype / variety	B1	B2	niacin	pantothenic acid	B6
Rudico	0.44	0.135	10.6	1.06	0.45
May-Emmer	0.33	0.108	8.4	0.95	0.27
Weisser Sommer	0.36	0.108	8.9	0.91	0.28
<i>T. dicoccon</i> (Dagestan)	0.29	0.111	9.7	0.78	0.27
<i>T. dicoccon</i> (Palestine)	0.36	0.113	9.7	1.04	0.38
<i>T. dicoccon</i> (Tapioszele)	0.36	0.115	10.2	0.92	0.39
<i>T. dicoccon</i> (Brno)	0.35	0.12	8.5	0.84	0.38
<i>T. dicoccon</i> (Tabor)	0.34	0.115	8.4	0.94	0.43
Vlasta (<i>T. aestivum</i> check)	0.36	0.071	6.8	0.95	0.37

The unit of “B1, B2, niacin, pantothenic acid, B6” is the same which is “mg/100g DM”.

antioxidant activity of polyphenols is described by Serpen et al. [15].

Catechin prevailed among polyphenolyic substances. Very low catechin content (57.5 mg/100g DM) was detected in Weisser Sommer, on the other hand, Rudico contained 149.5 mg/100g DM of catechin. Ferulic acid was another measurable polyphenol; its content ranged from 1.1 mg/100g DM in *T. dicoccon* (Tabor) to 2.5 mg/100g DM in Weisser Sommer. Contents of chlorogenic acid and epicatechin were immeasurable.

3.2.6 Vitamins of B Group in Emmer Accessions

A higher content of vitamins B1 and B2 was ascertained in Rudico (0.44 mg/100g DM, 0.135 mg/100g DM respectively) in comparison to May Emmer (0.33 mg/100g DM, 0.108 mg/100g DM respectively).

Also the highest contents of other B vitamins (niacin, pantothenic acid and B6) were found in the Rudico

Table 7 Content of E vitamin and carotenoids.

Genotype / variety	vitamin E (mg/100g DM)	Total carotenoids (mg/100g DM)
Rudico	1.24	20.23
May-Emmer	1.21	20.65
Weisser Sommer	1.09	23.88
<i>T. dicoccon</i> (Dagestan)	1.09	24.86
<i>T. dicoccon</i> (Palestine)	0.83	26.58
<i>T. dicoccon</i> (Tapioszele)	1.30	21.56
<i>T. dicoccon</i> (Brno)	1.03	20.43
<i>T. dicoccon</i> (Tabor)	1.09	18.31
Vlasta (<i>T. aestivum</i> check)	1.22	20.44

variety (Table 6).

3.2.7 The Content of E Vitamin and Carotenoids in Emmer Accessions

The highest content of E vitamin was measured in *T. dicoccon* (Tapioszele) (1.30 mg/100g DM). The total content of carotenoids ranged from 18.31 mg/100g DM in *T. dicoccon* (Tabor) to 26.58 mg/100g DM in *T. dicoccon* (Palestine) (Table 7).

4. Conclusions

In our experiments we have concluded that emmer wheat bread makes quality pure, because of the low swelling capacity of gluten. That is why emmer is suitable for other purposes as whole grain mixtures, cereal pure etc. than for classical yeast bread preparation.

The results described above indicate possibilities to select emmer wheat genotypes differing in grain composition, containing compounds with positive effects on human health.

Among tested emmer wheat accessions the Rudico variety had a set of positive characteristics such as: content of total dietary fibre, total polyphenol content with prevailing catechin and the highest amount of B group vitamins such as B1, B2, niacin, pantothenic acid and B6.

Acknowledgment

This research was supported by the research projects of the Ministry of Agriculture QH82272 and QI91B095.

References

- [1] EVIGEZ, Czech National Database of Plant Genetic Resources, 2010, available online at: <http://genbank.vurv.cz/genetic/resources>.
- [2] L. Dengcai, Z. Youliang, L. Xiujin, Utilization of wheat landrace Chinese Spring in breeding, *Scientia Agricultura Sinica* 36 (2003) 1383-1389.
- [3] J. Kotschi, Agrobiodiversity vital in adapting to climate change, *Appropriate Technology* 33 (2006) 63-66.
- [4] L. Dotlacil, Genetické zdroje a jejich význam pro šlechtění rostlin a setrvalý rozvoj zemědělství (Genetic resources - their importance for plant breeding and sustainable development in agriculture), *Genetické Zdroje* 87 (2002) 1-5.
- [5] A. Troccoli, P. Codianni, Appropriate seeding rate for einkorn, emmer, and spelt grown under rainfed condition in southern Italy, *European Journal of Agronomy* 22 (2005) 293-300.
- [6] S. Marino, R. Togetti, A. Alvino, Crop yield and grain quality of emmer populations in central Italy, as affected by nitrogen fertilization, *European Journal of Agronomy* 31 (2009) 233-240.
- [7] W.W. Collins, G.C. Hawtin, Conserving and using crop plant biodiversity in agroecosystems, in: W.W. Collins, C.O. Qualset, (Eds.), *Biodiversity in Agroecosystems*, CRC Press, Boca Raton, Florida, 1999, pp. 267-282.
- [8] G. Pardo, I. Aibar, J. Caverro, C. Zaragosa, Economic evaluation of cereal cropping systems under semiarid conditions: Minimum input, organic and conventional, *Scientia Agricola (Piracicaba, Braz.)* 66 (2009) 615-621.
- [9] J. Lachmann, V. Hosnedl, V. Pivec, Changes in the content of polyphenols in barley grains and pea seeds after controlled accelerated ageing treatment, *Scientia Agricultura Bohemica* 28 (1997) 17-30.
- [10] V.K. Laemmli, Cleavage of structural proteins during assembly of the head bacteriophage, *Nature* 227 (1970) 680-685.
- [11] P.I. Payne, G.J. Lawrence, Catalogue of alleles or the complex loci, Glu-A1, Glu-B1 and Glu-D1 which coded for high-molecular-weight subunits of glutenin in hexaploid wheat, *Cereal Research Communications* 11 (1983) 29-35.
- [12] H. Grausgruber, J. Scheiblauber, R. Schönlechner, P. Ruckebauer, E. Berghofer, Variability in chemical composition and biologically active constituents of cereals, in: J. Vollmann, et al. (Eds.), *Genetic Variation for Plant Breeding, EUCARPIA and BOKU – University of Natural Resources and Applied Life Sciences, Vienna*, Printed in Austria, 2004, pp. 23-26.
- [13] M. Marconni, R. Cubadda, Emmer wheat, in: E-S.M. Abdel-Aal, P. Wood (Eds.), *Speciality Grains for Food and Feed*, American Association of Cereal Chemists, St. Paul, 2005, pp. 63-108.
- [14] L.F. D'Antuoni, G.C. Galletti, P. Bocchini, Fiber quality of emmer (*Triticum dicoccum* Schubler) and einkorn wheat (*T. monococcum* L.) landraces as determined by analytical pyrolysis, *J. Sci. Food. Agric.* 78 (2) (1998) 213-219.
- [15] A. Serpen, V. Gökmen, A. Karagöz, H. Köksel, Phytochemical quantification and total antioxidant capacities of emmer (*Triticum dicoccon* Schrank) and einkorn (*Triticum monococcum* L.) wheat landraces, *J. Agric. Food Chem.* 56 (16) (2008) 7285-7292.

Separated Hydrolysis and Fermentation of Water Hyacinth Leaves for Ethanol Production

Buddhiporn Sornvoraweat and Jirasak Kongkiattikajorn

School of Bioresources and Technology, King Mongkut's University of Technology Thonburi, Bangkok 10150, Thailand

Received: August 06, 2010 / Accepted: November 26, 2010 / Published: March 30, 2011.

Abstract: Water hyacinth is a raw material for long-term sustainable production of cellulosic ethanol. In this study, the acid pretreatment and enzymatic hydrolysis were used to evaluate to produce more sugar, to be fermented to ethanol. Separated hydrolysis and fermentation (SHF) studies were carried out to produce ethanol from water hyacinth leaves. Dilute sulfuric acid pretreatment and enzymatic hydrolysis were conducted to select the optimum pretreatment conditions. The optimum pretreatment conditions included $T = 135\text{ }^{\circ}\text{C}$, $t = 30\text{ min}$, and sulfuric acid concentration = 0.1 M. The residue was enzymatically hydrolyzed using the mixture of enzymes cellulase, xylanase and pectinase. The maximum enzymatic saccharification of cellulosic material (76.8%) was achieved. SHF by mono-culture of *Saccharomyces cerevisiae* KM1195 achieved the highest yields of ethanol. Furthermore, ethanol production was accomplished with the co-culture of *S. cerevisiae* TISTR5048 and *Candida tropicalis* TISTR5045 which produced the highest increase in ethanol yield. In this case, the ethanol concentration of 3.42 (g/L), percentage of the theoretical ethanol yield of 99.9%, the ethanol yield of 0.27 g/g and the productivity of 0.22 g/L/h were obtained. This suggested that mild acid pretreatment and co-culture are promising methods to improve enzymatic hydrolysis and ethanol production from water hyacinth.

Key words: Ethanol, water hyacinth leaves, fermentation.

1. Introduction

Bioethanol, a renewable fuel is becoming increasingly important as a consequence of major concern for depleting oil reserves, rising crude oil prices and greenhouse effect [1]. Lignocellulosic feedstock is considered as an attractive raw material not only for the liquid transportation fuel but also for the production of chemicals and materials, i.e. the development of carbohydrate-based biorefineries [2]. Besides terrestrial plants, aquatic plants are also promising renewable resource.

The water hyacinth, *Eichhornia crassipes* (Mart.) Solms, is a tropical species belonging to the pickerelweed family (Pontederiaceae). The water hyacinth plant is a free-floating aquatic plant

originating from the Amazon River basin in South America and has spread to more than 50 countries on five continents. The plant tolerates extremes in water level fluctuations, seasonal variations in flow velocity, nutrient availability, pH, temperature and toxic substances [3]. Extremely high growth rates of up to 100-140 ton dry material $\text{Ha}^{-1}\text{ year}^{-1}$ were reported, depending on the location and time of the year [4-6]. The coverage of waterways by water hyacinth has created various problems. Examples are the destruction of ecosystems, irrigation problems and an increase in mosquito populations. These negative effects have pinpointed the water hyacinth as one of the world's weeds and stimulated the search for control measures.

Aquatic plants have many advantages such as growing on and in bodies of water without competing against most grains and vegetables for arable land; they are also used for water purification to extract nutrients and heavy metals. Especially, the vegetation form of

Corresponding author: Jirasak Kongkiattikajorn, Ph.D., research fields: food chemistry and biochemistry, fermentation, bioactive compounds, enzyme technology. E-mail: jirasak.kon@kmutt.ac.th.

free-floating aquatic plants will facilitate their movement and harvest. Due to its fast growth and the robustness of its seeds, the water hyacinth has since then caused major problems in the whole area. Attempts to control the weed have caused high costs and labour requirements, leading to nothing but temporary removal of the water hyacinths. The water hyacinth would have a great potential if seen as raw material for industries or if incorporated into agricultural practice. It can provide cellulosic sugars for bioconversion to fuel ethanol. The present study, investigated ethanol production from the defined lab media (i.e. simulated synthetic hydrolysate medium) water hyacinth cellulose acid and enzyme hydrolysate using mono-culture and co-culture of yeasts fermentation.

2. Experiment

2.1 Substrate Preparation

Fresh water hyacinth plant were harvested from the Chaophaya River in Bangkok. The collected leaves were washed manually using tap water to remove adhering dirt, dried at 45 °C in a hot-air oven for 4 days, milled, screened to select the fraction of particles with a size of 45-697 µm, homogenized in a single lot and stored until needed.

2.2 Batch Fermentation

Hydrolysate was prepared by autoclaving under 15 lb/inch² using 1.5 g dried powder of water hyacinth leaves with 100 mL of 0.1 M sulfuric acid, in Erlenmeyer flasks. Then, 250 mL filter-sterilized cellulase (20 Filter paper units (FPU) (g substrate)⁻¹; Sumitime C; Shin Nihon Chemical Co. Ltd., Japan); α -amylase 100 unit (g substrate)⁻¹; amyloglucosidase 100 unit (g substrate)⁻¹; xylanase activity: 500 unit (g substrate)⁻¹ and pectinase activity: 250 unit (g substrate)⁻¹ in 0.1 M sodium phosphate (pH 5.0) was added to the flask and reacted at 50 °C and 120 rpm for 48 h for hydrolysis. After the enzymatic reaction, the hydrolysate was centrifuged at 21,000 × g for 10 min.

The supernatant was supplemented with additional nutrients to give a base medium composition of: 1 g/L yeast extract; 2 g/L (NH₄)SO₄; 1 g/L MgSO₄·7H₂O. Batch fermentation was conducted in a 250 mL Erlenmeyer flask with a working volume of 100 mL was inoculated with 5% v/v inoculum (20 h culture, 1 × 10⁷ cells/ml) at 30 ± 0.2 °C in an Incubation shaker. The broth was kept under agitation at 50 rpm. Samples were taken at regular time intervals during fermentations to determine the concentrations of cell mass, ethanol and residual sugars in the broth. All experiments were carried out in duplicate.

2.3 Analytical Methods

Total solids (TSs) moisture and crude protein in water hyacinth were determined according to standards [6]. Cellulose, hemicellulose and lignin contents were determined by the detergent extraction method [7]. Culture dry weight was measured by centrifugation and drying at 105 °C, until no weight change between consecutive measurements was observed. Total reducing sugar was estimated by using dinitrosalicylic acid (DNS) reagent [8]. The fermentation was carried out at 30 °C for 32 h the broths were filtered through a 0.45 µm Millipore filter. Ethanol in the samples was determined by gas chromatograph using a 60:80 Carbopack B: 5% Carbowax 20 M glass column. The injector was operated at 200 °C; the flame ionization detector (FID) was kept at 200 °C and nitrogen gas was used as carrier gas at a flow rate of 30 mL/min. The temperature was programmed at 120 °C for 1.4 min, from 120 °C to 240 °C at 30 °C/min, then held 5 min at 240 °C.

2.4 Statistical Analysis

Data was analysed by one-way ANOVA and differences among treatment means were determined by Duncan's new multiple-range test.

3. Results and Discussion

The average composition of water hyacinth is summarized in Table 1.

Table 1 Chemical analysis of water hyacinths according to different sources.

Parameter (% on DM basis)	This study	Abdelhamid and Gabr [9]	Bolenz et al. [10]	Chanakya et al. [11]	Patel et al. [12]	Poddar et al. [13]
Hemicellulose	32.69	33.4	22	33.39	43.4	18.42
Cellulose	19.02	19.5	31	18	17.8	25.61
Lignin	4.37	9.27	7	26.36	7.8	9.93
Crude protein	10.20	20	-	-	11.9	16.25

3.1 Composition of Water Hyacinth

Water-hyacinth is considered to be a potential biomass source of cellulose and hemicellulose for conversion to useful products [14]. Due to its high moisture content (93-95%), it was dehydrated before use (Table 1). In this study, the average composition of water hyacinth leaves was: total solids (TSs): 8.7-11.5 (% of wet weight), moisture 40-45 (% of wet weight), hemicellulose (as % of TSs): 32.69 ± 0.024 , cellulose (as % of TSs): 19.02 ± 0.017 , lignin (as % of TSs): 4.37 ± 0.027 , crude protein (as % of TSs): 10.20 ± 0.032 and starch (as % of TSs): 4.16 ± 0.043 . Several studies on the chemical composition of the water hyacinths have been reported. In Table 1 the chemical composition of the water hyacinths from different sources is summarised. These results agreed fairly well with the data reported by other investigators [15, 16]. Hemicellulose content of water hyacinth was relatively high compared to that of cellulose, which is a rare case among plant biomass. Klass and Ghosh [15] reported hemicellulose content as high as 55% of TS in water hyacinth. The result indicated that water hyacinth leaves could be a source of cellulose for bioconversion. Water hyacinth also contains appreciable amounts of crude protein, which could provide nitrogen source in any bioconversion process.

3.2 Water Hyacinth Cellulose Acid and Enzyme Hydrolysate Preparation

The effect of both pretreatment temperature and time on water hyacinth biomass is shown in Tables 1, 2 and 3, representing glucose concentration and reducing sugars concentration, respectively, in the pretreated solids at the different operational conditions assayed.

Table 2 Effect of temperature on average sugar composition of water hyacinth cellulose acid and enzyme hydrolysate.

Temperature (°C)	Components % weight (TSs)	
	Glucose	Reducing sugars
120	$3.82 \pm 0.09a$	$4.05 \pm 0.04a$
125	$4.20 \pm 0.05b$	$4.33 \pm 0.07b$
135	$4.44 \pm 0.02c$	$5.14 \pm 0.06c$

Values in the same column with the different letters are significantly different ($P < 0.05$).

The highest experimental glucose and reducing sugars were 5.81% and 8.52 respectively (1.5 wt% based on the mass of oven-dried water hyacinth) and was obtained at $T = 135$ °C for 30 min and 0.1 M H_2SO_4 . The temperature had a profound effect on the yield, with leading to higher yields while the pretreatment time after 30 min had not significant effect on the yield.

The main issue when pretreating lignocellulosic materials is to solubilize the hemicellulosic sugars keeping, at the same time, as much cellulose as possible in the pretreated solid that may be enzymatically hydrolysed. Dilute sulfuric acid hydrolysis (0.1 M) under autoclaving under pressure of 15 lb/inch² at 135 °C for 10 min and enzyme hydrolysis as described in materials and methods was very effective in releasing a good amount of sugar from water hyacinth leaves (Table 2). Higher temperature, higher yield of glucose and reducing sugars were released. Approximately 14% and 21% of glucose and reducing sugars were released at 120 °C less than that of at 135 °C, respectively. So, temperature at 135 °C was suitable to hydrolyse the water hyacinth leaves for sugar production. Approximately 40% of the reducing sugars were released in the first 10 min of autoclaving and enzyme hydrolysis, at 30 min of autoclaving and enzyme hydrolysis, 99% of the reducing sugars were released after which only slight increase was observed.

After 30 min of autoclaving, sugar yield was 100% of dry biomass of D-glucose, 5.81% (Table 3). These sugars were derived primarily from cellulose component. The glucose yield (5.81%) was rather high, showing that cellulose almost practically hydrolyzed.

Pretreated water hyacinth sample was hydrolyzed by mixed enzymes (cellulose, xylanase and pectinase) at pH 5.0, 50 °C for 24 h. The hydrolysis yield was 57.07% after 24 h of hydrolysis, and prolonged hydrolysis time beyond 24 h helped little in increasing the hydrolysis yield (data not shown).

The improvement in enzymatic hydrolysis yields detected concomitantly with pretreatment time (Table 2) may be attributable, among other reasons, to the solubilization of the hemicelluloses fraction of the residue [17]. It seems that not only hemicellulose solubilization, but some other factors like cellulose crystallinity, surface area accessibility or lignin content also affect enzymatic hydrolysis [18]. The maximum overall sugar yield (57.07 g sugar/100 g raw material) was obtained at 135 °C and 0.1 M acid concentration. The enhancement detected in overall sugar yield is mainly attributable to a significant increase of hemicellulose-derived sugars in prehydrolysates when using dilute sulfuric acid. Lloyd and Wyman [19] reported an increase of the overall sugar yield from 56.8% (when using water pretreated corn stover) up to 93% by dilute sulphuric acid pretreatment. This improvement was attributed to the increase of xylan solubilization much faster than xylose degradation, due to acid action. Even if glucose is the most suitable fermentable sugar, the fermentation of C5 sugars, essential to the economy of the global process, is also

Table 3 Effect of time on average sugar composition of water hyacinth cellulose acid and enzyme hydrolysate.

Time (min)	Components % weight (TSs)	
	Glucose	Reducing sugars
10	4.44 ± 0.02a	5.14 ± 0.06a
30	5.81 ± 0.07b	8.52 ± 0.06b
60	5.80 ± 0.04b	8.51 ± 0.11b
90	5.84 ± 0.04b	8.56 ± 0.12b

Values in the same column with the different letters are significantly different ($P < 0.05$).

deserving a great deal of interest [20]. The pretreatment and enzymatic hydrolysis optimization are key features to be considered in order to reach the maximization of the overall sugar yield, taking into account all fermentable sugars.

3.3 Fermentation

The amounts of ethanol yield of water hyacinth leaves obtained by diluted acid steam pretreatment with enzymatic saccharification are given in Table 5. As summarized in Table 5, the ethanol yields per unit biomass were comparable to those reported for other agricultural biomasses, i.e., 0.16-0.27 g g-dry⁻¹ for water hyacinth leaves. It was found that different microorganism stain produced different amount of ethanol. The maximum amount of ethanol was obtained from fermentation of co-culture of *S. cerevisiae* TISTR5048 with *C. tropicalis* TISTR5045, followed by *S. cerevisiae* KM1195, *S. cerevisiae* TISTR5048, and *S. cerevisiae* KM7253. It was also found that *S. cerevisiae* KM1195 was suitable mono-culture for fermentation of the water hyacinth leaves. The results indicated that ethanol production depended on microorganism stain.

Since the chemical composition of cellulose acid hydrolysate is complex and could be expected to contain unknown, potentially toxic elements [21-23], the fermentation performance of the *S. cerevisiae* and *C. tropicalis* were evaluated in a simulated synthetic hydrolysate medium, the composition of which was designed and formulated to mimic the water hyacinth cellulose acid hydrolysate with respect to reducing sugars. The time-course for growth, sequential utilization of sugars, and ethanol production is shown (Fig. 1). *S. cerevisiae* and *C. tropicalis* consumed glucose and mannose. After hexoses were exhausted, xylose assimilation began. Xylose consumption was total, since no increase in the ethanol concentration occurred during its utilization. Sequential utilization of sugars have been reported by many authors [24-27]. The fermentation parameters for both yield

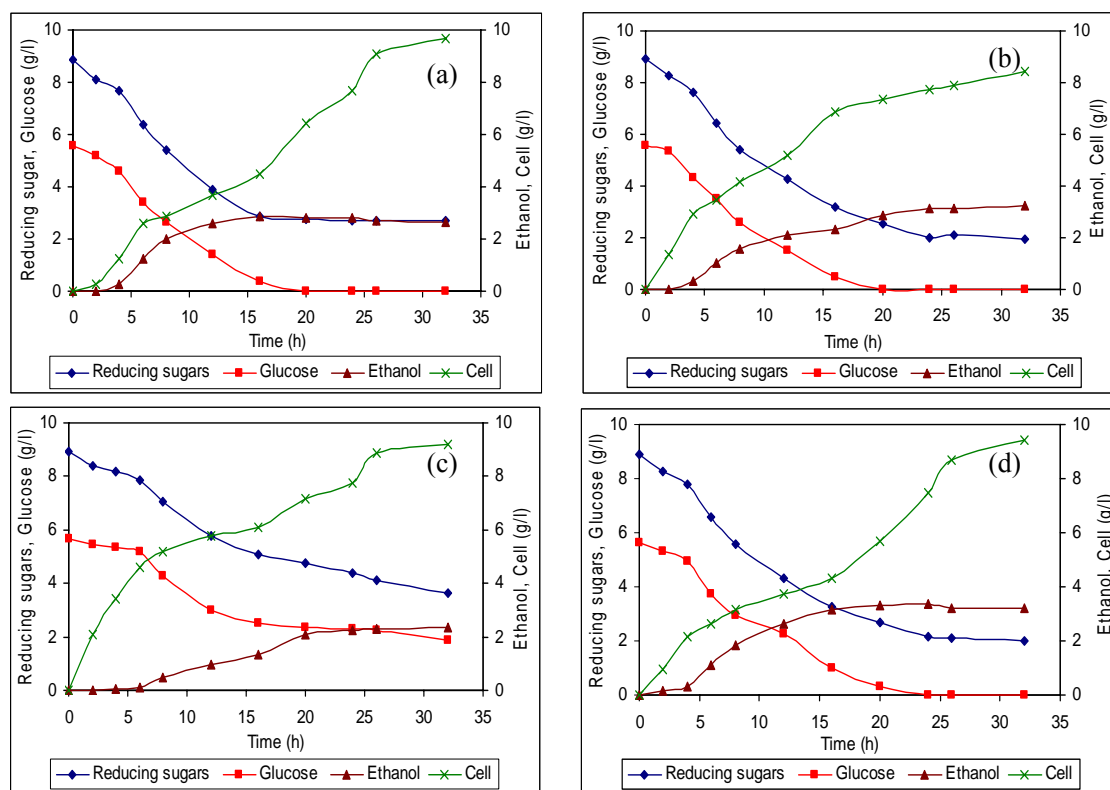


Fig. 1 The time course of growth, utilization of reducing sugars and glucose and ethanol concentration by *S. cerevisiae* TISTR5048 (a), *S. cerevisiae* KM1195 (b), *S. cerevisiae* KM7253 (c) and co-culture of *S. cerevisiae* TISTR5048 and *C. tropicalis* TISTR5045 (d) at 30 ± 0.2 °C and $\text{pH } 5.0 \pm 0.2$ using simulated synthetic hydrolysate medium.

and productivity are summarized (Table 4). At an inoculation cell density of the co-culture was about $0.25 \text{ g}\cdot\text{L}^{-1}$.

The highest values of ethanol yield per unit biomass (C_E), the maximum ethanol production (P_{\max}), ethanol production rate (Q_E) and product (ethanol) yield coefficient ($Y_{p/s}$) were found to be $0.27 \text{ g (g-biomass)}^{-1}$, 3.42 , 0.22 g/L/hour and $0.51 \text{ g (g-total sugar)}^{-1}$, respectively, by the fermentation of co-culture of *S. cerevisiae* TISTR5048 and *C. tropicalis* TISTR5045. The lowest values of ethanol yield per unit biomass (C_E), the maximum ethanol production (P_{\max}), ethanol production rate (Q_E) and product (ethanol) yield coefficient ($Y_{p/s}$) were found to be $0.16 \text{ g (g-biomass)}^{-1}$, 2.27 , 0.09 g/L/hour and $0.41 \text{ g (g-total sugar)}^{-1}$, respectively, by the fermentation of mono-culture of *S. cerevisiae* KM7253. It was found that mono-culture of *S. cerevisiae* KM1195 could produce relatively high ethanol yield almost equal to the co-culture (Table 4).

Table 4 Fermentation parameters of the mono-culture and co-culture of yeasts when grown in the water hyacinth cellulose acid and enzyme hydrolysate and simulated synthetic hydrolysate medium.

Strains	C_E	P_{\max}	Q_E	$Y_{p/s}$
SHF with mono-culture				
<i>S. cerevisiae</i> TISTR5048	0.19	2.84	0.21	0.45
<i>S. cerevisiae</i> KM1195	0.24	3.29	0.17	0.47
<i>S. cerevisiae</i> KM7253	0.16	2.27	0.09	0.41
SHF with co-culture incubation of				
<i>S. cerevisiae</i> TISTR5048 with <i>C. tropicalis</i> TISTR5045	0.27	3.42	0.22	0.51

C_E : Ethanol yield per unit biomass ($\text{g (g-biomass)}^{-1}$);

P_{\max} : Maximum ethanol production (g/L);

Q_E : Ethanol production rate (g/L/hour);

$Y_{p/s}$: Product (ethanol) yield coefficient ($\text{g (g-total sugar)}^{-1}$).

In fact, *S. cerevisiae* is unable to convert the C5-sugars present in hemicellulose, but *C. tropicalis* has the enzymatic machinery to ferment them. Fermentation of hydrolyzate from lignocellulosic residues is necessary to produce alcohol. For that purpose, both pentose-utilizing yeast strains (*C. tropicalis*) [32],

Table 5 Ethanol yields per unit biomass from various biomasses.

Biomass	Pretreatment	Fermentation mode	Fermentation strain	C _E	Reference
Water hyacinth leaves	Diluted acid steam pretreatment	SHF	<i>S. cerevisiae</i> TISTR5048	0.19	This study
Water hyacinth leaves	Diluted acid steam pretreatment	SHF	<i>S. cerevisiae</i> KM1195	0.24	This study
Water hyacinth leaves	Diluted acid steam pretreatment	SHF	<i>S. cerevisiae</i> KM7253	0.16	This study
Water hyacinth leaves	Diluted acid steam pretreatment	SHF	*	0.27	This study
Sorghum straw **	Diluted acid steam pretreatment	SHF	<i>S. cerevisiae</i> Ethanol Red™	0.18	Ref. [28]
Rice straw	Ammonia fiber expansion	SHF	<i>S. cerevisiae</i> 424A(LNH-ST)	0.18	Ref. [29]
Wheat straw	Lime pretreatment	SHF	Recombinant <i>E.coli</i> strain FBR5	0.26	Ref. [30]
Sugar cane bagasse	Steam pretreatment	SHF	TMB3001	0.18	Ref. [31]

C_E: Ethanol yield per unit biomass (g·(g-biomass)⁻¹). *: *S. cerevisiae* TISTR5048 with *C. tropicalis* TISTR5045. **: variety YSS-9.

and non-pentose-utilizing yeast strains (*Saccharomyces cerevisiae*) [33] have been used.

Fig. 1d shows the time-course for growth, sugar utilization and ethanol concentration in the cellulose acid hydrolysate medium at initial pH 5.0 ± 0.2 of co-culture of *S. cerevisiae* and *C. tropicalis*. The fermentation parameters are summarized in Table 4. The yield (C_E) and productivities (P_{max}, Q_E and Y_{p/s}) increased 1.42-, 1.2-, 1.05 and 1.13-fold, respectively, when mono-culture of *S. cerevisiae* TISTR5048 was grown in a medium cellulose acid hydrolysate as compared with the co-culture of *S. cerevisiae* and *C. tropicalis*. The higher ethanol yield of co-culture was due to *C. tropicalis* can utilize a very large variety of carbon sources including many sugars, disaccharides, phenols, alkanes, alkane derivatives, and fatty acids [34] and it can convert xylose to ethanol under aerobic conditions. *Candida* species are considered strong candidates for thermotolerance and ethanol tolerance needed to produce ethanol from lignocellulosic biomass. Moreover, it has the ability to tolerate concentrations of lignin-like polyphenols that are highly toxic to other yeast species. *C. tropicalis* is known by its vigorous growth on various carbon sources, which makes it a good candidate for industrial production of ethanol from renewable energy sources [32]. The results showed that co-culture of *S. cerevisiae* and *C. tropicalis* fermentation employed for the treatment of cellulose acid hydrolysate has partially used reducing sugars as substrate and improved the

fermentability.

The fermentation period of co-culture comparing to mono-culture of *S. cerevisiae* KM1195 or *S. cerevisiae* KM7253 was also reduced to about 33%. However, the fermentation period of co-culture for the cellulose acid hydrolysate was rather similar to that obtained with *S. cerevisiae* TISTR5048 (Table 4). This shows that there might be some leftover reducing sugars in the treated cellulose acid hydrolysate that are not used in the fermentation performance of *S. cerevisiae* TISTR5048. Table 5 shows ethanol yield of water hyacinth leaves and typical agricultural wastes. The results shows that the ethanol yield per unit biomass (C_E) in the SHF from water hyacinth leaves was comparable or a little higher than that obtained using the other agricultural wastes, suggesting that the cellulose and starch in the biomass were sufficiently hydrolyzed by this enzymatic hydrolysis stage. In co-culture fermentation, the other sugars derived from hemicelluloses hydrolysis were used for ethanol production by *C. tropicalis* TISTR5045. It is suggested that co-fermentation be used for economic conversing of lignocelluloses to ethanol. This study demonstrates that co-culture of *S. cerevisiae* and *C. tropicalis* is a very attractive system for bioethanol production.

4. Conclusions

The maximum values of ethanol yield (C_E), productivity (P_{max}, Q_E and Y_{p/s}) and percent sugar utilization were 0.27 g·(g-biomass)⁻¹, 3.42, 0.22

g/L/hour and $0.51 \text{ g}(\text{g-total sugar})^{-1}$, and 77.4%, respectively, at temperature $30 \pm 0.2 \text{ }^\circ\text{C}$ and $\text{pH } 5.0 \pm 0.2$, when co-culture of *S. cerevisiae* TISTR5048 and *C. tropicalis* TISTR5045 was grown in treated cellulose hydrolysate medium. Fermentation by mono-culture of *S. cerevisiae* KM1195 at the same condition improves the ethanol yield and productivity compared to the other mono-culture of *S. cerevisiae* TISTR5048 or *S. cerevisiae* KM7253. Therefore, the fermentation of water hyacinth leaves for ethanol production was carried out in a high yield by optimum treatment and appropriated yeast strain.

Acknowledgments

This work was financed by National Research Council of Thailand. The authors would like to thank Faculty of Agriculture, Kasetsart University, Thailand for helpful support of facilities.

References

- [1] G. Hu, J.A. Heitmann, O.J. Rojas, Feedstock pretreatment strategies for producing ethanol from wood, bark, and forest residues, *BioResources* 3 (1) (2008) 270-294.
- [2] A.E. Farrell, R.J. Plevin, B.T. Turner, A.D. Jones, M. O'Hare, D.M. Kammen, Ethanol can contribute to energy and environmental goals, *Science* 311 (5760) (2006) 506-508.
- [3] B. Gopal, *Water Hyacinth*, Elsevier, New York, 1987.
- [4] T. Kikuchi, M. Takagi, E. Tokuhisa, T. Suzuki, W. Panjaitan, M. Yasuno, Water hyacinth (*Eichhornia crassipes*) as an indicator to show the absence of *Anopheles suncaicus* larvae, *Med. Entomol. Zool.* 48 (1) (1997) 11-18.
- [5] C.C. Gunnarsson, C.M. Petersen, Water hyacinths as a resource in agriculture and energy production: A literature review, *Waste Manage* 27 (2007) 117-129.
- [6] Association of Official Analytical Chemists (AOAC), *Methods of analysis of the association of official analytical chemists*, Washington DC, 1975.
- [7] J.B. Robertson, P.J. van Soest, The detergent system of analysis and its application to human foods, in: W.P.T. James, O. Thiander (Eds.), *The Analysis of Dietary Fibers in Food*, Marcel Dekker, New York, 1981, pp. 123-158.
- [8] G.L. Miller, Use of dinitrosalicylic acid reagent for determination of reducing sugars, *Anal Chem* 31 (1959) 426-428.
- [9] A.M. Abdelhamid, A.A. Gabr, Evaluation of water hyacinth as feed for ruminants, *Arch. Anim. Nutr. (Archiv fuer Tierernahrung)* 41 (7/8) (1991) 745-756.
- [10] S. Bolenz, H. Omran, K. Gierschner, Treatments of water hyacinth tissue to obtain useful products, *Biol. Wastes* 33 (4) (1990) 263-274.
- [11] H.N. Chanakya, S. Borgaonkar, G. Meena, K.S. Jagadish, Solid phase biogas production with garbage or water hyacinth, *Bioresour Technol* 46 (1993) 227-231.
- [12] V. Patel, M. Desai, D. Madamwar, Thermochemical pretreatment of water hyacinth for improved biomethanation, *Appl. Biochem. Biotechnol.* 42 (1993) 67-74.
- [13] K. Poddar, L. Mandal, G.C. Banerjee, Studies on water hyacinth (*Eichhornia crassipes*) – Chemical composition of the plant and water from different habitats, *Indian Veterin J.* 68 (1991) 833-837.
- [14] A. Sharma, Eradication and utilization of water hyacinth: A review, *Curr. Sci. (India)* 40 (1971) 51-55.
- [15] D.L. Klass, S. Ghosh, Methane production by anaerobic digestion of water hyacinth (*Eichhornia crassipes*), in: D. L. Klass, G.H. Emert (Eds.), *Fuel from Biomass and Wastes*, Ann Arbor Science Publication Inc, MI, USA, 1981, pp. 129-148.
- [16] B.C. Wolverton, R.C. McDonald, Energy from vascular plant waste water treatment system, *Econ. Bot.* 35 (1981) 224-232.
- [17] M.A. Kabel, G. Bos, J. Zeevalking, A.G.J. Voragen, H.A. Schols, Effect of pretreatment severity on xylan solubility and enzymatic breakdown of the remaining cellulose from wheat straw, *Bioresour Technol* 98 (2007) 2034-2042.
- [18] L. Laureano-Perez, F. Teymouri, H. Alizadeh, B.E. Dale, Understanding factors that limit enzymatic hydrolysis of biomass, *Appl. Biochem. Biotechnol.* (121-124) (2005) 1081-1099.
- [19] T.A. Lloyd, C.E. Wyman, Combined sugar yields for dilute sulfuric acid pretreatment of corn stover followed by enzymatic hydrolysis of the remaining solids, *Bioresour Technol* 96 (2005) 1967-1977.
- [20] B.C. Saha, Hemicellulose bioconversion, *J. Ind. Microbiol. Biotechnol.* 30 (2003) 279-291.
- [21] J.E. Fein, S.R. Tallim, F.R. Lawford, Evaluation of D-xylose fermenting yeasts for utilization of a wood-derived hemicellulose hydrolysate, *Can. J. Microbiol.* (30) (1984) 682-690.
- [22] N. Nishikawa, R. Sutcliffe, J.N. Saddler, The influence of lignin degradation products on xylose fermentation by *Klebsiella pneumonia*, *Appl. Microbiol. Biotechnol.* 27 (1988) 549-552.
- [23] F.R. Frazer, T.A. McCaskey, Wood hydrolysate treatments for improved fermentation of wood sugars to 2,3-butandiol, *Biomass* 18 (1989) 31-42.
- [24] T.W. Jeffries, H.K. Sreenath, Fermentation of

- hemicellulose sugars and sugar mixture by *Candida shehatae*, *Biotechnol. Bioeng.* 31 (1988) 502-506.
- [25] J.P. Delgenes, R. Moletta, J.M. Navarro, Fermentation of D-xylose, D-glucose, and L-arabinose mixture by *Pichia stipitis*: effect of the oxygen transfer rate on fermentation performance, *Biotechnol. Bioeng.* 34 (1989) 398-402.
- [26] T. Bjorling, B. Lindman, Evaluation of xylose fermenting yeasts for ethanol production from spent-sulfite liquor, *Enzyme Microb Technol* 11 (1989) 240-246.
- [27] M.D. Ferrari, E. Neirotti, C. Albornoz, E. Saucedo, Ethanol production from Eucalyptus wood hemicellulose hydrolysate by *Pichia stipitis*, *Biotechnol. Bioeng.* 40 (1992) 753-759.
- [28] S. Mehmood, M. Gulfranz, N.F. Rana, A. Ahmad, B.K. Ahring, N. Minhas, et al., Ethanol production from *Sorghum bicolor* using both separate and simultaneous saccharification and fermentation in batch and fed batch systems, *Afr. J. Biotechnol.* 8 (12) (2009) 2857-2865.
- [29] C. Zhong, M.W. Lau, V. Balan, B.E. Dale, Y.J. Yuan, Optimization of enzymatic hydrolysis and ethanol fermentation from AFEX-treated rice straw, *Appl. Microbiol. Biotechnol.* 84(4) (2009) 667-676.
- [30] B.C. Saha, M.A. Cotta, Enzymatic hydrolysis and fermentation of lime pretreated wheat straw to ethanol, *J. Chem. Technol. Biotechnol.* 82 (10) (2007) 913-919.
- [31] C. Martin, M. Galbe, C.F. Wahlbom, B. Hahn-Hagerdal, L.J. Jonsson, Ethanol production from enzymatic hydrolysates of sugarcane bagasse using recombinant xylose-utilising *Saccharomyces cerevisiae*, *Enzyme. Microb. Technol.* 31 (2002) 274-282.
- [32] I. Ballestros, M. Ballestros, A. Cabanas, J. Carrasco, C. Martin, M.J. Negro, et al., Selection of thermotolerant yeasts for simultaneous saccharification and fermentation of cellulose to ethanol, *Appl. Biochem. Biotechnol.* (28-29) (1991) 307-315.
- [33] S.H. Krishna, K. Prasanthi, G.V. Chowdary, C. Ayyanna, Simultaneous saccharification and fermentation of pretreated sugarcane leaves to ethanol, *Process Biochem.* 33 (1998) 825-830.
- [34] H. Kawachi, K. Shimizu, H. Atomi, S. Sanuki, M. Ueda, A. Tanaka, Gene analysis of an NADP-linked isocitrate dehydrogenase localized in peroxisomes of the n-alkane-assimilating yeast *Candida tropicalis*, *Eur. J. Biochem.* 250 (1997) 205-211.

Allelopathic Potentials of Some Crop Residues on the Germination and Seedling Growth of *Chromolaena Odoratum* L.

Modupe Janet Ayeni and Joshua Kayode

Department of Plant Science, University of Ado-Ekiti, Ado-Ekiti 361010, Nigeria

Received: October 25, 2010 / Accepted: November 26, 2010 / Published: March 30, 2011.

Abstract: The allelopathic effects of aqueous extracts of rice husk (*Orza sativa* L.) and sorghum stem (*Sorghum bicolor* L.) on the germination and seedling growth of *Chromolaena odoratum* L. were investigated. The extracts of the two crop residues exhibited inhibitory effects on the germination and seedling growth of *Chromolaena odoratum* L. The degree of retardation demonstrated in both extracts was concentration dependent. However the results obtained revealed that the retardation was more pronounced in the rice husk extract-treated seeds. However statistical analysis ($P < 0.05\%$ level) revealed that the degrees of inhibition of radicle and plumule obtained from various extracts treated seeds of both extracts were not significantly different when compared to those obtained from the control experiments as well as those obtained from the varying extract concentrations.

Key words: Allelopathy, crop residues, germination, seedling growth, *Chromolaena odoratum*.

1. Introduction

Allelochemicals produced by some plants are now known to influence the growth and development of neighboring plants, when they are released into the environment. The allelochemicals may be present in various parts of the plant, they can be found in the roots, leaves, flowers, fruits, seeds or stems from where they are released into the soil through various processes such as volatilization, root exudation, leaching and decomposition of plant residues [1, 2].

Allelochemicals affect germination and growth of other species by, blocking hydrolysis of nutrient reserve and cell division [3, 4] causing significant reductions in the growth of plumule and radicle of various crops [5], retardation of seedling growth and poor seedling survival [6, 7].

Recent initiatives are now suggesting the use of allelochemicals in weed control particularly now that the extensive use of herbicides in modern agriculture has given rise to concerns about herbicides residues in the environment and the rapid development of herbicides resistant by weeds. It is now known that over 295 weed biotypes have acquired resistant to important herbicides. Thus non-herbicidal innovation, such as enhancing crop allelopathic ability are increasingly being required in managing weed populations [8]. It is expected that weed suppression by crop allelopathy during the early establishment period would reduce the need for commercial herbicides. Also allelochemicals being biosynthesized herbicides are easily biodegradable and are believed to be much safer than herbicides [9, 10].

In Nigeria, allelopathic studies reported so far had concentrated on the allelopathic potentials of weeds on agricultural crops. Some of these included the studies of Tijani-Eniola and Fawusi [11] on *Chromolaena odoratum*, Kayode [12-14] on *Euphorbia heterophylla*,

Modupe Janet Ayeni, M.Sc., research fields: plant physiology and ecology. E-mail: jayeni@yahoo.com.

Corresponding author: Joshua Kayode, Ph.D., professor, research fields: agroforestry and ecology. E-mail: jokayode@ymail.com.

Aspilia africana and *Calotropis procera* respectively. No study had been reported so far on allelopathic potentials of crop residues in the country. Consequent on the above, the study being reported here aimed at examining the allelopathic effects of aqueous extracts from residues of sorghum stem and rice husks on *Chromolaena odoratum*, a commonly occurring weed in Nigeria.

2. Materials and Methods

Freshly removed rice husks were obtained from a rice mill situated in Igbemo-Ekiti, a town situated at about 20 km from the campus of the University of Ado Ekiti while mature sorghum stem were harvested from the experimental farm of the Department of Plant Science, University of Ado- Ekiti, Ado-Ekiti, Nigeria. The sorghum stem were cut into small pieces to facilitate drying. The rice husks and sorghum were air dried for three weeks and later pounded using pestle and mortar.

Portions of 5 g, 10 g, 15 g, 20 g and 25 g were measured out from rice husks and sorghum residues. Each portion was soaked in 200 mL of distilled water in 500 mL conical flasks. The mixtures were shaken intermittently and left over for 24 hrs. The extracts were later filtered using Whatman No.1 filter paper and the filtrates were used afresh, some portions were kept inside the refrigerator for further usage.

Two layers of Whatman No. 1 filter papers were put in each Petri dish of 9 cm diameter and five seeds of *Chromolaena odoratum* obtained from a farm in University of Ado-Ekiti campus were placed in each Petri dish. The Petri dishes were moistened daily with the five different filtrates using syringe and needle. The experiments were replicated ten times in each treatment of the extracts.

Control experiments were set up with Petri dishes moistened with distilled water and were replicated ten times. All the Petri dishes were put in growth chamber at room temperature. The seeds were considered germinated upon radicle emergence. The germination, radicle and plumule growth elongation measurements were recorded at 24 hrs interval for six days. The results obtained from

the extracts treated seeds were compared, statistically using t-test analysis, to those obtained from the control experiments.

3. Results and Discussion

The effects of the aqueous extracts derived from rice husks and sorghum stem on the germination of *Chromolaena odoratum* are shown in Tables 1 and 2 respectively. The extracts brought about considerable inhibition on the germination of *Chromolaena odoratum* seeds. For example, in the rice husk extract (Table 1), while 30% of the seeds had germinated at 48 hrs experimental time in the control, no germination was obtained in all concentrations of the extract treated seeds until the 72 hrs experimental time. Similarly in the sorghum extracts, 26% of the seeds germinated at 48 hrs experimental time in the control experiment while only 12%, 6%, and 2% of the seeds germinated at the 5 g, 10 g and 15 g extract concentrations respectively, with no germination occurring at the 20 g and 25 g extract concentrations (Table 2).

In both extracts, the degree of inhibition increased with the increase in the concentration of the extracts suggesting that the effects of the extracts were concentration dependent. Table 1 revealed that while 12% of the seeds had germinated in the 5 g rice husk extract concentration in the 72 hrs experimental time, only 10%, 8%, 8%, and 6% of the seeds respectively germinated in the 10 g, 15 g, 20 g and 25 g extract concentrations. Also, in the sorghum extracts (Table 2), 26% of the seeds germinated at 5 g extract concentration but 10%, 8%, 6% and 4% germinated at 10 g, 15 g, 20 g and 25 g extract concentrations respectively. It was apparent from the results that the rice husk extracts had more inhibitory effects on the germination of *C. odoratum* as no germination was recorded until 72hrs of the experiment (Table 1).

The results of the effects of the aqueous extracts from the rice husks and sorghum stem on the radicle lengths of *Chromolaena odoratum* were shown in Tables 3 and 4 respectively. The radicle lengths were retarded in all the

Table 1 Effects of aqueous extracts from rice husk on the germination of *Chomoleana odoratum* L. (%).

Extracts (g/200mL)	Experimental time (Hrs)					
	24	48	72	96	120	144
5	0	0	12	14	16	2
10	0	0	10	14	6	4
15	0	0	8	12	10	4
20	0	0	8	12	6	4
25	0	0	6	10	4	2
Control	0	30	18	8	2	2

Table 2 Effects of aqueous extracts sorghum extracts on the germination of *Chromoleana odoratum* L. (%).

Extracts (g/200mL)	Experimental time (Hrs)					
	24	48	72	96	120	144
5	0	12	26	12	2	0
10	0	6	10	16	12	0
15	0	2	8	6	6	18
20	0	0	6	5	4	10
25	0	0	4	4	5	8
Control	0	26	16	10	6	4

extracts treated seeds when their lengths were compared to those from the control experiments. In the rice husk extract (Table 3), the radicle length in the control experiment was 0.22 cm at 144 hrs experimental time while the lengths were 0.14 cm, 0.08 cm, 0.07 cm, 0.05 cm and 0.05 cm respectively in the 5 g, 10 g, 15 g, 20 g and 25 g extract concentrations. Similar trend was obtained in the sorghum extract experiments (Table 4). Tables 3 and 4 also revealed that the degree of retardation in the radicle lengths increased with increase in concentration of the extracts, with the rice husk extracts demonstrating more inhibitory effects on the *C. odoratum* seeds as no radicle growth was recorded until 96 hrs of the experiment.

The aqueous extracts also retarded plumule lengths of *C. odoratum* (Tables 5 and 6). No growth was recorded in both extracts until 96 hrs of the experiment. The results tend to suggest that plumule growth was more retarded by both extracts than the radicle (Tables 5 and 6). These findings corroborated the earlier assertions of Turk et al. [5] that some plant residues demonstrated allelopathic effects by inhibiting plumule and radical lengths. However statistical analysis ($P < 0.05\%$ level) revealed that there were no significant

Table 3 Effects of aqueous extracts of rice on radical length (cm) of *Chromoleana odoratum* L.

Extracts (g/200mL)	Experimental time (Hrs)					
	24	48	72	96	120	144
5	0	0	0	0.03	0.09	0.14
10	0	0	0	0.02	0.06	0.08
15	0	0	0	0.02	0.05	0.07
20	0	0	0	0.01	0.04	0.05
25	0	0	0	0.01	0.04	0.05
Control	0	0	0.03	0.12	0.21	0.22

Table 4 Effects of aqueous extracts of sorghum extracts on radical length (cm) of *Chromoleana odoratum* L.

Extracts (g/200mL)	Experimental time (Hrs)					
	24	48	72	96	120	144
5	0	0	0.01	0.09	0.21	0.22
10	0	0	0	0.02	0.07	0.09
15	0	0	0	0	0.02	0.03
20	0	0	0	0	0.01	0.02
25	0	0	0	0	0.01	0.02
Control	0	0	0.04	0.13	0.24	0.27

Table 5 Effects of aqueous extracts of rice on plumule length (cm) of *Chromoleana odoratum*.

Extracts (g/200mL)	Experimental time (Hrs)					
	24	48	72	96	120	144
5	0	0	0	0.01	0.05	0.07
10	0	0	0	0.01	0.03	0.05
15	0	0	0	0	0.02	0.03
20	0	0	0	0	0.02	0.03
25	0	0	0	0	0.01	0.03
Control	0	0	0.01	0.07	0.14	0.15

Table 6 Effects of aqueous sorghum extracts on plumule length (cm) of *Chromoleana odoratum* L.

Extracts (g/200mL)	Experimental time (Hrs)					
	24	48	72	96	120	144
5	0	0	0	0.06	0.15	0.18
10	0	0	0	0.01	0.05	0.06
15	0	0	0	0	0.01	0.02
20	0	0	0	0	0.01	0.01
25	0	0	0	0	0.01	0.01
Control	0	0	0	0.08	0.17	0.02

differences in the plumule and radicle lengths of the extract treated seeds and those of the control in the two different aqueous extracts used in this study. Also there were no significant differences in the plumule and radical lengths in the varying concentrations of the two extracts.

4. Conclusion

Results from this study were similar to that of Jadher and Goyanar [15] who observed that the percentage seed germination, plumule and radicle lengths of rice and cowpea were decreased with increasing concentrations of *Acacia auriculiformis* leaf leachates and also with Quadhia [16] who observed that extracts from *C. gigantea* inhibited radicle and plumule growths of *Lathyrus sativa*.

Plant residues are now known to contain allelochemicals which are released into the soil during decomposition. Previous study by Cherney et al. [17] found vanillic acid, p-hydroxy-benzaldehyde, p-coumaric acid and Ferullic acid in four hybrids of sorghum. Cheema [18] revealed that mature sorghum contained acids-gallic acid, caffeic acid, ferulic acid and chlorogenic acid. Two other compounds dhurin and sorgoleone were also associated with allelopathy of sorghum. Sorgoleone is a long chain hydroxyquinone exuded from growing sorghum root. Rice allelopathy could be attributed to P-hydroxyl benzoic acid, syringic acid, vallinic, ferullic, P-coumaric and o-hydrophenyl acetic acid it contained [19]. Also Ebana et al. [20] identified seven Quantitative Trait Loci (QTLs) present in the plant that could be associated with rice allelopathic activity. Hence these chemicals must have been responsible for the inhibition of seed germination and the retardation of seedling growths of radicle and plumule of *Chromolaena odoratum* in this study. Further research activities might be required to enhance the utilization of this allelopathic feature of the plant residues in the control of this weed.

References

- [1] E.L. Rice, Allelopathy, Academic Press, New York, USA, 1984.
- [2] C.H. Chuo, The role of allelopathy in agro ecosystem studies from tropical Taiwan, Ecological Studies 78 (1990) 105-121.
- [3] B.P. Patil, Effects of *Gliricidia maculata* L. extracts on field crops, Allelopathy J. 1 (1994) 118-120.
- [4] A. Irshad, Z.A. Cheema, Influence of some plant water extracts on the germination and seedling growth of Barnyard grass (*E. crus-galli* L. Beauv), Pak. J. Sci. Ind. Res. 43 (3) (2004) 222-226.
- [5] M.A. Turk, A.M. Tawaha, Allelopathic effects of black mustard (*Brassica nigra* L.) on germination and growth of Wild oat (*Avena fatua* L.), Crop Protection 22 (4) (2003) 673-677.
- [6] S.G. Conard, Inhibition of *Abies concolor* radicle growth by extracts of *Ceanothus velutinus*, Madrono 32 (1985) 118-121.
- [7] A.E. Smith, The potential allelopathic characteristics of bitter sneezeweed (*Helenium amarum*), Weed Sci. 37 (1990) 665-669.
- [8] H. Wu, J. Pratley, D. Lemerle, T. Haig, Crop cultivars with allelopathic capacity, Weed Research 39 (1999) 171-180.
- [9] E.L. Rice, Biological Control of Weeds and Plant Diseases, Univ. Oklahoma Press, Norman, USA, 1995.
- [10] F.E. Dayan, J.G. Romagni, M. Tellez, A. Rimando, S. Duke, Managing weeds with biosynthesized products, Pecti. Outl. 10 (1999) 185-188.
- [11] H.A. Tijani-Eniola, O.A. Fawusi, Allelopathic activities of crude methanol extracts of Siam weed and wild poinsettia on seed germination and seedling growth of tomato, Nigerian Journal of Weed Science 2 (1989) 15-20.
- [12] J. Kayode, Allelopathic effects of aqueous extracts of *Euphorbia heterophylla* L. on the radicle and plumule growth of cowpea (*Vigna unguiculata* L. Walp), Bioscience Research Communications 10 (1) (1998) 23-26.
- [13] J. Kayode, Allelopathic potentials of aqueous extracts of *Aspilia africana* on radicle and plumule growth of *Zea mays*, Journal of Physical and Biological Sciences 2 (2004) 43-46.
- [14] J. Kayode, Allelopathic effects of aqueous extracts of *Calotropis procera* on the germination and seedling growth of maize, Pakistan Journal of Scientific and Industrial Research 47 (1) (2004) 69-72.
- [15] B.B. Jadhar, B. Gayanar, Allelopathic effects of *Acacia auriculiformis* in the germination of rice and cowpea, Indian J. Plant Phys. 1 (1992) 86-89.
- [16] A. Qudhia, Allelopathic effects of some obnoxious weeds on germination and seedlings Vigor of *Lathyrus sativas*, FABIS Newsletter 42 (1999).
- [17] D.J. Cherney, J.A. Patterson, J.H. Cherney, J.D. Axtell, Fibre and soluble phenolic monomer composition of morphological components of Sorghum stover, J. Sci. Food Agric. 54 (1991) 645-649.
- [18] Z.A. Cheema, Weed control in weed through sorghum allelochemicals, Unpublished Ph.D Thesis, Department of Agronomy, University of Agriculture, Faisalabad, Pakistan, 1988.
- [19] G.H. Chuo, S.J. Chiou, Antointoxication mechanism of rice II, Effects of culture treatments of the chemical nature on paddy soil on rice productivity, J. Chem. Eco. 5 (1979) 839-859.
- [20] K. Ebana, W.G. Yan, R.H. Dilday, H. Namai, K. Okuno, Analysis of QTL associated with the allelopathic effect of rice using water-soluble extracts, Breeding Science 51 (2001) 47-51.

Conditional Mutations in *Drosophila*

Boris F. Chadov, Nina B. Fedorova, Eugenia V. Chadova and Helena A. Khotskina

Institute of Cytology and Genetics, Siberian Department of Russian Academy of Sciences, Novosibirsk 630090, Russia

Received: June 24, 2010 / Accepted: September 16, 2010 / Published: March 30, 2011.

Abstract: The aim of this study was to obtain unusual mutations called conditional. The mutations manifest in some, not all representatives of a species. Collections of these mutations in chromosomes X, 2, and 3 of *Drosophila melanogaster* were established. Sex of fly or chromosomal rearrangement was the conditions providing “manifestation- non manifestation” of these mutations. The mutations differ from the usual by a set of properties. The salient differences in addition to conditional manifestation include: manifestation dependence on the spatial arrangement of chromosomal material in the genome, parental effects (maternal or paternal) of the mutant, capacity for transferring the genome from stable to unstable state. It is suggested that conditional mutations are mutant variants of *Drosophila* regulatory genes contained by the large Genomic Regulatory Network of *Drosophila*. Thus, the genes of this category can be detected by using special breeding procedures, mutations of these genes have unusual manifestation.

Key words: Conditional mutation, penetrance, modification, morphosis, dominant lethal, genetic instability, energy dissipation, *Drosophila melanogaster*.

1. Introduction

Gene mutation has been defined as hereditary change in the DNA sequence and also the manifestation of the DNA change at the organismal level. In a diploid organism, some changes are manifest when present in a single dose (dominant mutations), others when present in a double dose in the genome (recessive mutations). In both cases, dealt with is the autonomous manifestation of mutations that is independent of the rest of the genome. Classical genetics is concerned with precisely these “true” mutations. At the level of the phenotype these mutations manifest themselves outwardly, because present in any individual of a given species.

There exist mutations of another type. They are called conditional mutations [1]. The mutation of this category is not manifest in every individual of a given species, but only in some of them. Manifestation depends on the concrete genotype of an individual. As opposed to mutations with

incomplete penetrance whose causes of non-manifestation are undetermined [2, 3], genetic conditions of “manifestation-non- manifestation” for conditional mutations are clearly defined by the method used to obtain them. In the course of work with conditional mutations, mutations with lethal manifestation, conditional dominant lethals (CDLs) were obtained first [4, 5], then conditional mutants with visible manifestation [6]. Sex of mutant individual [4, 5] and chromosomal rearrangement [7] were conditions providing manifestation. At this juncture, local DNA damage whose manifestation at the organismal level depends (entirely or partly) on the structure of the other regions of the genome is called a conditional mutation.

Classical genetics is based on mutations with autonomous manifestation. From these mutations, the laws of inheritance of characters were derived, the concept of the existence of genes, particulate and independent units of inheritance was developed, chromosome theory of inheritance was worked out.

The authors are at the dawn of study specifically addressed to mutations with non-autonomous

Corresponding author: Boris F. Chadov, Ph.D., academician, research field: genetics. E-mail: chadov@bionet.nsc.ru.

manifestation, although they deserve attention not less than those with autonomous manifestation. There is good reason for believing that mutations with non-autonomous manifestation forms particular traits of the living organism. These traits compose the invariant part of the external appearance of the organism of a concrete species [1]. Such traits cannot be obtained by using autonomous mutations. Here, the authors review the study of conditional mutations conducted from 2000 when, using a specific approach, the first batch of conditional mutants in *Drosophila melanogaster* was obtained [4, 5].

2. Recovery of Conditional Mutations: Ways and Means

Mutations were induced by ionizing radiation. The searched mutation was manifested in one genetic background and not in another. Fig. 1 presents schematically how conditional dominant lethals (CDLs) were obtained in the X chromosome of *Drosophila melanogaster* [1, 7]. Males were gamma-irradiated and crossed with the attached-X females. Sons of the parents were individually crossed to yellow females. Sons that gave no female progeny from this cross were chosen as mutants. These sons contained the conditional mutation in the X chromosome. The mutation did not affect their viability and fertility. However, once in the female yellow/+ genome, it became a dominant lethal: daughters died at the embryonic stage, and the adult progeny was composed of sons only. In this exemplary case, the conditional mutation is a dominant lethal. It is called conditional because manifest as lethal in mutant females heterozygous for yellow (one genetic background) and not in mutant males (another genetic background).

Another cross was used to recover CDLs in chromosome 2 [1] (Fig. 2). The mutation behaved as a dominant lethal in the case when homologous chromosome 2 was structurally normal (one genetic background), but not as a lethal in the case when the

homologous chromosome contained the *Ins(2LR)Curly* inversion (another genetic background). The lethal effect of the mutation obtained with this scheme is sex-independent, unlike the case of the CDL in the X chromosome [4].

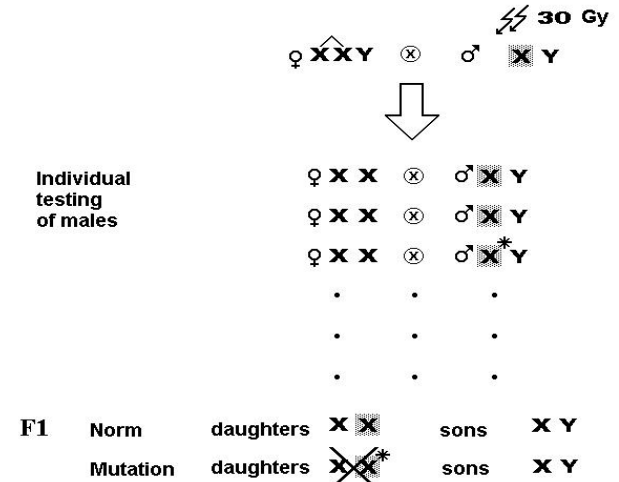


Fig. 1 Detection of conditional dominant lethals in the X chromosome of *D. melanogaster*. Gamma – irradiated (30 Gy) *Drosophila* males were mated to females containing attached-X chromosomes. Sons of this progeny were individually crossed to yellow females. X-chromosome of the irradiated male is hatched. Asterisk indicates the same chromosome with mutation. In contrast to sons without lethal mutation, those that received the X with dominant lethal were daughterless.

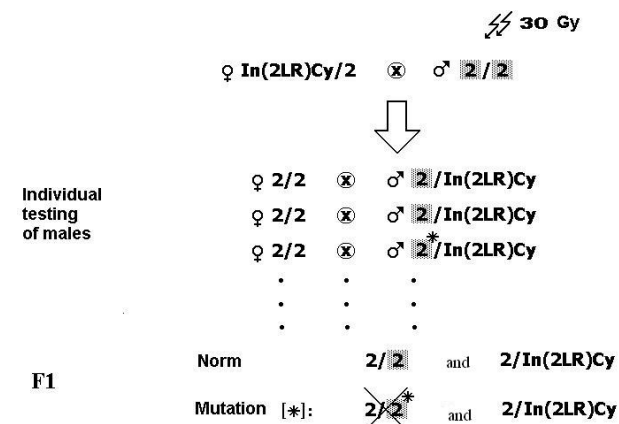


Fig. 2 Detection of conditional dominant lethals in chromosome 2 of *D. melanogaster*. Gamma-irradiated (30 Gy) *Drosophila* males were crossed to females containing inversion *In(2LR)Cy* with dominant marker *Curly* in one chromosome 2. Sons having this chromosome together with irradiated chromosome 2 (hatched) were individually crossed to yellow females, containing structurally normal chromosomes 2. Sons receiving chromosome 2 with dominant lethal produced *Curly* progeny only.

Yet another way of obtaining CDL in the X took advantage of a modified version of recovery of recessive lethal mutation by Muller-5 method [7]. A collection of these mutants as $\underline{l}/Muller-5$ females was mated to males with a marked structurally normal X chromosome. Four cultures with a recessive lethal mutation in the X showing unusual properties were distinguished. The lethal was a typical recessive lethal in cross of the $\underline{l}/Muller-5$ female with the *Muller-5* male (the routine way of maintaining recessive lethal mutations in the X chromosome). In this cross, mutant female yielded one type of daughters ($\underline{l}/Muller-5$) and one type of sons *In(1)M-5*. However, in crosses of $\underline{l}/Muller-5$ females to structurally normal males, there appeared sons of two, not one, phenotypes: *Muller-5* and wild type. The latter received also the recessive allele from the mutant female, but it ceased to behave as a lethal because the father's genotype with the inversion was changed [7].

In all the three schemes, conditional mutations were recessive lethal in an unusual background. In the two first schemes, the mutations became dominant lethals upon transfer to a provocative background. In the third, the mutation ceased being lethal upon transfer to it. "Usual" and "provocative" backgrounds are arbitrary. What is important is that the response of mutations to change in the genetic background is reproducible in repeated crosses [4, 5]. All the three approaches to recovery of the mutations were given the common term the "method of conditional lethals" [1].

In one of the experiments, after testing for dominant lethality using *yellow* females, four mutant females produced homozygotes with visible mutant phenotype (Fig. 3). These were only females that had two mutant X chromosomes. As for males that had one mutant X, their phenotype was normal. We initially designated these conditional mutations *dimorphic* because the same mutation could give rise to two phenotypes: one in the male (normal), the other in the female (mutant) [6].

The phenotype of females of the first dimorphic line, the authors designated *shorter leg*, was bizarre: oblique,

pulled down wings, absence of the second radial vein of wing, lymph filled blister on the wing, much shorter legs than normal with one segment of tarsus instead of the usual five (Fig. 3a). Females of the second line had both wings blistered (Fig. 3b). Females of the third and fourth lines had an interrupted second vein of wing with a somewhat differently located interruption. A female and a male of the "interrupted vein" line are shown in Fig. 3c, and Fig. 3d. Males of all the four lines were phenotypically normal.

These four mutants may also be referred to conditional mutations, but with visible phenotype. Sex here is the condition providing manifestation of the mutant phenotype. It will be recalled that these mutations also show the dominant lethal phenotype (absence of daughters) manifest in crosses of the mutant male to *yellow* females.

The formation of unilateral defects of individual development, termed morphoses, is a distinguishing feature of all the obtained conditional mutations. This phenomenon will be described in the "Conditional mutation and genomic instability" section. The fourth approach for obtaining conditional mutations relied on

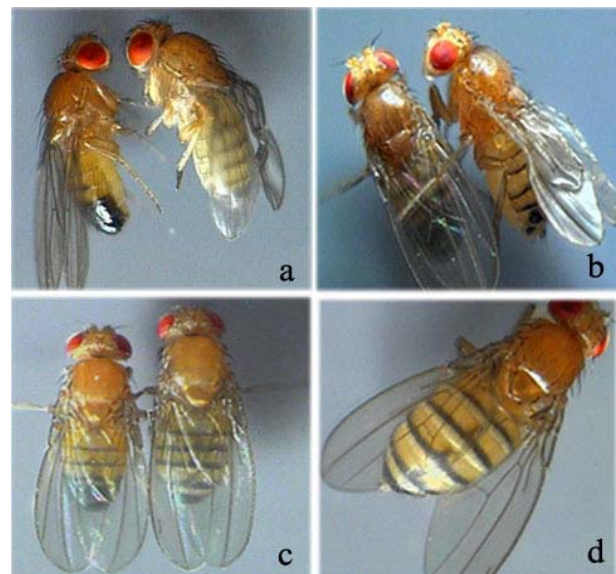


Fig. 3 Dimorphic mutations.

(a) "shorter leg" mutation: females have shorter legs, oblique wings, blisters on wings; males normal; (b) mutation "blisters on wings" female have blistered wings, male normal; (c) mutation "interrupted vein": radial vein L2 interrupted in females; males normal; (d) mutation "interrupted vein" in female (large-scale).

the property of forming morphoses. The idea was to select the individuals with developmental defects i.e. morphoses from the first generation progeny of irradiated parents. These flies were then tested for content of recessive lethals [8].

With this methodological strategy, yet another conditional mutation with visible phenotype was revealed. It was designated “*Small barrel*” (*Smba*) [8, 9]. It is located in chromosome 2. Pupae and adults were reduced in body size (Fig. 4). The mutation is dominant so far as the *Smba* phenotype arises in heterozygotes for the mutation. The mutation is conditional in that the presence of the *In(2LR)Curly* inversion in homologous chromosome 2 is needed for the mutant phenotype to appear (Figs. 4a and 4b). Maintenance of the mutant chromosome together with the *In(2LR)Plum* inversion chromosome causes disappearance of the *Smba* phenotype (Fig. 4b). The other features of the mutation will be dealt with below.

The total number of experiments the authors performed from 2000 to recover conditional mutations in *D. melanogaster* is 8. As a result, 60 CDLs were identified in the X chromosome, 10 in chromosome 2, and 4 in chromosome 3. Six mutations had visible

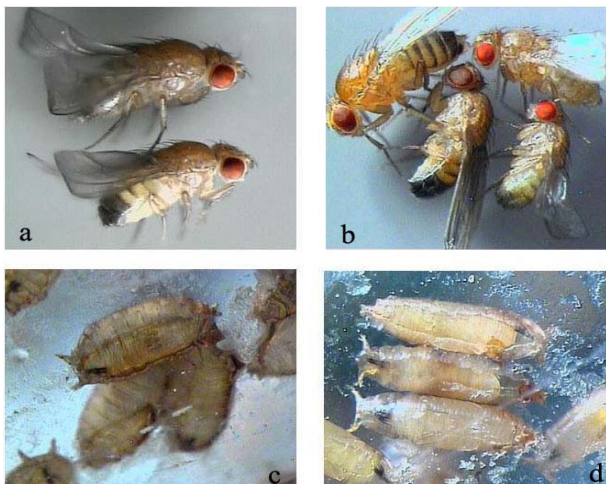


Fig. 4 Mutation “*Small barrel*” (*Smba*).

(a) general appearance of a mutant female and a male in the stock *Smba/In(2LR)Cy*; (b) left, female and male in stock *Smba/In(2LR)Pm* (body size normal); right, female and male in the stock *Smba/In(2LR)Cy* (body size reduced); (c) short pupae of stock *Smba/In(2LR)Cy*; (d) pupae of normal size of stock *Smba/In(2LR)Pm*.

phenotype. The total number of identified mutations will be defined after their complete localization on the polytene chromosome map. Work is underway.

3. Maintenance of Conditional Mutations in Culture

Conditional mutations were maintained in cultures, depending on specificity of each conditional mutation. CDLs in the X chromosome were maintained in two ways (Fig. 5). With the first way (Fig. 5A), the culture contained females, heterozygous for the mutation and the *Muller-5* inversion. Females produced *In(1)M-5* sons and “+” sons with the mutation. The latter were fertile, but no +/+ females appeared in the culture because the effect of the mutation was lethal in the homozygous females. With the second way (Fig. 5B), the mutant X chromosome was transmitted paternally only so that females in the line contained attached-X chromosomes.

Conditional recessive mutations in the X, derived from typical recessive lethals by the Muller-5 method, were maintained as typical recessive lethals in the X chromosome.

CDLs in chromosome 2 were maintained in culture containing the *In(2LR)Curly* inversion. Homozygotes for every one chromosome 2 were lethal.

CDLs in chromosome 3 were maintained in culture containing the *In(3LR)Dichaete* inversion. Homozygotes for every one chromosomes 3 were lethal.

Four dominant lethals in the X chromosome with the visible manifestation were maintained in the homozygous condition. In these cultures, homozygous females were mutant in phenotype, while hemizygous males were phenotypically normal.

Smba mutation was maintained in *In(2LR)Curly/Smba* culture. Homozygotes for *Smba* and *In(2LR)Curly* were lethal.

4. Factors That Affect Manifestation of Conditional Mutations

Sex was the prevailing influential factor. CDLs in

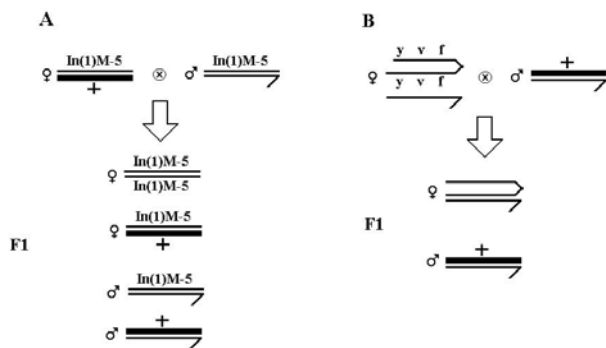


Fig. 5 Two ways for maintenance of conditional dominant mutations in the X chromosome.

(A) in heterozygous state in females containing an inverted *Muller-5* chromosome (*In(1) Muller-5*) and the mutant X (+, solid line). Daughters *In(1) Muller-5/+* and sons + receive the mutant X. Daughters *In(1) Muller-5/ In(1) Muller-5* and sons *In(1) Muller-5* do not receive the mutant X; (B) in culture with *attached-X* chromosomes (*y v f/y v f*). Sons, not daughters receive the mutant X chromosome.

the X are dominant or recessive lethals in females only. They exert no lethal effect in males. The four conditional mutations with visible manifestation also emerged, in female only.

Structural reorganization of the genome was the second factor that affected manifestation of conditional mutations. The presence of CDL in the male X caused absence of daughters in the progeny of *yellow* (*y/y*) females, in contrast, daughters appeared among progeny of females: 1) *y/y; In(2LR)Curly/+*, 2) *y/y;*

In(2LR)Pm/+, and 3) *y/y; In(3LR)D/+* with chromosomal rearrangements in chromosome 2 or 3 (Table 1) [7]. In these cases, chromosomal rearrangements in nonhomologous chromosomes were the modifying factors.

While lethal mutations in compound with a structurally normal *yellow* X gave a lethal combination, these mutations in compound with an inverted *Muller-5* chromosome did not give lethal combination. CDLs in the X chromosome are maintained precisely in this combination in our laboratory collection, as indicated above. Chromosomal rearrangement in homologous chromosome is also a factor eliminating lethal CDL effect.

Rearrangement in homologous chromosome is crucial for manifestation of conditional mutations in chromosome 2. Test for obtainment of conditional mutations in chromosome 2 [1, 10] is entirely based on the dependency of mutation manifestation on chromosomal rearrangement. Heterozygotes with mutations were viable only in the case when homologous chromosome 2 contained the *In(2LR)Curly* inversion. They became dominant lethals when the homolog was structurally normal.

Interaction among distinct DNA changes was the third factor on which manifestation of conditional

Table 1 Effect of rearranged chromosome 2 and 3 on lethality CDLs in the X chromosome delivered to the zygote together with sperm. {crosses of mutant males to females: 1) *y/y; +/+*; 2) *y/y; +/ In(2LR)Cy*; 3) *y/y; +/ In(2LR)Pm* and 4) *y/y; +/ In(3LR)D*}.

Male mutation line	Female <i>y/y; +/+</i>		Female <i>y/y; +/ Cy</i>				Female <i>y/y; +/ Pm</i>				Female <i>y/y; +/ D</i>			
	Daughter +	Son <i>y</i>	Daughter +		Son <i>y</i>		Daughter +		Son <i>y</i>		Daughter +		Son <i>y</i>	
			<i>Cy+</i>	<i>Cy</i>	<i>Cy+</i>	<i>Cy</i>	<i>Pm+</i>	<i>Pm</i>	<i>Pm+</i>	<i>Pm</i>	<i>D+</i>	<i>D</i>	<i>D+</i>	<i>D</i>
1	–	230	–	–	178	163	–	–	107	57	–	–	115	8
2	–	230	14	13	127	134	4	3	70	72	–	–	42	7
4	–	270	9	4	185	159	1	7	86	81	–	–	162	7
5	–	197	23	21	80	95	6	4	47	48	–	–	37	3
27	2	167	1	0	102	113	2	1	53	65	–	–	9	2
29	4	163	32	27	71	56	26	24	55	20	6	6	88	10
30	–	184	15	13	81	76	9	12	60	47	–	–	38	6
31	–	242	32	20	127	102	5	4	28	29	–	–	70	6
32	–	197	22	10	90	77	9	17	36	32	–	–	48	2
33	–	209	20	18	95	101	11	8	87	47	24	2	85	12
34	–	140	11	14	88	101	25	20	68	54	–	10	103	3

Table 2 Lethal interaction of mutation *Smba* in chromosome 2 in reciprocal crosses with deficiencies of chromosome 2.

Deficiencies of chromosome 2		Phenotypes of progeny of crosses			
		♀ <i>Smba</i> /Cy × ♂ <i>Df</i> (2)/Cy		♀ <i>Df</i> (2)/Cy × ♂ <i>Smba</i> /Cy	
Region	Deficiency	Cy	Cy+	Cy	Cy+
Df(2)	Df 3138	79	-	223	-
35B4-6; 35B10-C1	Df 3588	75	-	241	-
	Df 5574	111	-	147	-
	Df 5680	97	-	188	-
Df(2)	Df 7414	158	1	169	-
54B2; 54B17-C4	Df 7445	113	-	179	-
	Df 9596	125	1	255	-
Df(2)	Df 1547	141	-	174	-
55A; 55F	Df 6780	119	1	46	-

mutation depended. This dependency among defects in different chromosome regions was detected for the conditional mutation “*Small barrel*”. In a cross of the mutation to a set of deficiencies for chromosome 2 composed of 105 cultures, 9 deficiencies that responded to the presence of *Smba* were identified. A double heterozygote for *Smba* and deficiency proved to be lethal (Table 2). Nine responsive deficiencies cover three distinct regions of chromosome 2: 1) 35B4-6; 35B10-C1; 2) 54B2; 54B17-C4 and 3) 55A; 55F. Thus, three regions of chromosome 2 were damaged, one in the left, two in the right arm [9].

By recombination in the centromeric *pr - cn* region, *Smba* chromosome split into two crossover chromosomes containing the left or the right arm of mutant chromosome *Smba*. Cultures with either the left or right arm mutant chromosome ceased yielding the “*Small barrel*” phenotype. This meant that mutant phenotype resulted from combined effect of damage in the right and left arms of chromosome 2.

Thus, at this juncture, there is reason for regarding ordering of genetic material in the genome and structure of distinct chromosome regions in the genome as conditions for manifestation of a whole class of gene mutations the authors designated conditional. It cannot be ruled out that, with further study, the number of conditions related to genome structure will increase.

5. Conditionality and Unconditionality of Mutations

The usual mutations are manifest as dominant or recessive in all individuals of a given species. These mutations and their manifestation type may be called unconditional. Conditional mutations have at least two manifestations, in the presence or in the absence of the necessary conditions. In addition to the conditional manifestations, the conditional mutations we detected, had *unconditional* manifestations.

To illustrate, CDLs in the X selected on the basis of testing with *yellow* females, represent recessive lethals: they are not manifest in the heterozygote, but lethal in the homozygote. Recessive lethality is the unconditional manifestation of the detected mutations. However, these lethals cannot be referred to the usual recessive lethals in the X so far as mutations are without lethal effect in the male genome. As known, the usual recessive lethals in the X chromosome are lethal both in the homozygote female and in the hemizygote male.

Conditionality of recessive lethals in the X chromosome obtained by the modified Muller-5 method were manifested in the cross to structurally normal males: normal sons, along with M-5 sons, started to appear in progeny of mutant females. However, lethality loss was restricted to males, no females homozygous for

lethal chromosomes appeared. Therefore, lethality is a conditional trait in mutant males and, in contrast, it is a nonconditional trait in mutant females.

Dominant lethality of conditional mutations in chromosome 2 is due to the presence/absence of a specific inversion in homologous chromosome 2. The dominant lethality trait is conditional. However, these conditional mutations manifest in the hetero- and homozygote as typical recessive lethals. The recessive lethality is an unconditional trait of these conditional mutations.

Four conditional mutations with visible manifestation showed sex-dependence of mutant manifestation. In the cross to *yellow* females, they behave as dominant lethals, i.e., they are conditional mutants, too. Judged by the result of all the tests, these four mutations may be regarded as conditional in the sense of the word.

Smba is the most freakish of all the conditional mutations we recovered. Besides visible dominant manifestation, which is dependent on the presence of a particular rearrangement in the homolog, *Smba* also exerts conditional recessive lethal effect. Conditionality for visible phenotype and recessive lethality are not interrelated. For example, interrelations with deficiencies in chromosome 2 in regions 35 and 55 are the same for *In(2LR)Curly/Smba* and *In(2LR)Plum/Smba*, despite the fact that the former visibly manifest mutation and the latter do not.

Thus, manifestation of two types: conditional and unconditional, combined in the obtained mutations. It cannot be ruled out that unconditional manifestation may become conditional in some genotypes. Such genotypes are yet to be identified. The presence of not one, but two at least manifestation types, justifies the assumption that mutation may cause damage of not a single, rather several gene products, as observed for genes with alternative splicing.

6. Conditional Mutations and Genomic Instability

Conditional mutations make the genome pass from

the stable to unstable state. This was inferred from observations from previous studies on a set of phenomena in conditional mutations [11, 12]. Instability appeared in heterozygotes for conditional mutations. Stating it otherwise, instability was a dominant manifestation of mutations.

Loss of the lethal effect of CDLs in the X. CDLs were maintained in culture with the *In(1)Muller-5* inversion and with the attached-X chromosomes. A year after mutations were obtained, replicate test using *yellow* females revealed that some mutations lost their lethal effect. Mutant males started to produce daughters in crosses to *yellow* females. This prompted us to perform the test with *yellow* females regularly involving members of the entire collection of CDLs in the X. During the period of four years, of the 22 CDLs maintained on the attached Xs, 9 entirely lost lethal effect, while 4 became incompletely lethal (Table 3).

Loss of manifestation of visible mutations in the counterpart chromosome 2. Lethal mutations in chromosome 2 maintained in heterozygote state with the inverted chromosome *In(2LR)Cy*, *Cy Bl L⁴* are characterized by “loss” of dominant mutations *Cy*, *Bl*, and *L⁴* in the inverted chromosome. During the six months of mutation maintenance, 20 cases of manifestation loss occurred: one marker in 17, 2 markers in 3 (Fig. 6). In laboratory cultures, all the 3 visible dominant mutations are very well expressed and completely dominant. During the many years of maintenance of the *In(2LR)Cy*, *Cy Bl L⁴* complex in different cultures of laboratory stock, no loss of the dominant markers *Cy*, *Bl*, and *L⁴* was observed.

Loss of the X chromosome in meiosis of CDL mutants. A high number of patriclinous *yellow* sons appeared in crosses of females heterozygous for CDL and the *Muller-5* inversion with *yellow* males. They were found to occur in 20 CDL progenies of the 21 (Table 4). The frequency of patriclinous males in CDL progeny was 12.3%, on average, as opposed to the control in which it was 0%. The formation of patriclinous males is evidence of loss and nondisjunction of the X chromosome in female meiosis in individuals with CDLs.

Table 3 Loss of lethal manifestation of CDLs in the X chromosome obtained in 2000 (maintained in attached-X cultures).

CDL line	2000 year		2001 year		2002 year		2004 year	
	Total number of progeny	Proportion of daughters	Total number of progeny	Proportion of daughters	Total number of progeny	Proportion of daughters	Total number of progeny	Proportion of daughters
1	191	0.00	13	*0.46	199	*0.42	77	*0.52
2	435	0.00	4	0.00	259	0.02	36	0.03
3	180	0.00	20	*0.45	311	*0.43	95	*0.50
5	303	0.02	33	*0.45	265	*0.60	83	*0.41
6	283	0.02	2	0.00	111	0.02	39	0.05
7	100	0.00	3	0.00	44	**0.27	63	*0.40
8	216	0.07	5	0.00	90	0.09	49	**0.14
9	529	0.00	7	0.00	169	**0.21	81	0.04
10	297	0.04	7	0.00	69	**0.30	57	**0.26
11	409	0.06	4	0.00	82	**0.18	55	**0.16
26	89	0.01	-	0.00	175	0.07	40	0.02
27	161	0.00	29	*0.69	113	*0.56	92	*0.49
29	76	0.00	4	0.00	171	*0.54	80	*0.51
30	115	0.00	8	0.00	109	0.02	71	0.00
31	189	0.00	8	0.00	138	0.01	70	0.03
32	198	0.00	4	0.00	74	0.00	53	0.02
33	234	0.00	23	*0.52	214	*0.56	88	*0.51
34	198	0.00	-	0.00	62	0.00	54	0.02
35	115	0.04	12	0.00	162	**0.13	83	*0.48
36	110	0.01	5	0.00	106	0.02	54	0.07
38	84	0.01	3	0.00	80	*0.56	51	**0.33
41	100	0.01	5	0.00	331	*0.49	106	*0.52

* -loss mutation lethal effect; ** - decrease in mutation lethal effect.

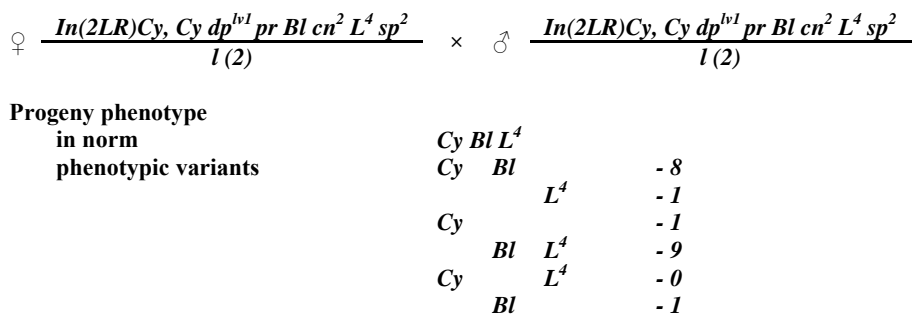


Fig. 6 Loss of dominant markers *Curly, Bristle, Lobe* in inverted chromosome *In(2LR)Cy, Cy Bl L⁴* under condition that is in compound with chromosome 2 containing the conditional mutation. In culture of conditional lethal *l(2)*, mutant chromosome 2 have the counterpart homolog containing three dominant markers *Cy, Bl, L⁴*. Twenty losses of dominant marker manifestation were found; of the 17 were manifestation loss of a single marker and 3 of two.

Formation of secondary mutations. In the course of maintenance of cultures with CDLs, some of the newly arisen phenotypic changes were inherited. Mutations with complete penetrance of the type: *plexus, dumpy, brown*, and also with incomplete penetrance of the type:

cubitus interruptus, radius incompletus, black arose. Visible mutations also continued to arise alone or as suites one after another, in progeny, occasionally over successive generations.

Loss of the X chromosome in somatic tissue:

Table 4 Progeny of females *In(1)Muller-5, w^a B/+* containing mutation in crosses to *yellow* males*.

Male line	Progeny phenotype					Total number of progeny	Proportion of patroclinous <i>yellow</i> males in progeny
	Female		Male				
	B	+	w ^a B	+	y		
1	65	5	56	1	47	174	0.27
2	93	59	80	31	54	317	0.17
3	28	19	32	23	20	122	0.16
5	52	63	60	53	14	242	0.06
6	147	105	102	74	73	501	0.15
7	124	86	64	68	35	377	0.09
8	83	88	72	89	31	363	0.09
9	88	44	37	31	50	250	0.20
10	50	49	51	44	0	194	0.00
11	76	66	72	63	14	291	0.05
27	54	38	36	21	49	198	0.25
29	77	85	44	60	19	285	0.07
30	109	70	85	58	56	378	0.15
31	132	89	83	77	79	460	0.17
32	57	65	57	44	3	226	0.01
33	45	31	53	23	10	162	0.06
34	99	63	42	27	33	264	0.13
35	142	56	85	37	124	444	0.28
36	138	97	98	100	48	481	0.10
38	140	107	119	120	18	504	0.04
41	93	88	66	84	28	359	0.08
Control	262	258	178	239	0	937	0.00

* - mutation was in chromosome (+).

formation of mosaics and gynandromorphs.

Chromosome loss was also observed in mitotically dividing cells of mutants. Segments of male tissue were formed in daughters of mutant females. For example, yellow spots in a grey background in female *y/+*, eyes of phenotype *Bar* and *white-apricot* in females *Bar/+* and *w^a/+*, respectively (Fig. 7). These cases may be explained by loss of the normal X chromosome in somatic tissue cells. Loss of the X during early embryogenesis gave rise to gynandromorphs – mosaics combined female and male body parts.

Formation of single and mass modifications.

Waves of phenocopies appeared in cultures of mutations. The same phenotype of known mutations

kept appearing in one or several generations: *black*, *purple*, *brown*, *trident*, among others; after wave-like appearance the recurring phenotypes disappeared. Fig. 8 gives examples of modifications. Attempts to fix the newly arisen phenotype failed.

Mass formation of morphoses. The new phenotypes in CDL cultures occurred in the background of the appearance of various unilateral morphological defects of clonal type designated *morphoses*. They are not inherited, but inheritance of CDL provides morphosis formation in every culture generation. Table 5 presents the formation frequencies of morphoses in one of the cultures. Fig. 9 shows some of the morphoses. The number of morphoses in our collection of digital

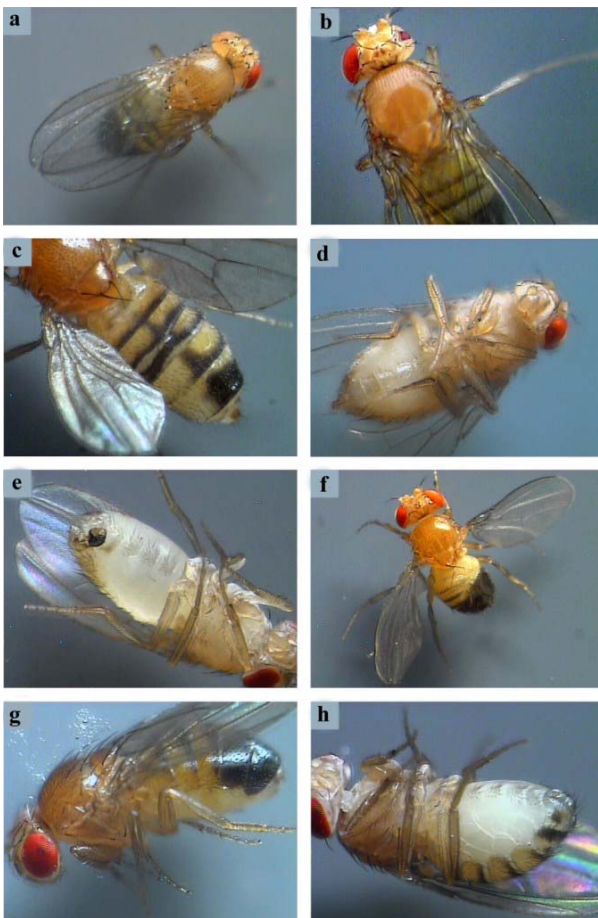


Fig. 7 Mosaics and gynandromorphs in lines with conditional dominant lethal.

(a) eyes of different color in progeny of $w^a/+$ female; (b) different shape of eyes in progeny of $B/+$ female; (c) colorless left half of last tergites; (d) right half of head and thorax are of male type (stripe-like eye, sex comb on prothoracic leg, yellow color legs), rest of the body of female type; (e) left part of the body is of male type (yellow body, shorter wing), right part of female type; mixed structure of external genitals; (f) left half of the abdomen of female type color, right, of male type; (g) left part of the fly is of male type; (h) right part of the same fly have female appearance.

images of morphoses is as high as 1,000. All parts of the fly's body were covered by morphoses of the type "+ tissue" or "- tissue".

Formation frequency of modifications, secondary mutations, morphoses. The data for the formation of new phenotypes (mutations, modifications and morphoses) are based on observations made on stocks during their maintenance or rarely during their involvement in experiment. In those cases, when the

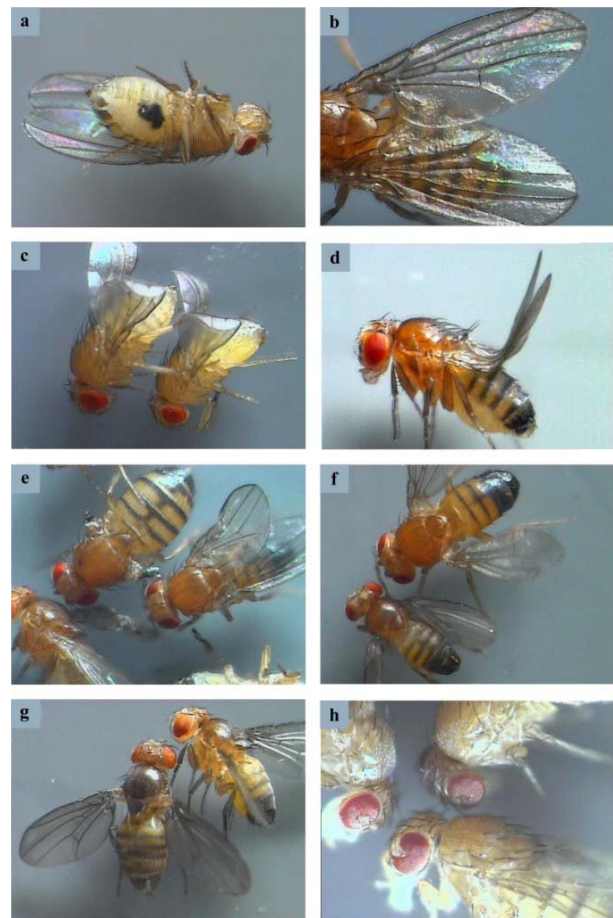


Fig. 8 Modifications in lines with conditional dominant lethal.

(a) "melanoma", body areas of dark color; (b) "blistered wing"; (c) pale "dwarves", freakishly small flies of light yellow color; (d) vertical curved wings; (e) "shortened wings": wings reduced to complete disappearance; (f) "dwarf", male reduced in body size, normal color, top - male of normal size; (g) female "black", right, male of normal color; (h) three individuals with the same defect of eyes.

facts themselves were unexpected, frequencies could not be rigorously estimated. However, it may be stated that: 1) the frequencies of the detected events were by several orders greater than in cultures with the usual *Drosophila* mutations; 2) the process of formation of new phenotypes was irregular, it is most intense immediately after mutations were obtained and in the case of hybridization to another culture; 3) the formation of novelties tended to damp during maintenance in culture.

Transposition of mobile element *mdg-2* in dimorphic lines. Two mutants with visible phenotypic

Table 5 Formation of morphoses in progeny of “*mutation/y² ec cv ct v f*” female.

Stock of mutation	Total number of progeny	Proportion of progeny with morphoses (%)
2	485	11.3
3	244	10.7
5	362	26.0
6	596	2.4
7	317	17.9
8	405	14.0
9	428	14.7
10	271	6.6
11	390	16.7
27	108	6.5
29	471	3.2
30	243	11.1
31	417	8.6
32	415	12.8
33	97	15.5
34	737	10.9
35	478	11.9
36	327	25.7
38	126	3.2
41	408	16.4
Control	3687	0

manifestation appeared among CDLs in the X derived from isogenic line. These were “*shorter-leg*” and “*interrupted vein*”. The mutations are dimorphic: females of mutant, males of normal phenotype. Transcriptional activity level of mobile element *mdg-2* was studied in “*shorter-leg*” and “*interrupted vein*” lines, and in two control line. The first control line was initial isogenic line itself, the second control line were obtained after irradiation in the same generation with “*shorter-leg*” and “*interrupted vein*” mutations. The dimorphic lines significantly differed from the initial isogenic and second control lines: line “*shorter-leg*” by insertions of element *mdg-2*, and line “*interrupted vein*” by its excision [13].

Thus, the presence of CDL results in genome destabilization: local destruction and reorganization. Destabilization effect in the genome is dominant and conditional. How long the effect will be maintained? This is an open question. Special observations will be required to estimate the time course of instability.

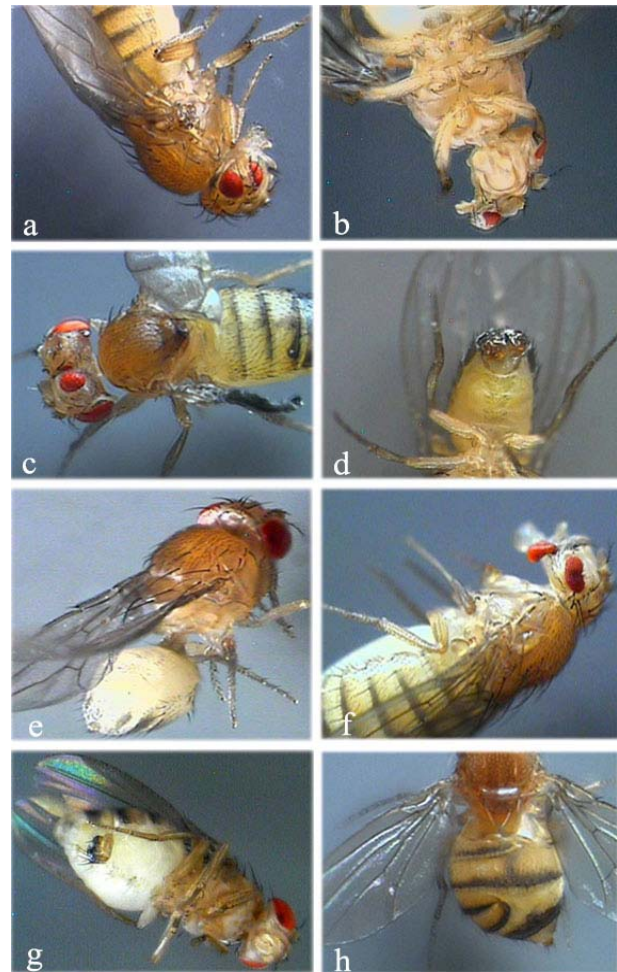


Fig. 9 Morphoses in lines with conditional dominant lethal. (a) and (b), two versions of a reduced head copy instead of eye; (c) two heads on one neck; (d) doubling of male external genitalia; (e) abdomen rotation by 180°; (f) eye division into two parts; (g) fragment of tergite on abdomen; (h) absence of two tergites on the right.

7. Increase in Energy Exchange in Individuals with Conditional Mutations

Increase in locomotor activity was observed after obtaining CDLs [1, 7]. Locomotor activity was studied using a special device (*Drosophila Monitor Activity, Model DAM2, TriKinetics Inc. USA*). Four lines with CDL in the X chromosome and two normal (control) lines were analyzed. Locomotor activity was estimated by the number of times a fly crossed the midline of the glass tube in which fly was placed. Locomotor activity was measured for 10 days. Fig. 10 shows hourly locomotion in 6 lines for 3 days. Diurnal rhythm and

prevalence of activity in mutant lines are seen. During the period of 10 days, all the 4 mutant lines showed locomotor activity significant higher than the control (Fig. 11, left histogram) [14].

Energy exchange was estimated by the method of indirect calorimetry in these 6 lines. Expired CO₂ expressed as mL per gram live weight for one hour exposure was studied in fly groups each consisting of 10 3-day old *Drosophila* males. The amount of expired CO₂ was measured in infrared gas analyzer. The CO₂ expiration values for all 4 mutant lines significantly exceeded those for the controls (Fig. 11, right histogram) [14].

Enhanced locomotor activity and respiration rates in mutants indicated that change in their energy status

resulted from CDL formation. This change was manifest as an increase in energy dissipation. Increase of energy dissipation in genetic mutants has not been previously described in the literature. Thus, CDL presence became the cause of an increase in energy dissipation in the organism [14].

8. Maternal and Paternal Effects of Conditional Mutations

The approach used to recover conditional mutations, allowed us to unequivocally assign a mutation to a particular chromosome pair. The localization was definite so that there was no need to reconsider it during further culture maintenance. However, the phenomenology of unusual mutation manifestation,

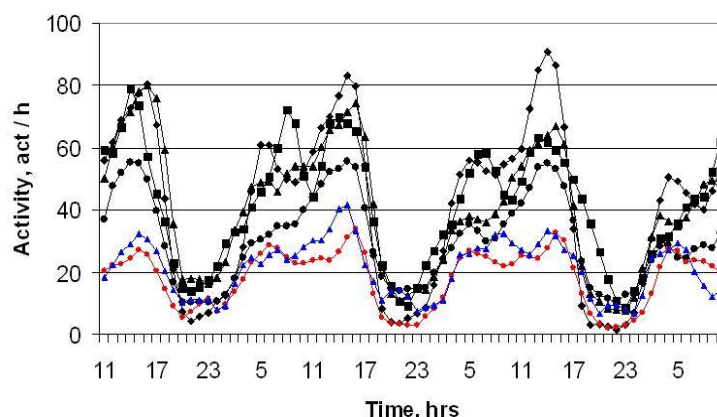


Fig. 10 Locomotor activity of an adults of *D. melanogaster* of 6 lines for 3 days. Four mutant lines: N7 (black diamond), N46 (black square), N101 (black circle), N103 (black triangle), and two control lines: N61 (light circle), N62 (light triangle). Along vertical line, number of times a fly crosses the tube midline, horizontal line, time of day, hrs.

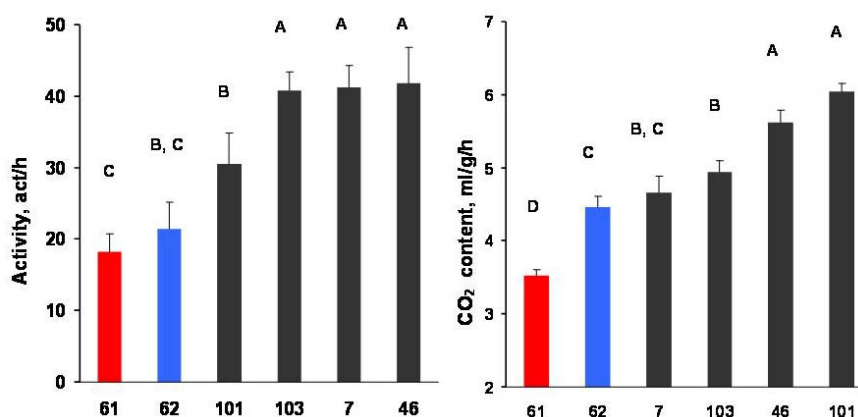


Fig. 11 Average diurnal locomotor activity (left panel) and CO₂ expiration (right panel) in control (No.61 and 62) and mutant (No.7, 46, 101, 103) lines.

Different letters above columns designate statistically significant different average values of locomotor activity ($F_{5, 123} = 7.34, P < 0.001$) and CO₂ expiration values ($F_{5, 148} = 31.89, P < 0.001$). Multiple comparisons of averages were done using the LSD test.

quite often showed an uncoupling between manifestation caused by a conditional mutation and its location. This uncoupling was expressed as maternal and paternal effects. Four examples follow.

Morphosis formation. When CDL in the X chromosome was maintained in the $l/In(1)M-5$ females (Fig. 5A), morphoses appeared not only in progeny with the mutant X, also in the mutant X-free progeny. This is a case of maternal inheritance of the capacity for mutation to give rise to morphoses in progeny. Morphoses were formed in progeny without CDL, when mutation was maintained paternally (Fig. 5B), too. Daughters, which did not receive the mutant X chromosome from the father, turned out to have morphoses [1]. Parental effect was causative in the capacity for inheritance of the property of giving rise to morphoses without inheritance of the mutations themselves.

Effect of the Y chromosome on the viability of males containing the CDL in the X. In *Drosophila*, males without the Y chromosome survived and could be obtained. If a son received the X with CDL from his mother, regardless of whether or not he got a Y chromosome, the son viability remained unaltered. By contrast, if a son received an X with CDL from his father, the son could not survive without the Y [1].

Parental effects on progeny of individuals containing CDLs in chromosome 3. Diallel reciprocal crosses between 4 lines containing CDL in one of chromosome 3 and inversion $In(3LR)Dichaete$ in the other 3 were performed (Table 6). If the direct cross ($\text{♀}55 \times \text{♂}46$) produced no progeny at all, the reciprocal cross yielded all the F1 classes at the expected ratio. No progeny was produced in cross ($\text{♀}34 \times \text{♂}46$), but progeny was arise in reversed cross ($\text{♀}46 \times \text{♂}34$). The difference in the reciprocal crosses could be considerable, not to the extent to be lethal. In cross $\text{♀}27 \times \text{♂}46$, the number of *Dichaete* progeny recovered proved to be 3.4 fold smaller (18.9%) than in the reverse cross (64.4%). So far as the set of progeny classes and their formation probability were the same in the reversed crosses, the difference in progeny between direct and reverse crosses could not be due to progeny viability.

The manifestation of the *Smba* mutation. This is a vivid example of parental effect. In the course of localization of this mutation, *Smba* males were crossed to females of 105 stocks with various deficiencies of chromosome 2. A 100% of progeny from every cross was of the *Smba* phenotype [9].

Taken together, all the above cases provide evidence indicating that the location of gene products, which

Table 6 Proportion of *Dichaete* progeny in reciprocal crosses of four lines *Dichaete/CDL(3),+* (No. 27, 34, 46, 55), containing conditional mutations in chromosome 3.

Reciprocal crosses	Progeny						Total number of progeny	<i>Dichaete</i> progeny (%)
	Norma			<i>Dichaete</i>				
	Females	Males	Total	Females	Males	Total		
$\text{♀}27 \times \text{♂}34$	49	47	96	20	13	33	129	25.58
$\text{♀}34 \times \text{♂}27$	56	41	97	114	67	181	278	65.11
$\text{♀}27 \times \text{♂}46$	132	147	279	34	31	65	344	18.90
$\text{♀}46 \times \text{♂}27$	63	68	131	102	135	237	368	64.40
$\text{♀}27 \times \text{♂}55$	88	158	246	29	28	57	303	18.81
$\text{♀}55 \times \text{♂}27$	37	30	67	97	59	156	223	70.00
$\text{♀}34 \times \text{♂}46$	0	0	0	0	0	0	0	0
$\text{♀}46 \times \text{♂}34$	73	95	168	109	95	204	372	54.80
$\text{♀}46 \times \text{♂}55$	145	166	311	264	279	543	854	63.60
$\text{♀}55 \times \text{♂}46$	0	0	0	0	0	0	0	0
$\text{♀}55 \times \text{♂}34$	0	0	0	81	65	146	146	100
$\text{♀}34 \times \text{♂}55$	0	0	0	114	91	205	205	100

formed on the mutant genes with conditional manifestation, is uncoupled from gene location. This uncoupling makes them markedly different from product formed on the classical genes. In the latter case, the gene and its product share a common location. Otherwise, classical genetics would simply not work.

9. Discussion

Modern genetics is based on the classical postulate of the existence of particulate independent units of inheritance. They are detected and mapped using methods applied to structurally - functionally independent units. The idea of independent genes is the cornerstone of population genetics and neo-Darwinian synthesis. In terms of other sciences, physiology in the first place, the living organism is a system and, like any other, should be composed of interdependent elements. Thus reasoning, genes in their manifestation should be dependent on each other. An element dependent and independent at the same time on the same factor is inconceivable. A way out from this impasse is by assuming that a living organism possesses elementary structures of two, at least, categories, one category of genes that are functionally dependent, the other independent of each other.

The idea of genes of two categories has been advanced some time ago. Promptly after the discovery of genes with incomplete penetrance, Timofeev-Resovskii has suggested two categories of genes, with some genes manifesting themselves in all, without exception, genotypes of a species, and others in some genotypes only [15, 16]. He coined the term the “constantly and variably manifesting themselves genes” to designate those of two categories [15]. The idea was short-lived. Timofeev-Resovskii modified it into the idea of dependence of manifestation of every gene on “the internal genotype conditions” [16].

The idea of the existence of a special category of genes (dependent on each other) underlies authors assumption of the existence of specific mutants the authors called them conditional. There is a broader

common biological foundation justifying the existence of these specific genes. These specific genes underlie similarity between individuals of the same species, as the authors would suggest [1]. Conditional mutations represent mutations in these genes.

The term “conditional” in application to gene mutations is already used for those whose manifestation is dependent on environmental conditions [17]. The authors extended the “conditional mutation” concept by including “conditions” of the genome itself, believing that the number of “internal conditions” should exceed by far that of external. Using specially designed methods, the authors established a fairly large collection of conditional mutations and started to study the properties of this class as a whole.

The term “conditional mutation” is presumably applicable to some of the previously detected mutations. To conditional mutations may be referred *Drosophila funebris* mutants Timofeev-Resovskii isolated from a natural population [2, 3], the incidentally found mutation *Sxl* whose manifestation is sex-dependent [18-20], the Y-suppressed sex-linked recessive lethals in *Drosophila* [21], cell cycle mutations detected by means of “interaction of mutations” [22, 23], among others. These mutations, like those the authors currently obtained, manifest themselves in general as mutations of the regulatory genes. They may be regarded as components of the large Genomic Regulatory Network for development [24]. It is thought that genes of this system organized as networks can be tackled by microchips and knockout and other more sophisticated approaches. Here, the authors demonstrate the feasibility of applying classical mutagenesis in combination with breeding analysis in search of genes of this category.

There have been no large collections of conditional mutations. This may be a reason why their most important properties passed unnoticed. The existence of a special group sharing quite specific properties

among *Drosophila* mutations came as a surprise. The properties include first of all: 1) dominant manifestation pattern; 2) dependence of manifestation on gene location in the genome; and 3) capacity to make the genome pass from stable to unstable state.

The above described properties are manifest in heterozygotes for mutations. Lethality, parental (maternal and paternal) effects, higher metabolic level, genome instability, including morphoses formation that are all dominant. In other words, conditional mutations are necessarily dominant.

The formation of two functioning gene products, one for each of two alleles, is characteristic of most genes of a diploid. For this reason, two manifestations of a mutation may be envisaged, recessive or dominant. The imperative dominance of conditional mutations may mean that there is a single functioning gene product for two alleles of a gene. This results from either gene imprinting silencing of one of the alleles [25] or from the dimeric structure of the regulatory gene product. A dimeric product is functionally capable only in the case of normal homozygosity for the gene, it is not, if at least one allele modified a normal nucleotide sequence. Monomorphism of the regulatory part of the genome follows upon acceptance of the dimeric structure assumption. Existence of monomorphism has been inferred from population study [26] and theoretical consideration of the possibility of the existence of the invariant portion of the species genome [1].

Conditional mutations differ by their response to spatial reorganization of the genome from the usual mutations of the structural genes. The usual mutations are, as a rule, indifferent to where they are located in the genome, moreover, to rearrangements in homologous chromosomes. Conditional lethal mutations in the X respond to inversion in the counterpart X and inversion in chromosomes 2, 3. Lethality also changes in chromosome 2, depending on structural rearrangement in the counterpart homolog. As for the *Smba* mutation, of importance is not only the

presence of inversion as such in the counterpart homolog, the concrete inversion type as well.

It may be suggested that conditional mutations are susceptible to changes in location of genomic chromosomal material, because the concerned genes are regulated at the level of small RNAs. In such a case, regulation is within the nucleus, and the distance from the formation site and the target gene is significant for the regulation to be efficient. The usual genes are insensitive to change in their position in the genome, because they are under the control of the regulatory proteins. They are produced in the cytoplasm and have unobstructed access to all chromosome regions within the nucleus.

Observations on mutant cultures showed that the mutant genomes reside in unstable state. Multiple manifestations of instability are obvious. Loss of lethality is indicative of instability of the mutated loci themselves. Non-manifestation of dominant mutations in the counterpart chromosome and the formation of new mutations indicate spread of instability to other loci. Loss of the X and its non-disjunction is evidence of meiotic irregularity, while the formation of mosaics and gynandromorphs evidence that mitosis is irregular. Morphoses formation is a sign of something going wrong in the mitotically dividing cells. Morphoses represent unilateral deviations of normal ontogenesis in a restricted group of somatic cells during development. Morphoses have been observed previously as a result of exposure of somatic cells to mutagens [27-30]. Morphoses evidence for triggering in the cells of an irregular chain of sequential developmental events.

Appearance of new mutant phenotypes with stable inheritance allowed us to imply disturbances in the structural genes and possible change in primary DNA sequence. However, the disturbances may also not affect the primary DNA structure. In our experiments, we observed mutation variants lasting for just one generation (typical phenocopy) or a "transient" variants with a mutation persisting through generation ("waves" of phenocopies). A transient change in a

DNA region in germline is possible, it may be passed on to generations, then disappears.

No account would be complete without paying due homage to McClintock's discovery of genetic transposition [31] as early as in the 1940s, for her subsequent insights culminating in discovery of movable genetic elements (full story in Ref. [32]). The significance of responses of the genome to challenge [33] cannot be overestimated. The phenomenon of genetic instability is widespread [34]. Instability is characteristic of carcinogenesis [35, 36], hybrid dysgenesis [34], remote consequences of radiation [37], although instability in these cases has been considered often apart. The current study imparts a new meaning to the instability problem. Based on the current data, it may be assumed that the instability state is a response of the genetic system to damage of specific gene regions. Their damage triggers genetic instability. Such regions are the damaged sites of mutated genes. The fact that instability was provoked by each and every one of the obtained mutations indicates that instability is a nonspecific response and a peculiar biologically "sanctioned" version of the genome's state. It is rather a complicated and evolutionary well-rehearsed scenario with determined set of players. The participants of the scenario are already well known: these are mobile elements. Analysis of the mobile genetic element *mdg-2* in some of the recovered mutations has demonstrated its high transposition rate [13].

The unusual properties of conditional mutations prompt new approaches to resolution of a wide range of issues. These include speciation [38, 39], consequences of radiation in human [40], mutagenesis in plants [41, 42]. The suggested existence of a number gene categories in the genome, not a single, encourages revision of some of the crystallized concepts of the genetic system [43-46]. A new aspect related to energy in the system's function also warrants consideration [47, 48].

Acknowledgments

The authors express their gratitude to Prof. John T.

Burns from Bethany College USA for consultations in chronobiology and for assistance in setting up in *Drosophila* experiments with locomotor activity measurements and also Russian Fund of Basic Research for financial support (grant No. 08-04-00094). The authors are also grateful to A. Fadeeva for translating this article from Russian into English.

References

- [1] B.F. Chadov, E.V. Chadova, S.A. Kopyl, E.V. Artemova, E.A. Khotskona, N.B. Fedorova, From genetics of intraspecific differences to genetics of intraspecific similarity, *Rus. J. Genetics*. 40 (9) (2004) 945-958.
- [2] N.V. Timofeev-Resovskii, On the phenotypic expression of the genotype: Genetic variation of *Radius incompletus* in *Drosophila funebris*, *Zh. Eksp. Biol., Ser. A* 1 (3-4) (1925) 93-142.
- [3] N.V. Timofeev-Resovskii, Association between genes and phenotypic characters, in: N.V. Timofeev-Resovskii (Selected Works), O.G. Gazenko, V.I. Ivanov (Eds.), *Izbrannye Trudy*, Moscow, Meditsina, 1996, pp. 59-84.
- [4] B.F. Chadov, E.V. Chadova, S.A. Kopyl, N.B. Fedorova, A new class of mutations in *Drosophila melanogaster*, *Dokl. Biological Sciences* 373 (2000) 423-426.
- [5] B.F. Chadov, Mutations in the regulatory genes in *D. melanogaster*, in: *Proc. Intern. Conf. Biodiversity and Dynamics of Ecosystems in North Eurasia*, Novosibirsk, Russia, Aug. 21-26, 2000, pp. 16-18.
- [6] B.F. Chadov, E.V. Chadova, S.A. Kopyl, E.A. Khotskina, N.B. Fedorova, Genes controlling development: Morphoses, phenocopies, dimorphs and other visible expressions of mutant genes, *Rus. J. Genetics*. 40 (3) (2004) 271-281.
- [7] B.F. Chadov, E.V. Chadova, E.A. Khotskina, E.V. Artemova, N.B. Fedorova, The main effect of chromosomal rearrangement is changing the action of regulatory genes, *Rus. J. Genetics*. 40 (7) (2004) 723-731.
- [8] N.B. Fedorova, E.V. Chadova, E.A. Khotskina, B.F. Chadov, Conditional mutations: Obtainment by the method of morphoses, in: V.A. Kunakh (Ed.), *Topics in Experimental Evolution of Organisms*, 8th ed., Logos, Kiev, 2010, pp.78-83. (in Russian)
- [9] N.B. Fedorova, E.V. Chadova, E.A. Khotskina, B.F. Chadov, Imprinting of homologous chromosome 2 in *D. melanogaster* (in press).
- [10] B.F. Chadov, N.B. Fedorova, The elementary event of development, *Dokl. Biological Sciences* 389 (2003) 183-187.
- [11] B.F. Chadov, E.V. Chadova, E.A. Khotskina, N.B. Fedorova, Mutation in the ontogene – genome instability – appearance of new forms, in: V.N. Stegnij (Ed.), *Evolution Biology*, 3rd ed., Tomsk State University Press, Tomsk, 2005, pp. 92-106. (In Russian)
- [12] B.F. Chadov, E.V. Chadova, E.A. Khotskina, N.B. Fedorova, Conditional lethal mutations shift the genome from stability to instability, *Rus. J. Genetics* 45 (3) (2009) 276-286.

- [13] N.B. Fedorova, E.V. Chadova, Mutation in ontogene causes transposition of retrotransposon 412, in: V.A. Kunakh (Ed.), Topics in Experimental Evolution of Organisms, Kiev: Logos, V.4, 2008, pp. 210-215. (in Russian)
- [14] B.F. Chadov, N.B. Fedorova, E.V. Chadova, E.A. Khotskina, M.P. Moshkin, D.V. Petrovski, Genetic mutation affects the energy status of drosophila, *Rus. J. Genetics*. 46 (9) (2010) 1062-1066.
- [15] N.W. Timofeev-Ressovskii, Relationship between the gene and external trait, in: G. Thieme (Ed.), Wissenschaftliche Woche zu Frankfurt, (1) Erbbiologie, Leipzig, 1934, pp. 92-115. (in German)
- [16] N.W. Timofeev-Ressovskii, V.I. Ivanov, Some problems of phenogenetic, in: S.I. Alikanian (Ed.), Timely Problems of Current Genetics, Publishing House of Moscow University, Moscow, 1966, pp. 114-130.
- [17] M. Ashburner, *Drosophila*, Laboratory Handbook, Cold Spring Harbor Laboratory Press, 1989, p. 1330.
- [18] H.J. Muller, S. Zimmering, Sex-linked lethal without evident effect in *Drosophila* male but partially dominant in females, *Genetics* 45 (1960) 1001-1002.
- [19] S. Zimmering, H.J. Muller, Studies on the action of the dominant female-lethal F1 and a seemingly less extreme allele F1^s, *Dros. Inf. Service*. 35 (1961) 103-104.
- [20] E.M. Maine, H.K. Salz, Th.W. Cline, P. Schedl, The sex-lethal gene of *Drosophila*: DNA alterations associated with sex-specific lethal mutations, *Cell* 43 (1985) 521-529.
- [21] D.L. Lindsley, C.W. Edington, E.S. von Halle, Sex-linked recessive lethals in *Drosophila* whose expression is suppressed by the Y chromosome, *Genetics* 45 (1960) 1649-1670.
- [22] C.L. Regan, M.T. Fuller, Interacting genes that affect microtubule function: The nc2 allele of the haywire locus fails to complement mutations in the testis-specific beta tubulin gene of *Drosophila*, *Genes Dev.* 2 (1988) 82-92.
- [23] H. White-Cooper, M. Carmena, C. Gonzalez, D. Glover, Mutations in new cell cycle genes that fail to complement a multiply mutant third chromosome of *Drosophila*, *Genetics* 144 (3) (1996) 1097-1111.
- [24] E.H. Davidson, J.P. Rast, P. Oliveri, A. Ransick, C. Caestani, C.H. Yuh, A genomic regulatory network for development, *Science* 295 (2002) 1669-1678.
- [25] D. Solter, Differential imprinting and expression of maternal and paternal genomes, *Annu. Rev. Genet.* 22 (1988) 127-146.
- [26] Y.P. Altukhov, Genetic Processes in Populations, *Academkniga*, Moscow, 2003, p. 431.
- [27] G. Frizen, Roentgenmorphoses in *Drosophila*, *Biol. Zh.* 4 (1935) 687-704.
- [28] I.A. Rapoport, Specific morphoses induced in *Drosophila melanogaster* by chemical compounds, *Byull. Eksp. Biol. Med.* 7 (1939) 415-417.
- [29] R. Goldschmidt, Theoretical Genetics, Berkley and Los Angeles, University of California Press, 1957, p. 564.
- [30] R. Goldschmidt, L. Piternick, The genetic background of chemically induced phenocopies in *Drosophila*, *J. Exp. Zool.* 135 (1957) 127-202 and 136 (1957) 201-228.
- [31] B. McClintock, Controlling elements and the gene, *Cold Spring Harb. Symp. Quant. Biol.* 21 (1956) 197-216.
- [32] R.N. Jones, McClintock's controlling elements: The full story, *Cytogenetics Research* 109 (2005) 90-103.
- [33] B. McClintock, Significance of responses of the genome to challenge, *Science* 226 (4676) (1984) 792-801.
- [34] R.B. Khesin, *Instability of the Genome*, Nauka, Moscow, 1985, p. 472.
- [35] P. Duesberg, C. Rausch, D. Rasnick, R. Hehlmann, Genetic instability of cancer cells is proportional to their degree of aneuploidy, *Proc. Natl. Acad. Sci. USA* 95 (23) (1998) 13692-13697.
- [36] P. Pongsaensook, L.E. Ritter, K.K. Parks, A.J. Grosovsky, Cis-acting transmission of genomic instability, *Mutat. Res.* 568 (1) (2004) 49-68.
- [37] S.P. Jarmonenko, A.A. Vainson, *Radiobiology of Man and Animals*, The Higher School, Moscow, 2004, p. 550.
- [38] B.F. Chadov, Mutations capable of inducing speciation, in: V.N. Stegnij (Ed.) *Evolution Biology*, 1st ed., Tomsk State University Press, Tomsk, 2001, pp. 138-162. (In Russian)
- [39] N.B. Fedorova, E.V. Chadova, E.A. Khotskina, B.F. Chadov, Genetic mutations preparing the speciation process, in: V.A. Kunakh (Ed.), Topics in Experimental Evolution of Organisms, 6th ed., Logos, Kiev, 2009, pp. 24-29.
- [40] N.B. Fedorova, Conditional dominant lethals in *Drosophila* and the remote consequences of radiation in human, in: *Modern Problems of Genetics, Radiobiology, Radioecology and Evolution*, Short Papers of the Second International Conference, Yerevan, Sept. 8-11, 2005, pp. 263-265.
- [41] K.K. Sidorova, *Genetics of Pea Mutants*, Nauka, Novosibirsk, 1981, p. 168. (in Russian)
- [42] K.K. Sidorova, Natural and induced mutability of pea mutants, in: *Modern Concepts of Evolutionary Genetics (Abstracts of Proceedings of the Scientific Conference Dedicated to prof. Dmitri K.Belayev)*, Part II, 1997, pp. 319-321. (In Russian)
- [43] B.F. Chadov, A new stage in the development of genetics and term *Epigenetics*, *Rus. J. Genetics* 42 (9) (2006) 1053-1065.
- [44] B.F. Chadov, Quasicycle "gene-progene" as an immanent feature of living material, *Philosophy of Science* 32 (1) (2007) 129-156. (in Russian).
- [45] M.R. Dietrich, From gene to genetic hierarchy: Richard Goldschmidt and the problem of the gene, in: P. Beurton, R. Falk, H.J. Rheinberger (Eds.), *The Concept of the Gene in Development and Evolution, Historical and Epistemological Perspectives*, Cambridge University Press, Cambridge, 2000, pp. 91-114.
- [46] M.R. Dietrich, R. Goldschmidt, Hopeful monsters and other heresies, *Nature Rev. Genetics* 4 (2003) 68-73.
- [47] B.F. Chadov, Power destiny of living and species formation, *Scientific Herald of Lugansk National Agricultural University, Biological Sciences (the Ukraine)* (1) (2009) 72-105. (in Russian).
- [48] B.F. Chadov, "Gene-progene" quasicycle and evolution, in: L.E. Grinin, A.V. Markov, A.V. Korotaev (Eds.), *Evolution: Problems and Discussions*, LKI/URSS, Moscow, 2010, pp. 280-301. (in Russian)

Status, Impact and Management of Certain Alien Plant Pests Proven to Be Invasive to Thailand's Ecology

Malee Thungrabeab and Suthap Tongma

Lampang Agricultural Research and Training Centre, Rajamangala University of Technology Lanna, Lampang Province 52000, Thailand

Received: April 12, 2010 / Accepted: June 21, 2010 / Published: March 30, 2011.

Abstract: Introduction of foreign plants and animals into Thailand's ecology has a long history, some arrived accidentally and others had a purpose. As global commerce increases, the issue of invasive alien species has become more urgent in Thailand. These agents are increasingly seen as a threat not only to biodiversity and ecosystem, but also to economic development and human well-being. They reduce yields of agricultural crops, forests and fisheries, decrease water availability, cause costly land degradation, block transport routes and contribute to the spread of disease. It is clear that since trade will not stop, dangerous alien species need to be controlled and managed and the strategies and control measures are to prevent, eradicate, contain, or effectively control the invaders. Implementation of these measures requires appropriate legislation, regulation and procedures. The impact of some invasive alien pests and their management on the agricultural sector of Thailand are presented.

Key words: Invasive alien plant pest, status, impact, management, Thailand.

1. Introduction

Invasive alien species are increasingly seen as a threat to biodiversity, ecosystem, economic development and human well-being. They reduce yields of agricultural crops, forests and fisheries. Thailand is a major producing country of agriculture products; its economic growth is significantly based on the agricultural sector. Thailand also imports an enormous number living organisms that become invasive alien species to their new host. These organisms range over a variety of species from vertebrates to insects, and cause severe agricultural losses. The risk of invasive alien species (IAS) has been growing though out the years. The existence of these invasive plant pests affects Thailand's agriculture and has caused dire economic losses, e.g., *Bemisia tabaci*, *Liriomyza* spp., *Plutella xylostella*, *Thrips*

tabaci, papaya ring spot virus, *Mimosa diplotricha*, *Meloidogyne* spp., *Pomacea canaliculata* [1]. Appropriate legislation, regulation and practical procedures are necessary to prevent the negative impact of alien species on Thailand's economic growth.

2. Methodology

Data sources from available literature, published reviews and direct consultation were analyzed for correlations between classification, origin, introduction pathway, impact on local ecology and management of invasive alien species.

3. Data Analysis

Thailand, a major producer of agricultural products, is increasingly susceptible to the reduction in yield of agricultural crops caused by invasive alien species. Detailed information on origin, pathways, status, impact and management of invasive alien agricultural pests, microorganisms, plants, insects and molluscs, was gathered and analyzed for potential correlations.

Corresponding author: Malee Thungrabeab, Ph.D., Asst. Prof., research fields: entomology, insect pathology. E-mail: sriwanmal@yahoo.com.

3.1 The Status of Alien Invasive Plant Pests in Thailand

3.1.1 Invasive Alien Microorganisms

All invasive alien microorganisms are unintentionally introduced, through fresh agricultural imports, e.g. flowers, vegetables, fruits or soil. The majority of invasive alien microorganisms caused severe agricultural losses in Thailand and are presented in Table 1.

3.1.2 Invasive Alien Plants

The introduction of plants has following pathways, i.e. as ornamental, feedstuff, green fertilizers and medicinal, etc. Some species have grower and spread very fast and escaped into agro-ecosystem; they are

Table 1 Important invasive microorganisms in Thailand.

Microorganism	Probable origin; year intercepted
<i>Papaya ringspot</i>	Queensland; 1975 [1, 2]
<i>Meloidogyne</i> spp. (Heteroderidae)	Not known [2]
<i>Fusarium oxysporum</i>	Not known [3]
<i>Ralstonia solanacearum</i>	Not known [2]
Rice tungro virus (Culimoviridae)	Not known [3]

Table 2 Some noxious weeds in Thailand.

Plant species	Family	Probable origin; year intercepted
<i>Ageratum conyzoides</i>	Compositae	America; not known [3]
<i>Ageratina adenophorum</i>	Asteraceae	Mexico via China; 1979 [3]
<i>Chromolaena odorata</i>	Asteraceae	Central and South America via Singapore; 1940 [4]
<i>Commelina benghalensis</i>	Commelinaceae	America; not known [3]
<i>Commelina diffusa</i>	Commelinaceae	America; not known [3]
<i>Cyanotis axillaries</i>	Commelinaceae	India; not known [3]
<i>Cyperus rotundus</i>	Cyperaceae	America; not known [3]
<i>Drymaria cordata</i>	Caryophyllaceae	Africa; 1952 [3]
<i>Echinochloa colona</i>	Poaceae	Eastern Asia; not know [3]
<i>Echinochloa crus-galli</i>	Poaceae	Eastern Asia; not know [3]
<i>Mimosa pigra</i>	Mimosaceae	Central and South America via Australia and Indonesia; 1950 [4, 5]
<i>Mimosa diplotricha</i>	Mimosaceae	Central and South America via Australia and Indonesia; 1950 [3]
<i>Eupatorium adenophorum</i>	Asteraceae	Mexico; not known [3]
<i>Euphorbia heterophylla</i>	Euphorbiaceae	Mexico via India; not known [3]
<i>Fimbristylis dichotoma</i>	Cyperaceae	Southeast Asia via Indonesia; not known [3]
<i>Fimbristylis miliacea</i>	Cyperaceae	Southeast Asia via Indonesia; not known [3]
<i>Imperata cylindrica</i>	Poaceae	South East Asia; not known [4]
<i>Leucaena leucocephala</i>	Leguminosae	Mexico and Central America; not known [4]
<i>Pennisetum pedicellatum</i>	Poaceae	Senegal via India; 1952 [3]

weeds. An inventory of IAS in Thailand showed over 1,763 alien plants that included both invasive and beneficial species. The plants that invaded agricultural areas and became weeds for the farming community are shown in Table 2.

3.1.3 Invasive Alien Insects

Among the insects that have been introduced to Thailand, forty-one of them are classified as serious insect pests of agricultural importance (Table 3). Most of the alien species do not become invasive or cause problems in their new locations and many even benefit society, i.e. as in agricultural, forestry and the pet industry. A total of 39 exotic insect species, 19 of those species were destined for biological control of various other insect pests and 20 as insect pests for biological control of both terrestrial and aquatic weeds. The lists of the exotic insect species used for biologically controlling various insect pests and weeds are given in Table 4.

3.1.4 Invasive Alien Mollusks

Mollusks introduced purposely to ornamental and

Table 3 Invasive alien insect species of agricultural importance in Thailand.

Species and common name	Probable origin; year intercepted
1. <i>Acraea violae</i> ; Towny custer (Lepidoptera: Acraeidae)	Africa via India; not known [3]
2. <i>Agrotis segetum</i> ; Cutworm (Lepidoptera: Noctuidae)	West Europe; not known [2]
3. <i>Aleurodicus destructor</i> ; Coconut whitefly (Homoptera: Aleyrodidae)	Central America; not known [6]
4. <i>Aleurodicus dispersus</i> ; Spiraling whitefly (Homoptera: Aleyrodidae)	Central America; 1982 [6]
5. <i>Amrasca biguttula</i> ; Cotton leafhopper (Homoptera: Cicadellidae)	India; not known [6]
6. <i>Amritodus atkinsoni</i> ; Mango leafhopper (Homoptera: Cicadellidae)	India; not known [6]
7. <i>Anomala antiqua</i> ; Sugarcane white grub (Coleoptera: Scarabaeidae)	India; not known [6]
8. <i>Aphis craccivora</i> ; Black legume aphid (Homoptera: Aphididae)	Europe; not known [6]
9. <i>Batocera rufomaculata</i> (Coleoptera: Cerambycidae)	South America India; not known [3]
10. <i>Bemisia tabaci</i> ; Tobacco whitefly (Homoptera: Aleyrodidae)	Pakistan; not known [1, 6]
11. <i>Brontispa longissima</i> ; coconut leaf miner hispid (Coleoptera: Hispidae)	Indonesia via Vietnam; 2002 [3]
12. <i>Conopomorpha cramerella</i> ; Cocoa pod borer (Lepidoptera: Gracillariidae)	Sri Lanka; not known [6]
13. <i>Frankliniella occidentalis</i> (Thysanoptera: Thripidae)	Cuba; 1960 [2]
14. <i>Gainaithrips ficorum</i> ; Cuban laurel thrips (Thysanoptera: Phlaeothripidae)	Cuba; 1967 [6]
15. <i>Helicoverpa armigera</i> (Lepidoptera: Noctuidae)	Mexico; not known [3]
16. <i>Ischnaspis longirostris</i> (Hemiptera: Diaspididae)	Africa; not known [6]
17. <i>Heteropsylla cubana</i> ; Leucaena psyllid (Homoptera: Psyllidae)	Central America; September 1986 [6]
18. <i>Homona coffearia</i> ; Leaf roller (Lepidoptera: Tortriadae)	India; not known [3]
19. <i>Icerya purchasi</i> ; Cottony cushion scale (Homoptera: Magaronidae)	Australia; not known [6]
20. <i>Leptocybe invasa</i> (Hymenoptera: Eulophidae)	Australia; not known [2]
21. <i>Liriomyza huidobrensis</i> ; Bean leaf miners <i>L. sativae</i> , <i>L. strigata</i> , <i>L. trifolii</i> (Diptera: Agromyzidae)	Europe; 1980s [6]
22. <i>Maruca vitrata</i> ; Bean pod borer (= <i>Maruca testulalis</i>) (Lepidoptera: Pyralidae)	South America; not known [6]
23. <i>Nezara viridula</i> ; Green stink bug (Hemiptera: Pentatomidae)	Southern Europe/North Africa; not known [6]
24. <i>Oligonychus coffeae</i> (Acari: Tetranychidae)	Africa; not known [3]
25. <i>Oligonychus mangiferus</i> (Acari: Tetranychidae)	Africa; not known [3]
26. <i>Parabemisia myricae</i> (Homoptera: Aleyrodidae)	Japan; not known [3]
27. <i>Pectinophora gossypiella</i> ; Cotton pink bollworm (Lepidoptera: Gelechiidae)	Australia; not known [6]
28. <i>Peregrinus maidis</i> ; Corn plant hopper (Homoptera: Delphacidae)	Central America; not known [6]
29. <i>Phthorimaea operculella</i> ; Potato tuber moth (Lepidoptera: Gelechiidae)	South America; not known [3]
30. <i>Phyllotreta striolata</i> ; Striped flea beetle (Coleoptera: Crysomelidae)	Europe; not known [6]
31. <i>Plutella xylostella</i> ; Diamondback moth (Lepidoptera: Yponomeutidae)	Southeastern Europe; not known [6]
32. <i>Pseudococcus longispinus</i> ; mealy bug (Homoptera: Pseudococcidae)	Egypt; not known [2]
33. <i>Saccharicoccus sacchari</i> ; Sugarcane scale (Homoptera: Pseudococcidae)	Papua New Guinea; not known [6]
34. <i>Scirpophaga innotata</i> ; Stem borer (Lepidoptera: Crambidae)	Indonesia, Pakistan, Philippines, and North Australia; not known [2]
35. <i>Scrobipalpa heliopa</i> ; Eggplant budworm (Lepidoptera: Gelechiidae)	Australia; not known [6]
36. <i>Stromatium barbatum</i> ; long horned borer (Coleoptera: Cerambycidae)	India; not known [2]
37. <i>Susica sinensis</i> ; plant hopper (Lepidoptera: Limacodidae)	China; not known [3]
38. <i>Tarophagus proserpina</i> (Homoptera: Delphacidae)	Australia; not known [3]
39. <i>Thosea sinensis</i> ; Chinese nettle caterpillar (Lepidoptera: Limacodidae)	China; not known [3]
40. <i>Thrip tabaci</i> ; Onion thrips (Thysanoptera: Thripidae)	Middle East; not known [6]
41. <i>Thrips simplex</i> (Thysanoptera: Thripidae)	Australia; not known [3]

Table 4 Insects introduced for biological control of pests in Thailand.

Target species	Natural enemies introduced	Origin, year of introduced
<i>Oryctes rhinoceros</i> : Coconut rhinoceros beetle (Coleoptera: Scarabaeidae)	<i>Scolia ruficornis</i> (Hymenoptera: Scoliidae)	West Caroline Island, Palau; 1963 [7]
<i>Plutella xylostella</i> : Diamondback moth (Lepidoptera: Yponomeutidae)	<i>Brachymeria</i> sp. (Hymenoptera: Chalcididae)	India; 1965 [7]
	<i>Cotesia plutellae</i> (Hymenoptera: Braconidae)	India; 1965 [7]
	<i>Diadegma insulare</i>	Canada; 1964 [7]
	<i>Diadegma semiclausum</i> (Hymenoptera: Ichneumonidae)	Taiwan; 1989 [8]
	<i>Diadromus collaris</i> (<i>Thyraeella collaris</i>) (Hymenoptera: Ichneumonidae)	India; 1965 [7]
	<i>Macromalon orientale</i> (Hymenoptera: Ichneumonidae)	India; 1965 [7]
	<i>Oomyzus sokolovskii</i> (<i>Tetrastichus sokolovskii</i>) (Hymenoptera: Eulophidae)	India; 1965 [7]
Scale insects, mealy bugs, aphids	Coccinellids: <i>Azya orbigera</i> (<i>Azya luteipes</i>)	Mexico via Hawaii; 1974-1977, 2002 [8]
	<i>Chilomenes lunata</i>	Kenya; 1982; NBCRC [7]
	<i>Coelophora pupillata</i>	Mexico via Hawaii; 1974-1977, 2002 [8]
	<i>Cryptolaemus montrouzeiri</i>	Australia via Hawaii; 1974-1977, 2002 [8]
<i>Heteropsylla cubana</i> : leucaena psyllid, (Homoptera: Psyllidae)	<i>Curinus coeruleus</i> (Coleoptera: Coccinellidae)	Mexico via Hawaii via Palau; 1987 [7]
	<i>Olla v-nigrum</i> (<i>Olla abdominalis</i>) (Coleoptera: Coccinellidae)	Mexico via Hawaii; 1989 Hawaii via Tonga; 1992 [8]
	<i>Orcus chalybeus</i> (Coleoptera: Coccinellidae)	Mexico via Hawaii; 1974-1977 [7]
	<i>Psyllaephagus yaseeni</i> (Hymenoptera: Encyrtidae)	Trinidad & Tobago via Hawaii; 1987-1988 [7]
	<i>Tamarixia leucaena</i> (Hymenoptera: Eulophidae)	Trinidad & Tobago via UK; 1991 [8]
<i>Aleurodicus dispersus</i> Spiraling whitefly	<i>Nephaspis oculatus</i> (<i>Nephaspis amnicola</i>) (Coleoptera: Coccinellidae)	Trinidad & Tobago via Hawaii; 1984 [7]
<i>Gynaikothrips ficorum</i> Cuban laurel thrips (Thysanoptera: Phlaeothripidae)	<i>Montandoniella moraguesi</i> (Hemiptera: Anthocoridae)	Philippines via Hawaii; 2001-2002 [8]
<i>Eichhornia crassipes</i> ; Water hyacinth (Pontederiaceae)	<i>Eccritotarsus catarinensis</i> (Hemiptera: Miridae)	Brazil via Australia; 1997 Brazil via Australia via South Africa; 1998 [8]
	<i>Neochetina bruchi</i> (Coleoptera: Curculionidae)	Argentina via Florida via Australia; 1990 [5]
	<i>Neochetina eichorniae</i> (Coleoptera: Curculionidae)	Argentina via Florida; 1977, 1979 [5]
	<i>Niphograptus albiguttalis</i> (Lepidoptera: Pyralidae)	Argentina via Florida via Australia; 1994 [8]
	<i>Xubida (Acigona) infusella</i> (Lepidoptera: Pyralidae)	South America via Florida via Australia; 1997 [8]
<i>Alternanthera philoxeroides</i> ; Alligator weed (Amaranthaceae)	<i>Agasicles hygrophila</i> (Coleoptera: Chrysomelidae)	Argentina via Florida via Australia; 1981 [5]

Table 4 (Continued).

Target species	Natural enemies introduced	Origin, year of introduced
<i>Mimosa pigra</i> ; Giant sensitive plant (Mimosaceae)	<i>Acanthoscelides puniceus</i> (Coleoptera: Bruchidae)	Mexico via Australia; 1984 [5]
	<i>Acanthoscelides quadridentatus</i> (Coleoptera: Bruchidae)	Mexico via Australia; 1984 [5]
	<i>Carmenta mimosa</i> (Lepidoptera: Sesiidae)	Mexico via Australia; 1989-1992 [8]
	<i>Chlamisus mimosae</i> (Coleoptera: Chrysomelidae)	Brazil via Australia; 1985 [5]
	<i>Coelecephalopion aculeatum</i> (Coleoptera: Apionidae)	Mexico via Australia; 1991-1992 [5]
	<i>Milothris irrorata</i> (Coleoptera: Cerambycidae)	Indonesia; 1981[5]
<i>Chromolaena odorata</i> ; Siam weed (Asteraceae)	<i>Acalitus adoratus</i> (Acarina; Eriophyidae)	Trinidad & Tobago via Guam; 2001 [8]
	<i>Cecidochares connexa</i> (Diptera: Tephritidae)	Trinidad & Tobago via Guam via Indonesia; 2001 [8]
	<i>Pareuchaetes pseudoinsulata</i> (Lepidoptera: Arctiidae)	Trinidad & Tobago via Guam; 1986-1988 [7]
<i>Ageratina adenophorum</i> ; Crofton weed (Asteraceae)	<i>Procecidochares utilis</i> (Diptera: Tephritidae)	Mexico via Hawaii; 1991-1992 [8]

because of poor sales, these mollusks were released into the natural. Invasive mollusks species are shown in Table 5.

3.2 Impact of Alien Invasive Plant Pests in Thailand

Alien species, introduced into Thailand both intentionally or by accident, eventually find their way into and colonize the agro-ecosystem. Often unchecked by natural enemies, many of these are become invasive plant pests that threaten natural plant health and also the agro-ecosystem itself. The losses caused by invasive alien species to Thailand's agriculture have been enormous. Among the effects of IAS are reduced cash incomes from low crop production, diminished food security, decreased exports due to poor quarantine, increased livelihood insecurity and increased public expense on food relief and breeding of disease resistant varieties. Additionally, the impact of IAS is immense, insidious, and usually irreversible. They not only cause great economic damage but also threaten native species through the degradation of habitats and ecosystems: The ecological cost is the irretrievable loss of native species and ecosystems.

3.3 Management of Invasive Species in Thailand

Should an IAS entry and establishment take place, in

general, management strategies and control measures are aimed to prevention, eradication, containment, or effectively control. Legislation, regulations and procedures augment the implementation of these measures [9].

3.3.1 Prevention

Practices for the prevention and management of IAS are given by law and regulation. For plants, insects, plant pathogens and biological control agents, the Department of Agriculture, Ministry of Agriculture & Cooperatives is the main agency for the prevention and tracking of imported alien species in Thailand. Several legislative enactments provide considerable support to prevent and manage IAS. The Water Hyacinth Eradication Act of 1913, the Plant Disease and Plant Pest Prevention Act of 1952, the Plant Quarantine Act of 1964 (revised 2006), the Plant Variety Act of 1975 (revised 1992) and the Plant Varieties Protection Act of 1999 provide the legal framework for dealing with dangerous alien pests of plants.

Effective implementation of this act could potentially prevent future introductions and establishment of IAS. However, the effectiveness of these regulations is restricted to the limited management resources and lack of adequate scientific data and evidence proving negative impacts. Furthermore, the existing law and

Table 5 The important invasive mollusks in Thailand.

Species and common name	Probable origin; year introduction
<i>Achatina fulica</i> : Giant Africa snail (Stylommatophora: Achatinidae)	East Africa; 1938 [3]
<i>Pomacea canaliculata</i> : Golden Apple snail (Mesogastropoda: Pilidae)	South America; 1990 [3]

regulation does not mention any technical-scientific guidelines or tools and methodologies for the quick detection, containment and control of IAS.

3.3.2 Eradication and Control

Most of IAS of economic and agricultural importance is amenable to various integrated pest management strategies from no control to single – component control. These employ various control techniques such as physical, mechanical, culture, genetic, chemical, biological, microbial control, mechanisms under the concept of “Integrated Pest Management”. Some of them are promoted as materials for handicraft, fertilizers, charcoal, souvenir, and animal feed.

4. Conclusion

Since trade will not stop, the risk of plant pest invasion will continue to grow. As a consequence, Thailand's agriculture will be seriously threatened. The detection of new invasive species and immediate control measures urgently must be taken to forestall their spread. Moreover, agricultural exportation will be blocked for failing to meet the quarantine required by other countries.

Acknowledgment

This work was supported by the European Commission under Asia-Link Program [CN/ASIA - LINK 1035 (129-036) (BIOSEC)].

References

[1] J. Nabhitabhata, Hundred of world's worst invasive alien

- species: Data of alien species in Thailand, in: Proceeding of International Day of Biological Diversity in Topic “Biodiversity and Management of Invasive Alien Species”, May 22-23, 2001, Office of Resource and Environmental Policy and Planning, Ministry of Science, Technology and Environment, Bangkok, 2002, pp. 34-47. (In Thai)
- [2] Office of Environmental Policy and Planning (OEPP), Proceeding of Alien Species in Thailand, Ministry of Science, Technology and Environment, Bangkok, Thailand, Oct. 24-26, 1996, p. 116. (In Thai)
- [3] Office of Resource and Environmental Policy and Planning, Proceeding of Invasive Alien Species, Ministry of Science, Technology and Environment, Bangkok, Thailand, 2007, p. 90. (In Thai)
- [4] S. Zungsontiporn, Global invasive plants in Thailand and its status and a case study of *Hydrocotyle umbellata* L., in: International Workshop on the Development of Database (APASD) for Biological Invasion, Taichung, Taiwan ROC, Sep. 18-22, 2006, p. 17.
- [5] B. Napompeth, Country report: Thailand, Biological control of paddy and aquatic weeds in Thailand, Weed Management, BIOTROP Special Publication No. 38, BIOTROP, Bogor, Indonesia, 1990.
- [6] B. Napompeth, C. Kongsawat, N. Iamsupasit, Current Status on Alien Species Management in Thailand, Abstract Book of 20th Pacific Science Congress, Bangkok, Thailand, Mar. 17-21, 2003.
- [7] B. Napompeth, Use of natural enemies to control agricultural pests in Thailand, in: The Use of Natural Enemies to Control Agricultural Pests, FFTC Book Series No. 40, Food and Fertilizer Technology Center (FFTC), Taiwan, 1990.
- [8] B. Napompeth, Management of Invasive Alien Species in Thailand, Extension Bulletin 544, Food & Fertilizer Technology Center (FFTC), Taiwan, 2004.
- [9] Office of Resource and Environmental Policy and Planning, Measure, Prevents, Control and Eradication of Alien Species, Ministry of Science, Technology and Environment, Bangkok, 2009, p. 28. (In Thai)